SUMMARY

The deterioration of polymers in the atmospheric environment can be simulated in the laboratory by accelerated weathering techniques. In the case of polystyrene, sample purity and the wavelengths used have lead to conflicting results concerning the nature of the initiation steps involved. In this thesis, the photo-oxidation of a series of hydrocarbon copolymers of styrene are studied using wavelengths greater than 300 nm (pyrex covered reaction cell) and the full spectrum of the light (quartz covered reaction cell) supplied by a medium pressure mercury lamp. The copolymers provide a high standard of purity and a tailor-made system, whereby the effect of changing chemical structure on the photo-oxidative stability can be closely examined for both wavelength regions. The main investigation of the copolymers' relative stabilities under a variety of conditions is carried out using data from oxygen-uptake versus time measurements. From a study of the production of gaseous products and the oxygen-uptake results,an initiation reaction for each wavelength region is proposed for the copolymers. Because of the close similarity in structure and behaviour between polystyrene and its copolymers, it is also proposed that the same general mechanisms apply to polystyrene itself.

A STUDY OF THE PHOTO-OXIDATION OF SOME STYRENE COPOLYMERS

A Thesis
presented for the degree of
DOCTOR OF PHILOSOPHY
in the Faculty of Science of the
University of St. Andrews
by

DAVID ALEXANDER RAMSAY, B. Sc.

August 1975

United College of St. Salvator
and St. Leonard, St. Andrews.

DECLARATION

I declare that this thesis is my own composition, that the work of which it is a record has been carried out by me, and that it has not been submitted in any previous application for a Higher Degree.

This thesis describes results of research carried out at the Department of Chemistry, United College of St. Salvator and St. Leonard, University of St. Andrews, under the supervision of Dr. J. R. MacCallum since the 1st of October 1972.

David A. Ramsay.

CERTIFICATE

I hereby certify that David Alexander Ramsay has spent twelve terms of research work under my supervision, has fulfilled the conditions of Ordinance General No. 12 and Resolution of the University Court 1967, No. 1, and is qualified to submit the accompanying thesis in application for the degree of Doctor of Philosophy.

J. R. MacCallum
Director of Research
Department of Chemistry
University of St. Andrews.

ACKNOWLEDGEMENTS

I should like to record my gratitude to Dr. James R. MacCallum for his help and encouragement in all aspects of this work.

I am indebted to the E. R. D. E., Waltham Abbey (Ministry of Defence), for the award of a Research Studentship during the period 1972-1975, and to Professor P. A. H. Wyatt for research facilities in the chemistry department during this time.

My thanks are also due to Dr. A. Davis of the E. R. D. E., Waltham Abbey, for his helpful advice throughout.

Finally, may I express my gratitude to all the teaching and technical staff of the University of St. Andrews Chemistry Department, especially Mr. J. Rennie, Mr. J. G. Ward and Mr. N. G. West for their technical assistance, and Mrs. E. J. West who typed this thesis.

CONTENTS

	Page
Declaration	(ii)
Certificate	(iii)
Acknowledgements	(iv)
Contents	(v)
List of Figures	(ix)
List of Tables	(xi)
Summary	(xiii)
CHAPTER 1 : Introduction	
I. Photochemistry	2
1. Photophysical Processes	2
A. Energy Transfer	3
i) Radiative	3
ii) Non-Radiative	4
a) Resonance Excitation Transfer	4
b) Exchange Energy Transfer	4
c) Energy Transfer in Collisions	4
B. Excimer Emission Spectra	5
2. Photochemical Processes	5
II. Photo-oxidation Reaction Monitoring	5
1. Change in Physical Properties	6
2. Product Analysis	6
3. Oxygen-uptake	6
III. Reactivity of Polymers	6
1. Chemical Structure	6
2. Physical Structure	8
3. Polymer State	8
4. Polymer History	8

	Page
IV. Photo-oxidation of Polystyrene	9
1. Reaction Sites and Consequences of Photo-oxidation	9
2. Initiation Reaction	9
a) Wavelengths 200 nm to 280 nm	10
i) Direct Bond Break	10
ii) Reaction with Singlet Oxygen	10
iii) Reaction with Ozone and Atomic Oxygen	12
iv) Miscellaneous Impurities	13
b) Wavelengths Greater Than 280 nm	13
i) Reaction with Singlet Oxygen	13
ii) Impurities	14
iii) Reaction with Molecular Oxygen	14
iv) Reaction of Residual Radicals	14
v) End-of-Chain Phenyl Alkyl Ketone Groups and 'Norrish Type' Reactions	15
3. Propagation Reaction	17
4. Decomposition of Hydroperoxides and Chain Branching	18
5. Termination Reaction and Products	21
CHAPTER 2 : Experimental	
1. Synthesis of Copolymers	23
i) Purification of Materials	24
ii) Experimental Method	25
2. Characterisation of Copolymers	26
i) Microanalysis	26
ii) Infra-red Spectroscopy	26
iii) Nuclear Magnetic Resonance Spectra	27
iv) Ultra-violet Spectroscopy	30
v) Excimer Emission Spectra	33
vi) Molecular Weight	33
3. The Photo-oxidation Apparatus	33
i) The Light Source	34
a) Stabilisation	34
b) Filters	34
c) Calibration	34

Page

ii) Factors Influencing the Design of the Apparatus 38
iii) Photo-oxidation Apparatus and Experimental Procedure 40
a) Cell A, Absorbers and Sample Holder 40
b) Manometer System and Method of Measurement - Apparatus One 41
c) Experimental Procedure - Apparatus One 43
d) Manometer System and Method of Measurement - Apparatus Two 44
e) Experimental Procedure - Apparatus Two 45
f) Film Casting 46

4. The Heating Effect Apparatus 47

5. Product Analysis 48

CHAPTER 3 : Results

1. Rate Measurement and Experimental Errors for Apparatus One and Two 49
2. Blank, Consistency and Film Casting Technique Checks 49

3. Results from Apparatus One 51
A. Reactions Under Quartz 52
B. Reactions Under Pyrex 54

4. Results from Apparatus Two 55
A. Reactions Under Pyrex 55
i) Relative Rates of the Copolymers 55
ii) Variation of Rate with Intensity 56
iii) Energy of Activation 56
B. Reaction Under Quartz 57
i) Relative Rates of the Copolymers 57
ii) Variation of Rate with Intensity 58
iii) Energy of Activation 59

5. Product Analysis 59

Page

6. Irradiation in Nitrogen and Vacuo 61

7. Effect of Absorber Removal on Rate 62
a) Under Quartz 62
b) Under Pyrex 62
i) Absorber Removal Only 62
ii) Absorber Removal and Variation in 313 nm Line Intensity 63

8. Heating Effect 65

CHAPTER 4 : Discussion
Photo-oxidation Reaction 69
A. The Reaction Under Quartz 69
i) Initiation and Oxygen-uptake 69
ii) Relative Rates of Copolymers Under Quartz 70
a) Extinction Coefficient Contribution 71
b) Polymer Structure Contribution 71
iii) Propagation, Products and Termination of the Reaction 72
B. The Reaction Under Pyrex 77
i) Initiation 77
ii) Relative Rates of Copolymers Under Pyrex in Apparatus Two 78
iii) Oxygen-uptake, Propagation, Products and Termination of the Reaction 81

BIBLIOGRAPHY 84

LIST OF FIGURES

Figure	TITLE	Following Page
1	Cell A	40
2	Sample Holder	40
3	Apparatus One, Manometer System	41
4	Enlargement of Plunger Trip Mechanism	41
5	Apparatus Two, Manometer System	44
6	Film Casting Apparatus	46
7	Cell B	47
8	Rate of Oxygen-Uptake Versus Sample Weight For Apparatus Two	50
9	Example of Change Produced in U.V. Spectra of the Films After Irradiation	52
10	Apparatus One. Oxygen-Uptake versus Time Under Quartz	52
11	Apparatus One. Oxygen-Uptake Versus Time For Polystyrene Under Pyrex	54
12	Apparatus Two. Oxygen-Uptake Versus Time Under Pyrex	55
13	Apparatus Two Under Pyrex Rate of Oxygen-Uptake Versus $(\text{Intensity})^{\frac{1}{2}}$	56
14	Apparatus Two. Energy of Activation Plots Under Pyrex	57
15	Apparatus Two Under Quartz Rate of Oxygen-Uptake Versus Time	57
16	Apparatus Two Under Quartz Rate of Oxygen-Uptake Versus Intensity	58

Figure	TITLE	Following Page
17	Change in Ultra-Violet Spectra in Air Versus Time	61
18	Change in Optical Density (Δ O. D.) After 5 Hours Irradiation in Air Divided by the Origional Optical Density of Films($(O. D.)_o$) Versus Wavelength	61
19	Effect of Heat on Irradiation Product	61
20	Apparatus Two. Effect of Removal of Absorbers on the Rate of Oxygen-Uptake Under Quartz	62
21	Apparatus Two. Effect of Removal of Both Absorbers on the Rate of Oxygen-Uptake Under Pyrex	62
22	Effect of The Removal of Absorbers on the Rate of Oxygen-Uptake Under Pyrex	63
23	Apparatus Two. Effect of the Removal of Both Absorbers on the Rate of Oxygen-Uptake Under Three Pyrex Discs	64
24	Heating Effect. Intensity Versus Temperature Increase Under Quartz	67
25	Heating Effect. The Volume Increases and Decreases when Lamp was Switched off and on During the Photo-oxidation Reaction of the p-Xylene/Styrene Copolymer Under Pyrex	67
26	The Optical Density (O. D.) Maximum at 364 nm for Polystyrene Films Containing Anthracene Versus Temperature Increase on Irradiation Under Quartz. Corrected for Polystyrene	68
27	Ultra-Violet Spectrum of Acetophenone	73

LIST OF TABLES

Table	TITLE	Page
1	Microanalyses Results for the Copolymers	26
2	Aliphatic/Aromatic Hydrogen Ratios in the ^{1}H n.m.r. Spectra of the Copolymers	28
3	Assignments of the Aliphatic Peaks in the ^{1}H n.m.r. Spectra of the Copolymers	28
4	Experimentally Determined γ Values of the Aliphatic Peaks in the ^{1}H n.m.r. Spectra of the Copolymers	29
5	Experimentally Determined γ Values of the Aromatic Peaks in the ^{1}H n.m.r. Spectra of the Copolymers	29
6	Extinction Coefficients Determined from the Peaks in the U.V. S pectra of the Copolymers	31
7	Extinction Coefficients Determined from the Peak Maxima in the U.V. Spectra of the Copolymers Corrected for the Number of Benzene Rings Per Repeat Unit	32
8	Excimer Emission Spectra Maxima	33
9	Variation of U.V. Lamp Intensity with Distance and Filter Determined by Actinometry	35
10	Relative Line Intensities from U.V. Source	36
11	Variation of 365 nm : 313 nm Line Intensity Ratio with Filter	37
12	Variation of 313 nm Line Intensity with Filter While Maintaining 365 nm Line Intensity Constant by Altering Arc to Sample Distance	38
13	Variation of U.V. Lamp Intensity with D.V.M. Reading Determined by Actinometry	38

Table	TITLE	Page
14	Rate of Oxygen-uptake for the Copolymers Under Quartz in Apparatus One	53
15	Rate of Oxygen-uptake for the Copolymers Under Pyrex in Apparatus Two	56
16	Energies of Activation for the Copolymers Under Pyrex	57
17	Rate of Oxygen-uptake for the Copolymers Under Quartz in Apparatus Two	58
18	Heating Effects for the Copolymers Under Quartz	67

SUMMARY

The deterioration of polymers in the atmospheric environment can be simulated in the laboratory by accelerated weathering techniques. In the case of polystyrene, sample purity and the wavelengths used have lead to conflicting results concerning the nature of the initiation steps involved. In this thesis, the photo-oxidation of a series of hydrocarbon copolymers of styrene are studied using wavelengths greater than 300 nm (pyrex covered reaction cell) and the full spectrum of the light (quartz covered reaction cell) supplied by a medium pressure mercury lamp. The copolymers provide a high standard of purity and a tailor-made system, whereby the effect of changing chemical structure on the photo-oxidative stability can be closely examined for both wavelength regions. The main investigation of the copolymers' relative stabilities under a variety of conditions is carried out using data from oxygen-uptake versus time measurements. From a study of the production of gaseous products and the oxygen-uptake results, an initiation reaction for each wavelength region is proposed for the copolymers. Because of the close similarity in structure and behaviour between polystyrene and its copolymers, it is also proposed that the same general mechanisms apply to polystyrene itself.

TO

MY PARENTS

CHAPTER 1

INTRODUCTION

Styrene, its polymers and copolymers have been known since about 1840. They became extremely important during and after the Second World War when their emergency use as superior insulating plastics and as all purpose synthetic rubbers caused a dramatic growth in their production. New reactions and technologies have resulted in new applications and the continued expansion has necessitated a great deal of research and development.

In use,polymers are subjected to a variety of different conditions. Whether natural or man-made, the environment will eventually cause deterioration in the polymer. This results in irreversible loss of the polymer's useful properties. Although the predictability of this loss is fairly well documented, the fundamental chemical processes involved must be known before efficient stabilisers or degraders are found. Studies of environmental ageing and subsequent polymer failure are therefore of direct commercial concern.

The best tests for weatherability of polymers are field tests[1]. However they are the slowest and still not infallible since variation of weather makes results inconsistent and in commercial terms prolonged experiments are not economically viable. The chemist is thus faced with the problem of accelerating the ageing of a polymer while as closely as possible simulating outdoor conditions.

The weather and the atmosphere contain many complex variables. It is, however, possible to identify the main agents of polymer deterioration.

Water is very important especially when dealing with condensation polymers[1] but the present investigation is limited to the effects of heat, light and oxygen.

Problems arising from simulation of temperature and gas environments prove minor in comparison to the choice of artificial light source. Sunlight is the main energy source in the environment. Once it has filtered through the earth's upper atmosphere, its photochemically active wavelengths are limited to near-ultra-violet region, 300-400 nm (400-300 kJ mol^{-1}). It is in this region, therefore, that our alternative source must correspond.

The principal ultra-violet radiation sources used are carbon arcs, fluorescent lamps, mercury arcs or lamps and various types of xenon arc. Although xenon arcs approximate most closely to sunlight[1], much of the more recent work has been done using mercury lamps. These provide sufficient chemical change to allow monitoring of the reaction after only a matter of minutes.

I Photochemistry

The combined effects of light and oxygen give rise to the photo-oxidation reaction. To help understand these reactions, a knowledge of basic photochemistry is required.

When a molecule absorbs a quantum of light in the absence of oxygen it is activated to an electronically excited state. The extent of this activation depends on the wavelength of the light absorbed. The energy thus gained can be dissipated in a variety of ways.

1. Photophysical Processes

The absorbed energy can be emitted as fluorescence, excimer

fluorescence, phosphorescence, energy transfer to another molecule or radiationless conversion as heat. In the event of bond scission the latter gives rise to 'hot' radicals which may take part in ground state thermal reaction.

The transfer of electronic energy and the emission of excimer fluorescence are extremely important processes and as such require fuller descriptions.

A. Energy Transfer

Energy transfer has been observed in solids[2], liquids[3,4] and gases[5] and between gaseous and solid phases[6]. It can be intramolecular or intermolecular and radiative or non-radiative. The requirements for energy transfer are an initial absorber (or donor) and an energy quencher (or acceptor). The actual transfer is between the excited energy level of the donor and a level of lower energy in the acceptor. In the presence of oxygen only singlet - singlet transfer occur because long - lived triplets are quenched by oxygen[7]. In the absence of oxygen, triplet - triplet transfer predominates because excited singlet states are brief.

The mechanisms by which energy transfer may occur can be broadly grouped into radiative and non-radiative processes.

i) Radiative

The acceptor absorbs light emitted by the donor. To do this the absorption spectrum of the acceptor must overlap the emission spectrum of the donor.

ii) Non-radiative

Non-radiative processes are of three types.

a) Resonance Excitation Transfer

By a mechanism which is thought to be due to dipole - dipole interaction, a donor molecule can transfer its excitation energy over distances of 5 to 10 nm.

b) Exchange Energy Transfer

In this type of energy transfer, the electron clouds of the excited donor and acceptor molecules overlap. The energy transfer involves an excited electron moving from the donor to the acceptor. This is a short range interaction (1 to 1.5 nm).

c) Energy Transfer in Collisions

When diffusion is rapid i.e. gas to solid surface, energy transfer can occur as a result of collisions between donor and acceptor molecules.

B. Excimer Emission Spectra

Excimers[8,9] are complexes of electronically excited molecules with molecules of the same species in their ground state. Excimer complexes may be intermolecular or intramolecular and can only exist in the excited state from which they dissociate into monomers upon radiative or radiationless deactivation. Their most prominent feature is that their emission spectra is a broad and characterless fluorescence band shifted to lower frequencies relative to the molecular fluorescence.

Yanari [10] was the first to suggest that the fluorescence of polystyrene might be of the excimer type. Some diphenyl and triphenyl alkanes[11] and vinyl polymers[12] were also shown to have intramolecular excimer fluorescence.

Hirayama[10] observed that excimers are formed in diphenyl and triphenyl alkanes only if the interacting benzene rings are separated by three carbon atoms. This has been confirmed for chromophores other than benzene rings[13,14].

The probable excimer structure in polystyrene is of the 1,3-diphenyl propane type[8].

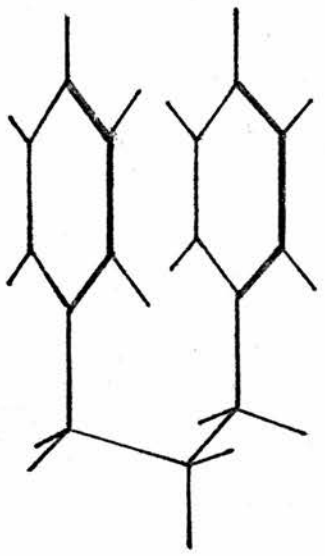

2. Photochemical Processes

The energy of photons can be sufficient to break single bonds and hence induce chemical reactions. These include formation of free radicals, photoinitiations, cyclisation, intermolecular and intramolecular rearrangements and fragmentations.

II Photo-oxidation Reaction Monitoring

When oxygen is introduced into the photoactivation and subsequent photodegradation steps, the processes involved become more complicated. Attempts to monitor the photo-oxidation reaction fall into three main groups. Each can be a useful tool when checking weatherability.

1. Changes in Physical Properties

By watching the change of ultra-violet and infra-red spectra, a picture of the reaction can be built up. Similarly, changes in molecular weight and mechanical properties aid mechanistic investigations.

2. Product Analysis

If a polymer produces easily detectable products, an accurate measure of polymer breakdown can be made. However, in many cases, attempts to produce sufficient initial product for analysis can result in complication by secondary reactions.

3. Oxygen-Uptake

This is a technique whereby the amount of oxygen taken up by a polymer is correlated with the extent of reaction. Most methods employ either manomeric or volumetric determinations and, depending on the sensitivity, very useful data can be obtained.

The combination of results from all three methods provides a comprehensive examination of the reactions involved.

III Reactivity of Polymers

The way in which a polymer reacts is dependent on several factors.

1. Chemical Structure

Pure polymers vary widely in stability on exposure to similar environments and it is this variation which is due primarily to chemical structure. The strength of a polymer lies in its weakest bond and rupture of this leads to ultimate deterioration. The rate of oxidation is usually dependent on the

strength of a carbon/hydrogen bond in the polymer. How easily the hydrogen is abstracted depends on its structural environment and should follow the normal order of carbon/hydrogen bond strengths. Take for example the stability series of polystyrene > polyethylene > polypropylene.

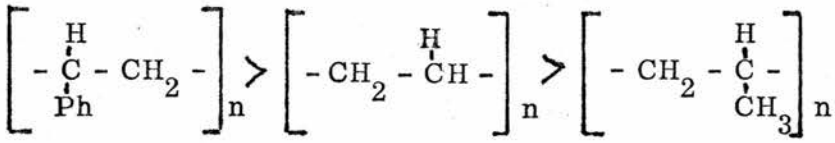

The order of polyethylene and polypropylene comes as no surprise. The labile hydrogens are respectively secondary and tertiary and, as could be predicted, the tertiary hydrogen is more easily abstracted. However the placement of polystyrene at first sight appears wrong. As with polypropylene there is only one labile hydrogen but removal of this from polystyrene would give a resonance stabilised benzylic radical and hence enhance the reaction.

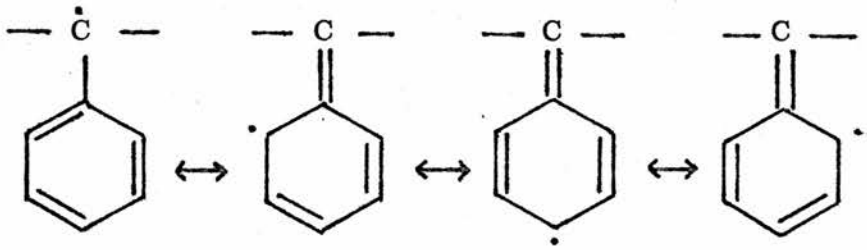

Attempts to explain this effect[15,16] have been that ;

a) The phenyl shields the benzylic hydrogen and prevents abstraction.

b) There is a loss of resonance if the phenyl groups are incorrectly orientated.

There is further support[16] for the shielding theory in the thermal oxidative stability series polystyrene > poly (3-phenyl - 1 - propene) > poly

(4 - phenyl - 1 - butene) > poly (6 - phenyl - 1 - hexene) ;

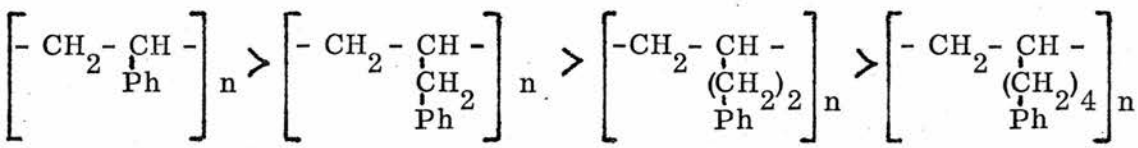

2. Physical Structure

Whether a polymer is in an ordered or disordered physical state effects its stability. Many polymers exist in a semicrystalline state which contains both ordered crystalline and disordered amorphous areas[17,18]. It is thought[19,20] that it is in the amorphous parts that oxidation occurs most readily. The crystalline area is either impermeable to oxygen or the oxidation rate is hindered by diffusion control.

3. Polymer State

The mechanism of reaction can be altered markedly by changing from the solid state to solution. A reactive species formed in solution has far more mobility that its solid state counterpart and has also the possibility of interaction with the solvent. In both cases diverging mechanistic routes can be visualised.

4. Polymer History

The processing a polymer receives during its production and storage can have a marked effect on its performance in use. Most industrial preparations involve high temperatures without adequate exclusion of oxygen. This gives rise to a number of impurities in the polymer. These impurities are often chromophoric oxygen groups such as peroxides and carbonyls in the polymer backbone itself. They could also be traces of monomers, oligomers or anomolus linkages. In any case such impurities have a detrimental effect on

polymer stability and lead to an inconsistency in polymer samples.

It comes as no surprise, then, that when photo-oxidation research is carried,out there are so many conflicting results.

IV Photo-oxidation of Polystyrene

1. Reaction Sites and Consequences of Photo-oxidation

When considering pure polystyrene we have three main reaction sites for photo-oxidation. Namely the benzene ring, the tertiary benzylic hydrogen atom and the methylenic group.

To examine the interaction of these with oxygen and ultra-violet irradiation a brief look at the consequences of polystyrene photo-oxidation should be helpful. Photo-oxidation at ambient temperatures produces ;

1) Yellow colouration.
2) Loss of mechanical properties eg. embrittlement.
3) Fluorescent and phosphorescent groups.
4) Carbonyl and hydroxyl functional groups in the polymer.
5) Overall build up in the ultra-violet spectrum of the polymer.
6) Solubility decrease.
7) Carbon dioxide and water as only volatile products.

Explanations of these phenomena have been made using several initiation and subsequent reaction mechanisms.

2. Initiation Reaction

The main initiating reactions and mechanisms,which have been proposed for the photo-oxidation of polystyrene,fall into two main areas. Those in which

light of wavelengths between 200 nm and 280 nm are used and those where the wavelengths used are above 280 nm.

a) Wavelengths 200 nm to 280 nm

The quanta of these wavelengths can be directly absorbed by pure polystyrene, but their energy is far greater than that associated with sunlight. Any suggested mechanism, therefore, for weathering thus accelerated must be considered with this in mind. The main theories so far postulated are as follows.

i) Direct Bond Break

Grassie and Weir[21] suggest that light of wavelength 253.7 nm is directly absorbed by the benzene rings of polystyrene in a $\pi \longrightarrow \pi^*$ transition. The energy corresponding to 253.7 nm quanta is 468 k J mol^{-1}. The bond strengths of the C - H bonds in polystyrene are, in the benzene ring, 435 k J mol^{-1}, in the secondary methylenic groups, 318 k J mol^{-1} and in the tertiary benzylic bonds, 297 k J mol^{-1}. The latter being lower due to the possibility of benzylic resonance stabilisation. The energy which is absorbed is then thought to be transmitted intramolecularly from the benzene rings to break the relatively weak tertiary C - H bond uniquely. The low quantum yield (approximately 8×10^{-2}) is explained because this dissociation affords only a small dispersion route for the absorbed energy. This theory is supported by E.S.R. work[22] and by studies of deuterated polystyrene[15].

ii) Reaction with Singlet Oxygen

When molecular oxygen ($^3\Sigma g^-$) is excited it can give rise to two excited

singlet molecules, ($^1\Delta$ g) and ($^1\Sigma$ g^+) which lie 0.98 e.v., (94.5 k J mol $^{-1}$) and 1.63 e.v., (157 k J mol $^{-1}$) respectively above the ground state. In this excited form singlet oxygen has quite significantly different properties from those of the ground state[23,24,25]. The theory of oxidation of polymers by singlet oxygen has been applied previously to polyethylene[26,27] and polybutadiene[28,29,30] and more recently to polystyrene[30,31]. Ranby et al.[6,31] suggest that when polystyrene's benzene rings or phenyl/oxygen charge transfer complexes are excited they can, by energy transfer, generate singlet oxygen (equations 1a and 1b).

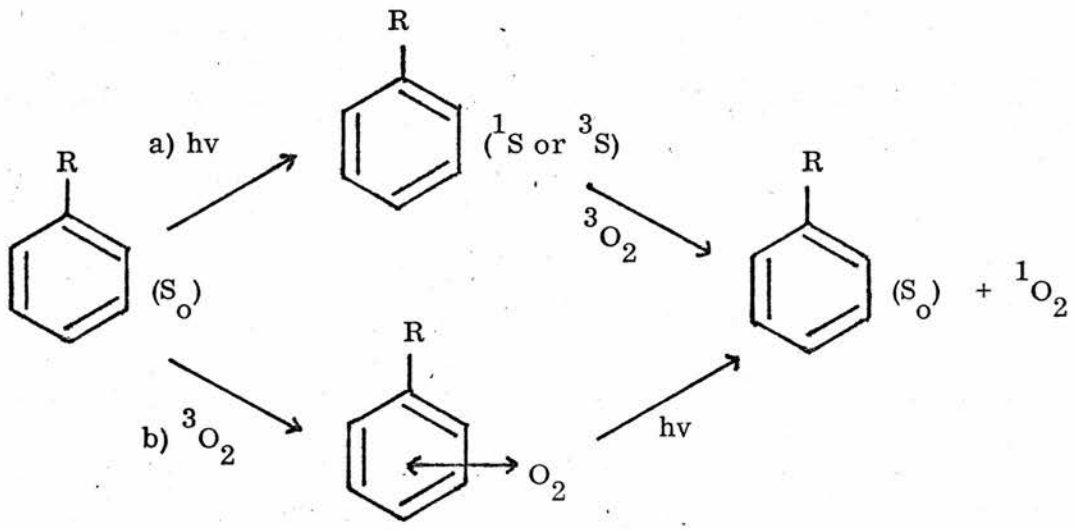

This singlet oxygen then attacks the tertiary carbon/hydrogen bond to produce hydroperoxides or abstract a hydrogen atom (equations 2a and 2b).

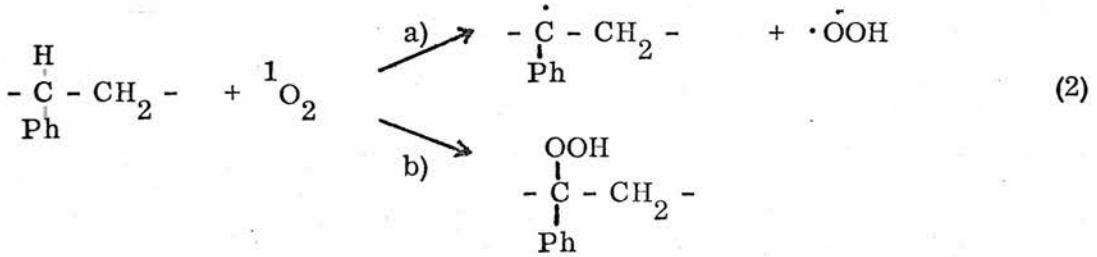

iii) Reactions with Ozone and Atomic Oxygen

Ozone

Kwei[32] has observed the formation of ozone from oxygen under 253.7 nm light. Although the concentration is low, oxidative degradation can be initiated by ozone attack on the polymer. The reactions of polyolefins[33,34] and polystyrene itself[35,36] with ozone in the absence of light have been studied. During the reaction polystyrene becomes brittle and coloured. This is attributed to crosslinking and oxidative degradation at the polymer's surface. The reaction produces carbonyl, peroxide and carboxyl groups. Polystyrene can initially undergo two reactions with ozone. These are ozonolysis of the aromatic ring and attack on the tertiary benzylic hydrogens to give peroxyl and hydroxyl radicals (equations 3a and 3b).

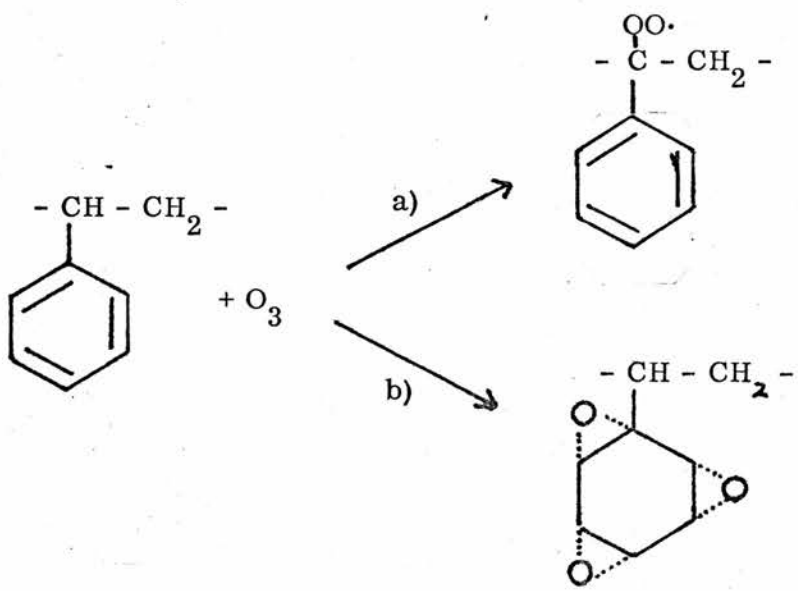

(3)

Atomic Oxygen

The weak $O-O_2$ bond in ozone can break under exposure to near-ultraviolet or visible light to form atomic oxygen[37] (equation 4).

$$O_3 + h\nu \longrightarrow O_2 + O \qquad (4)$$

Atomic oxygen is then thought to undergo a hydrogen abstraction reaction on the polymer surface[6] (equation 5).

$$PH + O \longrightarrow \dot{P}\cdot + \cdot OH \qquad (5)$$

iv) Miscellaneous Impurities

If the polymer is impure, whether the impurity is built into the polymer or not, any energy source might cause the formation of reactive species and initiate degradation. This route for photo-oxidation is probably more relevant when dealing with industrially prepared polymers or wavelenghts of less energy.

b) Wavelengths greater than 280 nm

At these wavelengths pure polystyrene should not absorb energy directly. It is, however, these wavelengths that more closely represent natural sunlight and therefore it is in these regions we must look for more accurate accelerated weathering data. The problem now is to find out what initially absorbs the energy in the polymer to give us a photo-oxidation reaction. The main routes which have been suggested are as follows .

i) Reaction with Singlet Oxygen

As previously discussed[31] singlet oxygen is said to be produced by the action of ultra-violet irradiation on a charge transfer complex between molecular oxygen in the ground state at the benzene rings of polystyrene. Charge transfer complexes between aromatic molecules and oxygen are well known[38-43] and they have been put forward as an explanation for the apparent ultra-violet tail in the spectrum of polystyrene which extends into the near-ultra-violet region[31]. Ranby et al.[31] have proposed that it is these charge transfer

complexes which absorb light of wavelengths comparable to sunlight and hence produce singlet oxygen. This then reacts as above.

ii) Impurities

In an attempt to explain the absorption of polystyrene at these higher wavelengths Achhamer et al.[44] have suggested that when styrene polymerises photolabile and thermolabile structures are incorporated in the polymer backbone. Lawrence and Weir[45], working with polymer solutions, propose that these photolabile groups or "weak links" may be double bonds, head-to-head linkages or oxygenated structures like peroxides. A study of anomolus links in the context of thermal degradation has been carried out by Cameron[46]. These groups can absorb energy under comparatively mild conditions and produce reactive species which will initiate photo-oxidation at longer wavelengths.

iii) Reaction with Molecular Oxygen

Ingold[47] reported that molecular oxygen can abstract hydrogen directly from a hydrocarbon (equation 6).

$$RH + O_2 \longrightarrow R^{\cdot} + HO_2^{\cdot} \qquad (6)$$

This reaction is 125 to 190 k J mol^{-1} endothermic[45] depending on the strength of the R - H bond. The energy required to break a chemical bond directly is 290 - 420 k J mol^{-1} but since this energy is not readily available when longer wavelengths are employed this reaction may be possible explanation for initiation at these wavelenghts and higher temperatures.

iv) Reaction of Residual Radicals

Mesrobian[48] suggested that the initial stage in the process of ageing

was probably the formation of hydrocarbon free radicals by abstraction of a hydrogen atom on the polymer chain. This could occur by the action of free radicals left over from the polymerisation process eg. a catalyst molecule or fragment (Scheme 1).

SCHEME 1

$$\text{PHOTOSENSITIVE RADICAL} + h\nu \longrightarrow \text{RADICAL}$$

$$\text{RADICAL} + \text{POLYMER} \xrightarrow[\text{abstraction}]{\text{hydrogen}} \text{POLYMER RADICAL} \downarrow \text{PHOTO-OXIDATION REACTION}$$

v) End-of-Chain Phenyl Alkyl Ketone Groups and 'Norrish Type' Reactions

From phosphorescence and spectral analysis, George et al.[49] concluded that the industrial polymerisation process involves the formation of peroxide links which then decompose to give phenyl alkyl ketone end groups (Scheme 2).

SCHEME 2

$$-CH_2-\underset{Ph}{\overset{}{CH}}\cdot \xrightarrow{O_2} -CH_2-\underset{Ph}{\overset{O-O\cdot}{CH}}$$

$$\downarrow \text{NORMAL POLYMERISATION}$$

$$-CH_2\overset{O}{\overset{\|}{C}}\underset{Ph}{} + HOCH_2-\underset{Ph}{CH}- \xleftarrow{E_a} -CH_2-\underset{Ph}{CHOOCH_2}-\underset{Ph}{CH}-$$

$$150\ \text{kJ mol}^{-1}$$

When ketones decompose photochemically they can split in three ways[50, 51].

1) 'Norrish Type 1' Reaction (equations 7a and 7b)

$$R\overset{O}{\overset{\|}{C}}R' + h\nu \xrightarrow{a)} R\overset{O}{\overset{\|}{C}}\cdot + R'\cdot \qquad (7)$$

$$\xrightarrow{b)} R'\overset{O}{\overset{\|}{C}}\cdot + R\cdot$$

This reaction becomes more selective as the energy of the quantum decreases.

2) 'Norrish Type II' Reaction (equation 8)

$$R_2CHCR_2\overset{O}{\overset{\|}{C}}R_2CR' + h\nu \longrightarrow CR_2=CR_2 + \underset{\text{ENOL}}{CR_2=CR'OH} \qquad (8)$$

It is suggested that this reaction goes via a six-membered intermediate. The resultant enol converts to its keto form.

3) 'Norrish Type III' Reaction

A further reaction has been suggested which not only involves a split but also a transfer of a β - hydrogen atom (equation 9).

$$CH_3\overset{O}{\overset{\|}{C}}\overset{H}{\overset{|}{C}}(CH_3)_2 + h\nu \longrightarrow CH_3\overset{O}{\overset{\|}{C}}H + CH_2=CH-CH_3 \qquad (9)$$

This however is negligible at wavelengths comparable to sunlight.

The suggested initiation step which George et al.[49] propose is that these end-of-chain ketones degrade by the 'Norrish type II' mechanism (equation 10).

$$-CH_2\underset{Ph}{\overset{|}{C}}HCH_2\overset{O}{\overset{\|}{C}}\underset{Ph}{\overset{|}{C}} \xrightarrow{h\nu} -CH=\underset{Ph}{\overset{|}{C}}H + CH_3\overset{O}{\overset{\|}{C}}\underset{Ph}{\overset{|}{C}} \qquad (10)$$

The resultant ketone, when excited in a $n \rightarrow \pi^*$ transition[52], can produce singlet oxygen by energy transfer[31] (equation 11a). This can then react with the carbon double bonds to form hydroperoxides (equation 12). The ketone can also undergo a photoreduction reaction by abstracting a hydrogen from an adjacent polystyrene chain (equation 11b).

$$CH_3\overset{O}{\overset{\|}{C}}Ph + h\nu \xrightarrow{a)} CH_3\overset{O^*}{\overset{\|}{C}}Ph \xrightarrow{+{}^3O_2} CH_3\overset{O}{\overset{\|}{C}}Ph + {}^1O_2 \qquad (11)$$

$$\xrightarrow[+RH]{b)} CH_3\dot{C}PhOH + R\cdot$$

$$-CH = CHPh + {}^1O_2 \longrightarrow -CH_2 - \overset{OOH}{\overset{|}{C}}-Ph \qquad (12)$$

3. Propagation Reaction

To date, theories of photo-oxidation of polymers have been based on the mechanisms proposed by Bolland and Gee[53, 54, 55] for the oxidation of olefins. In the case of polystyrene, post initiation hydroperoxides are most probably involved in the propagation steps[56]. The photo-oxidation reaction can be initiated by a variety of chemical and physical means as seen above and the full reaction now becomes that shown in scheme 3.

SCHEME 3

INITIATION	$P-H \longrightarrow P\cdot + H\cdot$	(1)
PROPAGATION	$P\cdot + O_2 \longrightarrow PO_2\cdot$	(2)
	$PO_2\cdot + PH \rightarrow PO_2H + P\cdot$	(3)
TERMINATION	$2P\cdot \longrightarrow$	(4)
	$2PO_2\cdot \longrightarrow$ INACTIVE PRODUCTS	(5)
	$PO_2\cdot + P\cdot \rightarrow$	(6)

Macroradicals produced in step (1) of scheme 3 can easily react with oxygen to form peroxyl radicals. Investigation of low molecular weight radicals shows that the rate of oxygen addition depends on the radical's structure[57]. It is also thought that the addition of oxygen to radicals involves a polar transition state[57] (equation 13).

$$R\cdot + O_2 \longleftrightarrow \left[R^{+}\,{}^{-}O\text{-}O\cdot\right] \longleftrightarrow RO_2\cdot \qquad (13)$$

An alternative reaction of the macroradical is hydrogen abstraction but in the case of a benzylic radical this is 10^{10} times slower than combination with oxygen[57].

Step (3) of scheme 3 involves the abstraction of hydrogen by a peroxyl radical. The peroxyl radicals are strongly resonance stabilised and are relatively selective electrophilic species. They therefore abstract tertiary hydrogen atoms in preference to secondary or primary. Abstraction reactions are strongly dependent on activation energy and are sensitive to steric and polar effects especially in solution[58].

A retardation reaction is visualised by Hendry[59] if the macroradical reacts very slowly to form the peroxyl radical in step (2) of scheme 3. This may lead to premature termination by a radical combination step giving the peroxide (equation 14).

$$P\cdot + PO_2\cdot \longrightarrow POOP \qquad (14)$$

4. Decomposition of Hydroperoxides and Chain Branching

The hydroperoxide formed in steps (2) and (3) of scheme 3 can, under light irradiation, decompose. Hydroperoxide decomposition has been investigated by a number of workers[60, 61]. The hydroperoxide group can decompose by homolytic scission in three places, a), b) and c).

$$R \overset{a)}{\text{---}} O \overset{b)}{\text{---}} O \overset{c)}{\text{---}} H$$

The bond strengths are, from left to right, 293, 178 and 376 k J mol^{-1} [62]. The weakest bond is therefore the (- O - O -) bond, b), which will undergo

scission in preference to the others. Such scissions give rise to an alkoxyl radical (RO·) and a hydroxyl radical (· OH) which then take part in a chain branching step (scheme 4).

SCHEME 4

$$POOH \longrightarrow PO\cdot + \cdot OH$$

$$PO\cdot + PH \longrightarrow POH + P\cdot$$

$$HO\cdot + PH \longrightarrow P\cdot + H_2O \qquad \text{etc.}$$

These reactions produce alcohols, water and polymer radicals capable of reaction with oxygen. Further decompositions and reactions of alkoxyl radicals have been studied[63] and fall into three main groups.

1) Abstraction of hydrogen.

2) Combination with radicals.

3) β scission to give ketones and radicals.

When considering polystyrene the most likely position of the hydroperoxide is on the tertiary benzylic carbon atom[21, 64]. Its model compound would be cumene hydroperoxide.

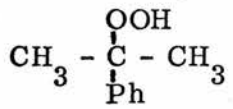

Its reaction with light and subsequent decomposition have been studied[50] and follows reaction scheme 5.

SCHEME 5

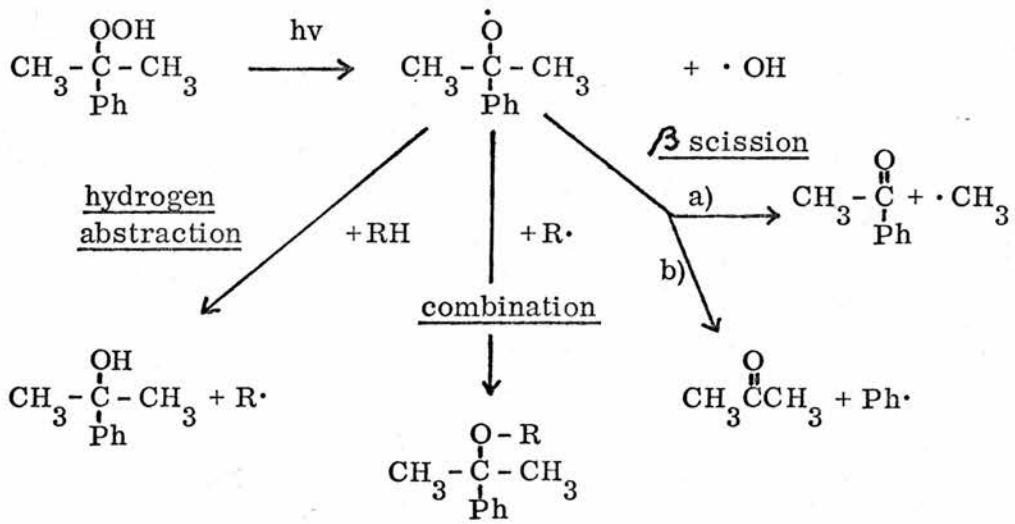

Walling[63] has studied the competing reactions of hydrogen abstraction and β scission in alkoxyl radicals. He points out that the β scission reaction b) in scheme 5 is extremely unlikely and proposes that the conjugative stability of acetophenone in the transition state ensures that reaction a) in scheme 5 is predominant. He also suggests that there is a considerable polar contribution to the transition state in β scission (equation 15).

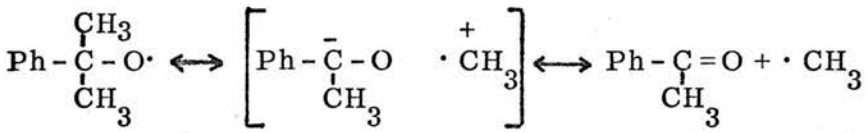

(15)

The terminal acetophenone structure has been observed in polystyrene photo-oxidation and is thought to be responsible for phosphorescence in photo-oxidised polystyrene[21, 56, 65, 66].

Subsequent reactions of the carbonyl group involves 'Norrish type' processes[50, 51] or photoreduction and products include carbon monoxide formed by the reaction of 'hot' radicals resulting from a 'Norrish type I' scission[50] (equation 16).

$$R'-\overset{\overset{O}{\|}}{C}-R \xrightarrow{h\nu} \left[R-\overset{\overset{O}{\|}}{C}\cdot\right]^{HOT} + R\cdot \qquad (16)$$

$$\downarrow$$

$$R'\cdot + CO$$

5. Termination Reaction and Products

Termination of the reaction involves combination of radicals to form inactive products. Which radicals actually take part depends on radical mobility and availability of oxygen. For example, in polymer films, large radicals are unlikely to be able to diffuse and find other macroradicals. It is therefore up to smaller radicals to terminate the reaction. Also,at high oxygen partial pressure,surface radicals are liable to be mostly peroxyl radicals and termination is a combination of these. This combination could involve stable cyclic peroxides or epoxides if peroxyl radicals are adjacent. It is also possible that scission and crosslinking may occur simultaneously. It has been postulated that crosslinking is responsible for the observed embrittlement and decrease in solubility[21]. However,if the radical centre were at the chain ends,we would expect the combination to produce an increase in molecular weight and a corresponding decrease in solubility.

The yellowing, infra-red bands and ultra-violet build up which are noticed in photo-oxidised polystyrene have been attributed to several chemical structures. They include, when oxygen is present, quinomethanes[44], benzalacetophenone[15], acetophenones[21, 56, 65, 66] and conjugated dialdehydes formed by ring opening of benzene[31]. Grassie and Weir[67] found that the yellow colouration appeared even in vacuum and explained this by proposing conjugated carbon-carbon unsaturation as the cause of colouration. An explanation was put forward by Ranby et al.[31] that what actually was happening was isomerism

of the benzene ring to fulvene and benzvalene.

Phosphorescence in photo-oxidised polystyrene has been attributed to acetophenone type structures and fluorescence to a trans-stilbene type structure[68].

Grassie and Weir have found that water and carbon dioxide are the major volatile products[21]. It can easily be seen, from reactions mentioned above, that water should be formed but no suitable explanation has been found for the presence of carbon dioxide in such large quantities.

CHAPTER 2

EXPERIMENTAL

1 Synthesis of the Copolymers

The copolymers used in this work were originally prepared by Richards and co-workers[69]. Their technique was based on the 'living' polymer method of polymerisation developed by Szwarc[70,71] and was chosen because it gave good structure control and purity. Richards et al.[69] found that monomers which were capable of anionic polymerisation could also form regular copolymers when reacted with an alkali metal in the presence of linking agents such as alkyl dihalides. The method involved the production of an initiating dianion ($^{-}M-M^{-}$) from a vinyl monomer (M) by the reaction of an alkali metal or alkali metal alloy. Subsequent reaction with a dihalide (X-R-X) yielded regular copolymers with the repeat unit (-M-M-R-).

The copolymers under consideration in this thesis were prepared using styrene as the vinyl monomer and lithium as the alkali metal. Four copolymers were prepared using the dibromides of methane, propane, butane and p-xylene. The reaction can be formulated as shown in scheme 6 overleaf.

SCHEME 6

$$2\,CH_2{=}\underset{Ph}{CH} + 2\,Li \longrightarrow 2\,Li^+ + 2\,CH_2{=}\overset{-}{\underset{Ph}{C}}H$$

$$2\,CH_2{=}\overset{-}{\underset{Ph}{C}}H \longrightarrow \overset{-}{\underset{Ph}{C}}H-(CH_2)_2-\overset{-}{\underset{Ph}{C}}H$$

$$\overset{-}{\underset{Ph}{C}}H-(CH_2)_2-\overset{-}{\underset{Ph}{C}}H + Br-R-Br \longrightarrow \overset{-}{\underset{Ph}{C}}H-(CH_2)_2-\underset{Ph}{CH}-R-Br + Br^-$$

$$\overset{-}{\underset{Ph}{C}}H-(CH_2)_2-\underset{Ph}{CH}-R-Br + \overset{-}{\underset{Ph}{C}}H-(CH_2)_2-\overset{-}{\underset{Ph}{C}}H \longrightarrow \overset{-}{\underset{Ph}{C}}H-(CH_2)_2-\underset{Ph}{CH}-R-\underset{Ph}{CH}-(CH_2)_2-\overset{-}{\underset{Ph}{C}}H$$

The reaction in scheme 6 thus produces a polymer with the repeat unit,

$$-\left[\underset{Ph}{CH}-(CH_2)_2-\underset{Ph}{CH}-R\right]-$$

where $R = CH_2$ for the methane/styrene copolymer,

$R = (CH_2)_3$ for the propane/styrene copolymer,

$R = (CH_2)_4$ for the butane/styrene copolymer,

and $R = CH_2-Ph-CH_2$ for the p-xylene/styrene copolymer.

i) Purification of Materials

Styrene monomer was shaken with sodium hydroxide to remove the stabiliser and then washed several times with distilled water. It was dried, by standing over molecular sieves and magnesium sulphate, before being distilled under vacuum. The styrene monomer could then be kept over long periods in a refrigerator at $-15^{\circ}C$.

Dibromomethane, 1,3-dibromopropane and 1,4-dibromobutane were dried over molecular sieves and purified by vacuum distillation.

α, α' - Dibromo-p-xylene was recrystallised from benzene.

Lithium used in the preparation was washed in petroleum ether and then ethanol.

The solvent, tetrahydrofuran (T. H. F.), was purified by the addition of lithium aluminium hydride and finally by distillation. Sodium wire was added to the T. H. F. to ensure that it remained dry.

ii) Experimental Method

The lithium metal (0. 8 mol) in the form of 0. 5 mm diameter wire was added to the T. H. F. (500 ml), while it was being stirred under nitrogen, in a one-litre three necked round bottomed flask. After a few minutes a mixture of styrene (0. 4 mol) and dihalide (0. 2 mol) in T. H. F. (20 ml) was added. The reaction was allowed to proceed for about four hours during which time the solution became opaque due to the formation of lithium bromide. The temperature of the reaction was not rigorously controlled but an ice-water bath was kept around the flask, and the temperature inside the flask did not exceed 30^{o}C. After four hours the excess lithium was removed from the flask and the solution filtered. The solution was placed in a dropping funnel and allowed to drip slowly into a beaker containing four litres of methanol which was being agitated by a vibrating stirrer. The methanol was cooled in an ice bath as uncooled precipitation gave 'sticky', difficult-to-dry, polymers. The polymers which precipitated as fine white powders were filtered and dissolved in methylene chloride and the precipitation procedure in cold methanol repeated three times. After filtration, the polymer was placed in a vacuum oven at room temperature

for two weeks to remove any solvent still remaining. The yields ranged between 50 and 55%. The polymers were stored in a dessicator when not in use.

2 Characterisation of the Copolymers

i) Microanalysis

A microanalysis was performed on each copolymer to determine the carbon and hydrogen content. The results of the analyses are shown in table 1.

Table 1

CO-POLYMER	COMPOSITION			
	THEORETICAL		EXPERIMENTAL	
	% C	% H	% C	% H
P-XYLENE/STYRENE	92.3	7.7	91.55	7.36
METHANE/STYRENE	91.89	8.11	91.56	8.11
PROPANE/STYRENE	91.20	8.80	90.64	8.73
BUTANE/STYRENE	90.91	9.09	90.25	9.05

Since the theoretical compositions of the copolymers are very similar to each other, and the error in the analysis for each element is 0.3%, the micranalyses do not yield much information on the characterisation of each copolymer. They do,however,show that the sum of the carbon and hydrogen percentages in each case is very close to 100%, indicating that very little impurity can be present.

ii) Infra-red Spectroscopy

The infra-red spectra of the copolymers were recorded on a Perkin - Elmer 257 grating infra-red spectrophotometer. A film of each copolymer on

a sodium chloride disc was obtained by evaporating off the solvent from solutions of the copolymers in spectroscopic carbon tetrachloride. The spectra of the copolymers derived from aliphatic dihalides were all very similar to the spectrum of polystyrene except for the relative intensities of the peaks, which changed as the proportion of methylene groups in the repeat unit changed[72]. In the case of the p-xylene/styrene copolymer there were slight differences in the 2000 - 1600 cm^{-1} and 950 - 650 cm^{-1} regions which showed the presence of the para disubstituted benzene ring[73]. Three additional peaks also occurred. They were at 1515 cm^{-1} (medium), 1420 cm^{-1} (very weak) and 1035 cm^{-1} (weak). They remain unidentified but must have been associated with the inclusion of the p-xylene grouping in the main chain.

iii) Nuclear Magnetic Resonance Spectra

^{1}H n.m.r. spectra of the copolymers were recorded using a Varian HA 100 100 M.Hz. n.m.r. Samples were run at 70°C to increase peak resolution. Spectroscopic deuterated chloroform was used as solvent and chemical shifts were measured relative to tetramethylsilane as internal standard.

Each spectrum had the same general characteristics. An aromatic region at about 3 τ and an aliphatic region between 7 and 9 τ. By measuring the ratio of the aliphatic to aromatic protons and comparing the results with the theoretical values based on the assumption of the repeat unit described previously, the characterisation of each copolymer was possible. This ratio was calculated for each copolymer and is shown in Table 2, together with the theoretical values and the experimental results obtained by Richards and

coworkers[69] and Paterson[74].

Table 2

CO POLYMER	ALIPHATIC : AROMATIC RATIO			
	THEORY	RICHARDS	PATERSON	EXPERIMENTAL
P-XYLENE/STYRENE	0.71	—	—	0.72
METHANE/STYRENE	0.80	0.80	0.70	0.80
PROPANE/STYRENE	1.20	1.18	1.10	1.16
BUTANE/STYRENE	1.40	1.35	1.33	1.41

The agreement between the theoretical and experimental values was close and thus supported the assumption of the repeat units of the copolymers. On the basis of several readings for each copolymer, Richards et al.[72] assigned the aliphatic peaks in the ^{1}H n.m.r. spectra to the different proton environments present in each repeat unit. Table 3 shows these results with the assigned protons underlined.

Table 3

AVERAGE τ VALUE	ASSIGNMENT	PEAK NO.
8.40	$-CHPh-\underline{CH_2}-CHPh-$	1
8.70	$-\underline{CH_2}-CHPh-$	2
9.00	$-CH_2-\underline{CH_2}-CH_2-$	3
7.80	$-CH_2-\underline{CH}Ph$	4

These average τ values can be compared with the experimentally measured values for the copolymers in table 4. The numbers in brackets after the τ values refer firstly to the number of protons represented and secondly to the corresponding peak numbers of table 3.

Table 4

COPOLYMER	VALUES OF ALIPHATIC PEAKS
P-XYLENE/STYRENE	7.38(4,-), 7.79(2,4), 8.52(4,2)
METHANE/STYRENE	7.72(2,4), 8.45(2,1), 8.90(4,2)
PROPANE/STYRENE	7.81(2,4), 8.71(8,2), 9.13(2,3)
BUTANE/STYRENE	7.80(2,4), 8.68(8,2), 9.06(4,3)

The only aliphatic peak which could not be accounted for is that at 7.38 τ in the p-xylene/styrene copolymer. This was due to the methylene groups adjacent to the main chain benzene ring.

The aromatic region of the spectra for the copolymers is shown in table 5. The numbers in brackets are the number of protons corresponding to each peak.

Table 5

COPOLYMER	VALUES OF AROMATIC PEAKS
P-XYLENE/STYRENE	2.93(6), 3.14(4), 3.39(4)
METHANE/STYRENE	2.92(6), 3.31(4)
PROPANE/STYRENE	2.87(6), 3.10(4)
BUTANE/STYRENE	2.90(6), 3.06(4)

All but the p-xylene/styrene copolymer had two peaks. Bovey et al.[75] ascribed the peak at lower field to the meta - and para - hydrogens and the peak at higher field to the ortho - hydrogens in the pendant benzene rings of polystyrene. The shift to higher field in the case of the ortho protons was explained as a result of the increased shielding experienced when adjacent phenyl groups are orthogonal to one another.

The p-xylene/styrene copolymer showed three peaks in the aromatic region. The new peak had to be associated with the main chain aromatic protons. It was, however, difficult to assign the peaks. It has been observed[72,74] in the series of copolymers of repeat unit $-\left[\text{CHPh}-(\text{CH}_2)_2-\text{CHPh}-(\text{CH}_2)_n\right]-$ that as n increases the two peaks which arise from the pendant phenyl group protons gradually merge. This can also be seen in table 5 where there are examples of n = 1, 3 and 4. It seems likely that the inclusion of the group $-\text{CH}_2-\text{Ph}-\text{CH}_2-$ would decrease the separation of the peaks compared to that in the methane/styrene copolymer. The peak at 3.39 γ was therefore assigned to the main chain benzene ring protons.

iv) Ultra-violet Spectrometry

Ultra-violet spectra of the copolymers in spectroscopic cyclohexane were recorded on a Unicam SP 800 grating ultra-violet spectrophotometer. Since the Θ point for polystyrene in cyclohexane is approximately 34°C, samples were thermostated at 40°C in the spectrophotometer. The spectra of the copolymers all have absorption maxima at 260 nm, although the maximum absorption for polystyrene is at 262 nm. With the exception of the p-xylene/

styrene copolymer they all have the same form of fine structure as polystyrene. The absorption is below 290 nm and is due to electrons in the π orbitals of the benzene ring being excited to the π^* level. The fine structure arises from the vibrational sublevels which accompany the transitions.

The p-xylene/styrene copolymer has an extra peak at 274 nm which is due to the para-disubstituted benzene[76,77].

The optical densities of the copolymers were measured for the spectral peaks and the extinction coefficients were calculated using the relationship,

$$\text{Extinction coefficient} = \frac{\text{Optical density}}{\text{Concentration}\left(\begin{array}{c}\text{mol of repeat}\\ \text{unit per litre}\end{array}\right) \times \text{Path length (cm)}}$$

Table 6 gives the calculated extinction coefficients for the peaks in the region 240-280 nm with p-xylene, benzene and toluene[77] for comparison.

Table 6

WAVELENGTH (nm)	243	249	254	256	260	262	265	269	274
COMPOUND	EXTINCTION COEFFICIENTS								
BENZENE	110	190	-	-	170	-	-	11	-
P-XYLENE	100	220	240	280	420	360	580	620	760
TOLUENE	-	120	180	190	215	260	175	240	-
POLYSTYRENE	94	135	181	180	208	212	175	166	-
METHANE/STYRENE	409	482	555	552	573	558	462	415	-
PROPANE/STYRENE	193	266	347	341	405	399	320	306	-
BUTANE/STYRENE	236	326	412	409	468	463	365	345	-
P-XYLENE/STYRENE	414	503	614	612	710	692	655	594	321

Since the repeat units contain different numbers of benzene rings, table 7 shows the extinction coefficients for the absorption maxima and the last column shows the extinction coefficient per benzene ring.

Table 7

POLYMER	EXTINCTION COEFFICIENT	
	AT ABSORPTION MAXIMA	PER BENZENE RING IN REPEAT UNIT
POLYSTYRENE	212	212
METHANE/STYRENE	573	286.5
PROPANE/STYRENE	405	202.5
BUTANE/STYRENE	468	234
P-XYLENE/STYRENE	710	236.7

The high extinction coefficient of the methane/styrene copolymer relative to the others cannot be easily explained. The effect has also been observed[78] for the n = 1 copolymer in the series of copolymers with repeat unit $-\left[CCH_3Ph-(CH_2)_2-CCH_3Ph-(CH_2)_n \right]-$. It was explained by the fact that overlap was occuring between the band under consideration and a more intense band which existed for the main part at a shorter wavelength. It was supposed that the n = 1 copolymer existed in preferred configurations which overlapped to give a breakdown in fine structure and an increase in absorption intensity. The methane/styrene copolymer, however, showed no breakdown in fine structure compared to the other copolymers. The phenomenon must be due to the preferred configurations of the benzene rings in the copolymer but no absolute

explanation could be found.

v) Excimer Emission Spectra

Fluorescence spectra of films of the copolymers were carried out on a Perkin Elmer Hatachi MPF - 2A spectrofluorimeter. The methane/styrene copolymer was the only one to show any excimer emission. This was to be expected as it is the only copolymer which had the 1,3-diphenyl propane type structure. Table 8 shows the wavelengths of the excimer fluorescence (V_E^{MAX}) and the normal molecular fluorescence wavelength (V_M^{MAX}) of the methane/styrene copolymer, polystyrene[12] and 1,3-diphenyl propane[11].

Table 8

COMPOUND	V_E^{MAX} (cm^{-1})	V_M^{MAX} (cm^{-1})
1,3-DIPHENYL PROPANE	30,000	35,400
POLYSTYRENE	29,900	36,000
METHANE/STYRENE	31,850	-

vi) Molecular Weight

In their work on the copolymers, Richards and coworkers[79] reported that the molecular weights of the samples obtained by the method described previously, were of the order of 10,000. This was not verified experimentally.

3 The Photo-oxidation Apparatus

Methods of monitoring the photo-oxidation reaction of a polymer sample were mentioned in the introduction. The main method employed in the present work was following the oxygen-uptake of a polymer sample on irradiation.

i) The Light Source

The photo-oxidation reactions of polystyrene and the copolymers mentioned are slow. Light of sufficient energy and intensity had therefore to be available if meaningful results were to be obtained quickly. The range of wavelengths of particular interest lay in the near-ultra-violet region. They had to be long enough not to be absorbed by air and short enough to effect the polymer. A 500 watt medium pressure Hanovia lamp (supplied by Engelhard) was used to fulfil these criteria. The arc is of type 509/10 and has a life of 1000 hours.

a) Stabilisation

As well as the intensity stabiliser supplied with the lamp, it was necessary to add a variable transformer ('variac') because of the fluctuating voltage experienced from the power supply. An intensity monitoring photodiode (RCA 935, S5 Response,C s-Sb) together with a photodiode power supply and current amplifier and display digital voltmeter (Solatron LM 1619 D.V.M.) were also included in the set up. By adjusting the 'variac', the intensity could be maintained at $\pm$ 2%.

b) Filters

The use of monochromatic light, via a monochromator or glass or solution filter, was not feasible as the intensity after filtering was not large enough. Instead pyrex and quartz discs were used for the wavelength range above 295 nm and the full line spectrum respectively.

c) Calibration

The medium pressure lamp emits radiation over a wide range of

wavelengths in the ultra-violet and visible regions. The main experimental facts which could be obtained from potassium ferrioxalate actinometry[80, 81] were the total output of the lamp below 450 nm, the output when pyrex or multi layers of pyrex were used as filters and the variation of these intensities with arc to sample distance. These are summarised in table 9.

Table 9

FILTER	ARC to SAMPLE DISTANCE (cm)	INTENSITY * quanta cm^{-2} sec^{-1} x 10^{-15}
NONE	29.9	7.6
NONE	33.0	6.1
NONE	35.5	5.6
NONE	39.5	4.5
NONE	52.7	2.4
PYREX DISC	27.3	4.8
PYREX DISC	29.9	4.0
PYREX DISC	35.5	3.2
3 PYREX DISCS	27.3	3.5
3 PYREX DISCS	29.9	2.9
3 PYREX DISCS	35.5	2.3

*All intensities are corrected for the inclusion of a quartz disc.

The results show that the light intensity is inversely proportional to the square of the arc to sample distance. This is in agreement with theory[82].

The validity of the makers figures for the relative line intensities were checked using the photodiode and D.V.M. system with a monochromator (high intensity U.V. grating assembly Cat. no. 33-86-01 manufactured by Bausch and Lomb). Light was passed through the monochromator and readings (V_λ) were taken on the D.V.M. for a series of wavelengths (λ) in the region 220-400 nm.

The response curve for the photodiode given by the makers showed a range of 220-640 nm with a maxima at 340 nm. This curve was used as a weighting factor for the relative line intensities. The relative line intensites over the range of wavelengths were then calculated using the relationship,

$$\text{Relative line intensities } (\lambda) \propto \frac{V_\lambda}{\text{Response factor}}$$

The largest relative line intensity was that at 365 nm and therefore all the other relative line intensities were scaled to the 365 nm having a value of 100. Values obtained experimentally, from the makers and from Calvert and Pitts[50] are tabulated in table 10.

Table 10

WAVELENGTH (nm)	RELATIVE LINE INTENSITIES		
	CALVERT AND PITTS	MAKERS	EXPERIMENTAL
222	14.0	—	7.0
232	8.0	—	9.9
236	6.0	2.8	10.6
238	8.6	5.4	10.5
240	7.3	4.9	11.5
248	8.6	12.3	17.6
254	16.6	15.8	24.3
257	6.0	1.8	25.9
265	15.3	22.8	24.4
270	4.0	5.3	19.8
274	2.7	3.9	16.3
280	9.3	12.8	15.9
289	6.0	6.0	16.5
296	16.6	17.2	28.9
302	23.9	33.0	37.5
313	49.9	63.3	57.8
334	9.3	8.6	15.8
365	100	100	100
404	42.2	26.5	—

As can be seen, there were variations in the values but the shape of the overall energy distribution was similar.

Although both the 313 nm and 365 nm line intensities were reduced by the introduction of pyrex filters, the reduction of the 313 nm line intensity was proportionally greater. The ratio of the 365 nm line intensity to the 313 nm line intensity was checked using the method described previously. The results are shown in table 11 and are corrected for the inclusion of a quartz disc.

Table 11

FILTER	RATIO OF LINE INTENSITIES 365 nm : 313 nm
NONE	1.73 : 1.0
ONE PYREX DISC	3.41 : 1.0
TWO PYREX DISCS	4.43 : 1.0
THREE PYREX DISCS	5.92 : 1.0
FOUR PYREX DISCS	8.01 : 1.0

Since the variation of the overall intensity at the sample by altering the arc to sample distance has no effect on these ratios, this provided a means of changing the relative intensity of the 313 nm line while maintaining the 365 nm line intensity at a constant value.

Table 12 shows, for each filter, the arc to sample distance necessary to maintain the 365 nm line intensity at a constant value and the relative values of the 313 nm line intensity obtained, corrected for the inclusion of a quartz disc.

Table 12

FILTER	ARC To SAMPLE DISTANCE (cm)	RELATIVE 313 nm LINE INTENSITY
ONE PYREX DISC	29.9	100
TWO PYREX DISCS	28.6	77
THREE PYREX DISCS	27.3	58
FOUR PYREX DISCS	26.4	43

To check the reliability of the photodiode and the D.V.M., the actual intensity measured by actinometry was compared to a few D.V.M. readings obtained by adjusting the 'variac'. Table 13 shows that the D.V.M. reading is proportional to the intensity at the sample for constant arc to sample distance and photodiode position.

Table 13

INTENSITY (quanta cm^{-2} sec^{-1}) x 10^{-15}	D.V.M. READING (VOLTS)
5.6	0.470
4.5	0.360
2.4	0.200

ii) Factors Influencing the Design of the Apparatus

The measurement of oxygen-uptake of polymers on irradiation has led to a number of apparatus designs[83, 84, 85]. Basically they all have a manometer system with a reaction cell attached. The main problem with any volumetric measurement is accurate temperature control. This is accentuated in polystyrene and the copolymers under investigation as very small amounts of

oxygen consumption had to be monitored due to the very slow rate of oxidation. The apparatus, therefore, had to be highly sensitive for studying the early stages of the reaction and very well thermostated. With this in mind the apparatus was made as simple and small as possible yet capable of accommodating a relatively high area of film under conditions of uniform irradiation.

It is also important that there should be no mercury contamination either in the system, due to the manometer fluid or mercury diffusion pumps, or on the films, due to the casting procedure. Since the mercury light source obviously produces lines readily absorbed by mercury vapour an internal filtering would occur with the result that the light intensity incident on the surface of the polymer would be markedly reduced. In addition, there is the much more serious possibility of the photosensitised production of ozone which would complicate the overall reaction. The absorption of 253.7 nm radiation by mercury vapour in an atmosphere of oxygen results in production of excited mercury atoms (equation 17).

$$Hg\ (6\ ^1S_o) + h\nu \longrightarrow Hg^*\ (6\ ^3P_1) \qquad (17)$$

In the absence of collisions these become deactivated by fluorescing, but oxygen quenches this fluorescence and produces atomic oxygen and ozone[86] (equations 18 and 19).

$$Hg^*\ (6\ ^3P_1) + O_2 \longrightarrow O + HgO \qquad (18)$$

$$O + O_2 + M \longrightarrow O_3 + M \qquad (19)$$

The manometer fluid chosen was silicone fluid. It has low vapour pressure, low reactivity, low absorption of ultra-violet light and gives a large

sensitivity increase compared to mercury because of its low specific gravity. Its absorption of oxygen during the reaction was minimised by ensuring that it was saturated by bubbling oxygen through it and allowing equilibriation overnight before each experiment.

iii) Photo-oxidation Apparatus and Experimental Procedure.

a) Cell A, Absorbers and Sample Holder

A diagram of cell A is shown in figure 1. The main casing and top were made out of brass because of its high thermal conductivity. During the reaction samples were irradiated from above and depending on the wavelength range required pyrex and quartz discs 1 mm in thickness were used. Silicone high vacuum grease and an O-ring were used to ensure that there were no leaks when the cell was screwed together. The indentations in the base of the casing well were for absorbers. Grassie and Weir[21] observed that under 253.7 nm irradiation carbon dioxide and water were the only volatile products obtained. Obviously any genuine oxygen-uptake measurement must allow for the evolution of gaseous products. 'Carbosorb' (B. D. H. Chemicals Ltd) and Silica gel (Crosfield Chemicals Ltd) were used as carbon dioxide and water absorbers respectively. To ensure that the absorbers were effective, the 'carbosorb' was of the self indicating type and the silica gel was kept in a vacuum oven when not in use. Excess of the absorbers was used.

The sample holder shown in figure 2 was made of brass and constructed so that several films could be stacked in it by using brass spacer rings. Holes and grooves in the holder and spacers ensured that oxygen was available at all

FIGURE 1
CELL A (SECTION)

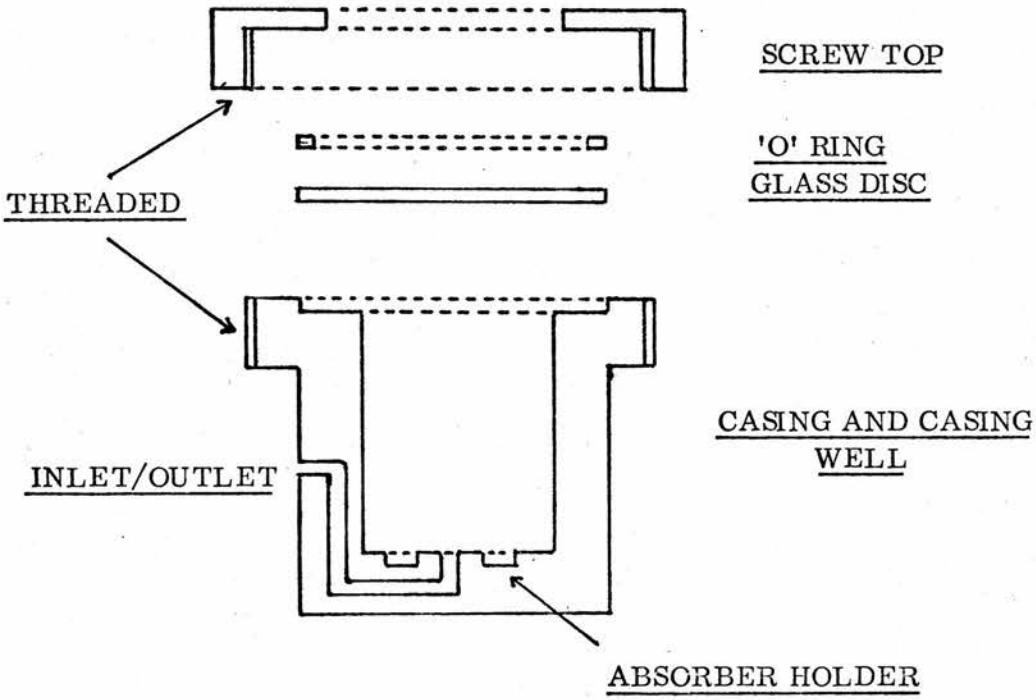

FIGURE 2
SAMPLE HOLDER (SECTION)

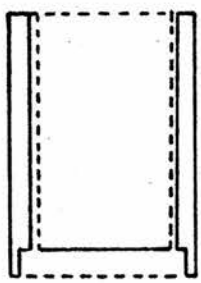

the film surfaces and any gases evolved had free access to the absorbers.

b) The Manometer System and Method of Measurement - Apparatus One

Cell A was joined to the glass manometer system, shown in figure 3, by a thin copper tube which was soldered to the cell and inserted in a rubber seal in the glassware. Copper was chosen not only for its high thermal conductivity but also for its flexibility. The manometer system consisted of two parts, the reference and the reaction sections, which could be isolated from one another by closing tap A. The apparatus was filled and evacuated through tap B by means of a two-way tap attached externally. The pumping system used was a rotary oil pump and the oxygen supply came from cylinders via a purification column filled with molecular sieves, anhydrous copper sulphate and 'carbosorb'. The manometer system was constructed of large bore capillary glass with a reference bulb C of approximately 50 ml volume. The taps were 'rotaflo' type TF6/13.

The plunger trip mechanism which made the monitoring of the reaction automatic is shown in figure 4. It consisted of two platinum wires which each had one of their ends heat - rounded to maximise electrical contact. Wire 1 was placed vertically in the manometer fluid and its unrounded end was dipped into mercury which lay on top of a glass to metal seal. The side arm on the other side of the seal also contained mercury. Silicone fluid was placed on top of the mercury to prevent any mercury vapour escaping. Wire 2 was placed vertically above the manometer fluid and its unrounded end was wrapped around a copper wire which in turn was wrapped around the lower part of a glass to metal seal

FIGURE 3

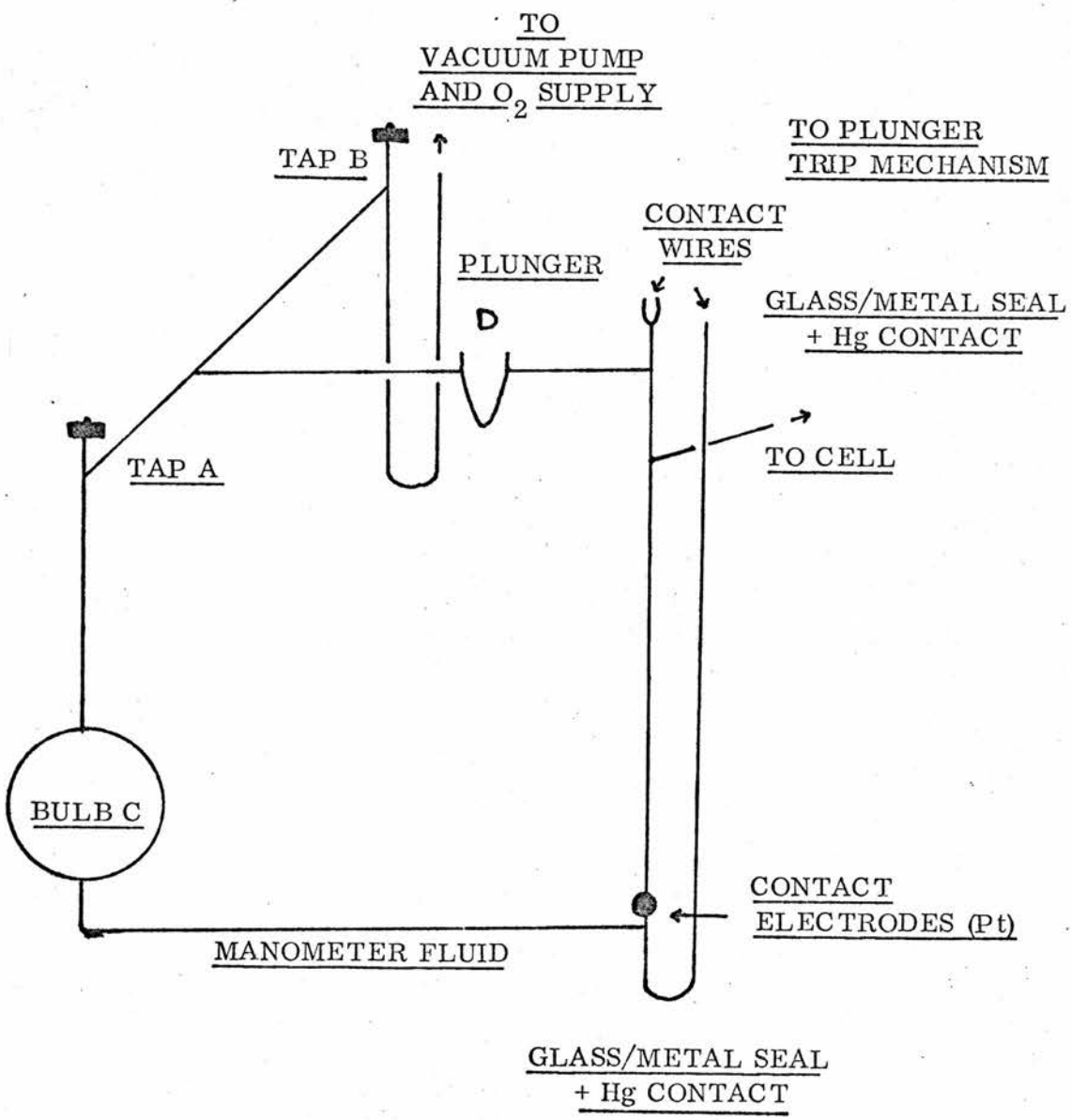

APPARATUS ONE

(AUTOMATIC)

FIGURE 4
ENLARGEMENT OF PLUNGER TRIP MECHANISM

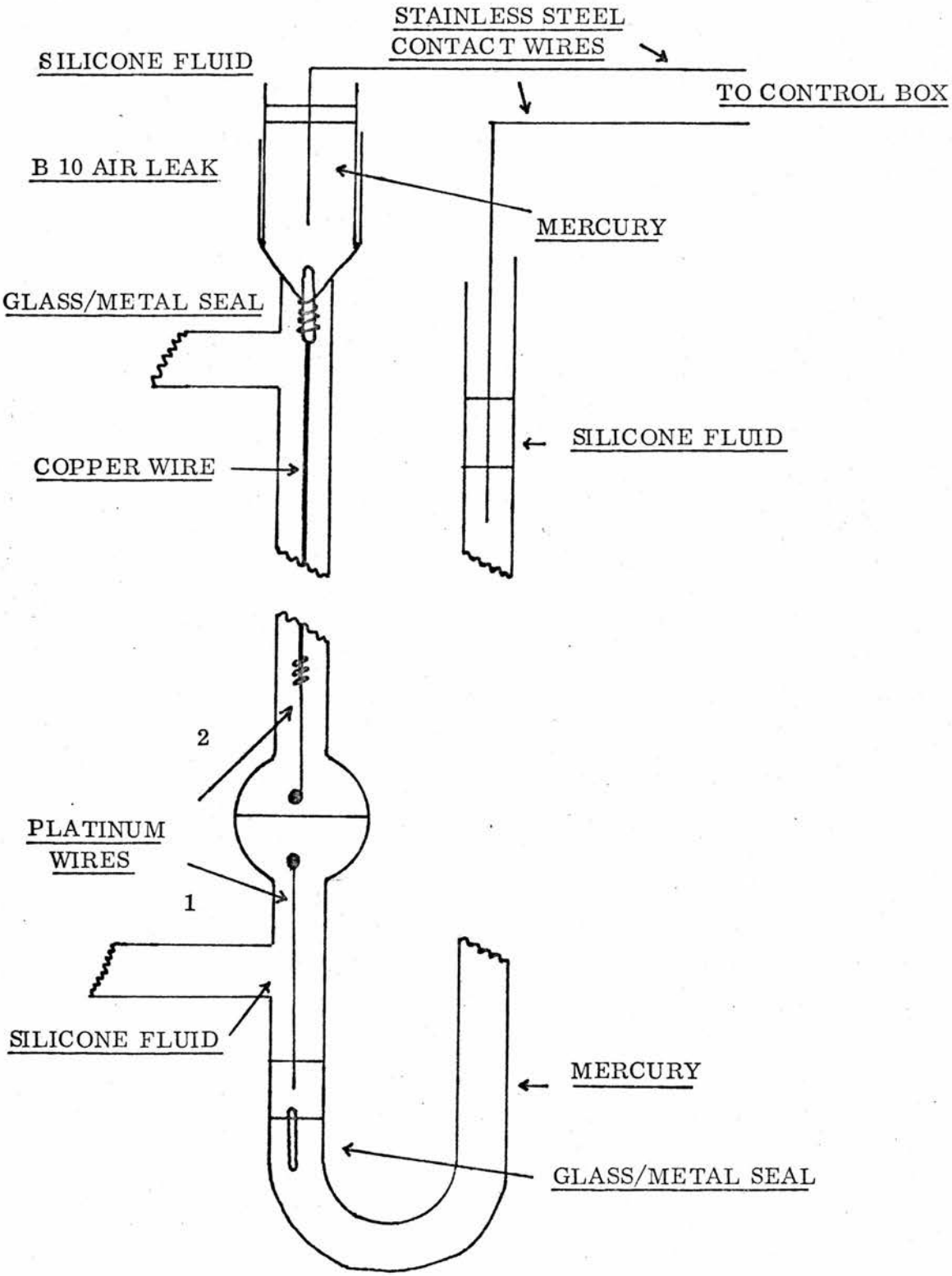

which was incorporated in a B 10 air leak. The upper part of the seal was covered by mercury which again had silicone fluid on top. Stainless steel wires were placed in the mercury of the side arm and the air leak. Their other ends were attached to terminals in a control box. The control box was linked up to an event recorder and a plunger. The event recorders used were of a variety of types. The main one used was a switchboard type ten channel event recorder type H30 (supplied by Henry's Radio Ltd.). The use of chart recorders over long periods of time, however, involved a number of malfunctions such as pen blockage and chart paper snagging. The plunger and the control box were constructed by the department workshop.

The plunger was a simple screw type which was activated by the twisting of a flexible wire. The plunger was attached to the manometer system by a B 24 hollow brass cone at point D. The trip mechanism was activated by the upper platinum wire touching the manometer fluid. Both wires were therefore positioned so that they did not touch the glass wall as this could have led to premature and inconsistent event recording due to the manometer fluid moving unevenly. Once the trip mechanism had been activated, the event was recorded and the plunger screwed down by one revolution. If taps A and B were closed when a turn took place the manometer fluid moved downwards on the reaction side of the apparatus. Thus a series of readings for oxygen-uptake versus time could be obtained. The volume displaced by one revolution of the plunger was calculated by measuring the pitch and area of the screw. This value and hence the sensitivity of the apparatus was equivalent to 1.5×10^{-6} moles of

oxygen at atmospheric pressure.

The whole manometer system except for the top of the air leak, side arm and plunger screw could be immersed in a thermostated water bath. The temperature was controlled by means of a contact thermometer connected to two 150 watt light bulbs. To ensure that the temperature was constant throughout the bath, a water pump was used to circulate the water. A check of the bath temperature at various positions in the bath was maintained by the use of conventional thermometers. A water cooled copper coil in the bath was used to compensate for high room temperatures and the heat of the lamp. These methods made possible extremely accurate temperature control. Unless otherwise stated reaction temperatures were $30^{o}C \pm 0.01^{o}C$.

c) Experimental Procedure - Apparatus One

The cell and manometer system were evacuated for 30 minutes with taps A and B open. As a rough check for leaks in the system tap B and then tap A were closed. Any rapid motion of the manometer fluid indicated a leak. Slow movement meant that some degassing was still taking place. When this test gave no movement after 10 minutes, the apparatus was then flushed with oxygen by repeated evacuation and charging. After the sixth filling action tap B was closed. It was shown by gas chromatography analysis that by this time no original air remained and the apparatus was filled with oxygen. The oxygen was then allowed to equilibriatefor 30 minutes at the end of which time tap B was reopened for 10 minutes to allow the oxygen to reach atomospheric pressure. Atmospheric pressure for the reaction was then measured using a barometer.

Tap B was then closed and the apparatus allowed to equilibriate overnight.

Tap A was now closed and the manometer level on the reaction side was adjusted to just above the lower platinum wire. The plunger wire was connected, a cover was placed over the cell and the lamp allowed to stabilised for 30 minutes. As previously stated the samples were irradiated from above. To ensure that for each reaction the lamp and cell positions were the same, a careful marking of boss, clamp and rod positions was carried out. The photodiode position was never altered so a check could be made on any variations. The arc to sample distance, which unless otherwise stated was 29.9 cm, was also checked before each reaction.

In an attempt to minimise the heating effect, which will be discussed later, a quartz disc was placed between the lamp and the cell. When the lamp had stabilised the cell cover was removed and the reaction proceeded.

d) The Manometer System and Method of Measurement - Apparatus Two

Cell A was again attached to a manometer system by a thin copper tube. One end of the tubing was soldered to the cell while its other end was soldered to a needle valve attached to a B 14 hollow brass cone. The needle valve was made by Edwards. The cone was fitted into a greased socket in the manometer system. The manometer system is shown in figure 5. Its design was similar but it was smaller in volume compared to the manometer system of apparatus one. It also had a reference and reaction side which could be isolated from each other by closing tap A. The main difference was that apparatus two had now to be manually operated. When the needle valve was turned, with taps A

FIGURE 5

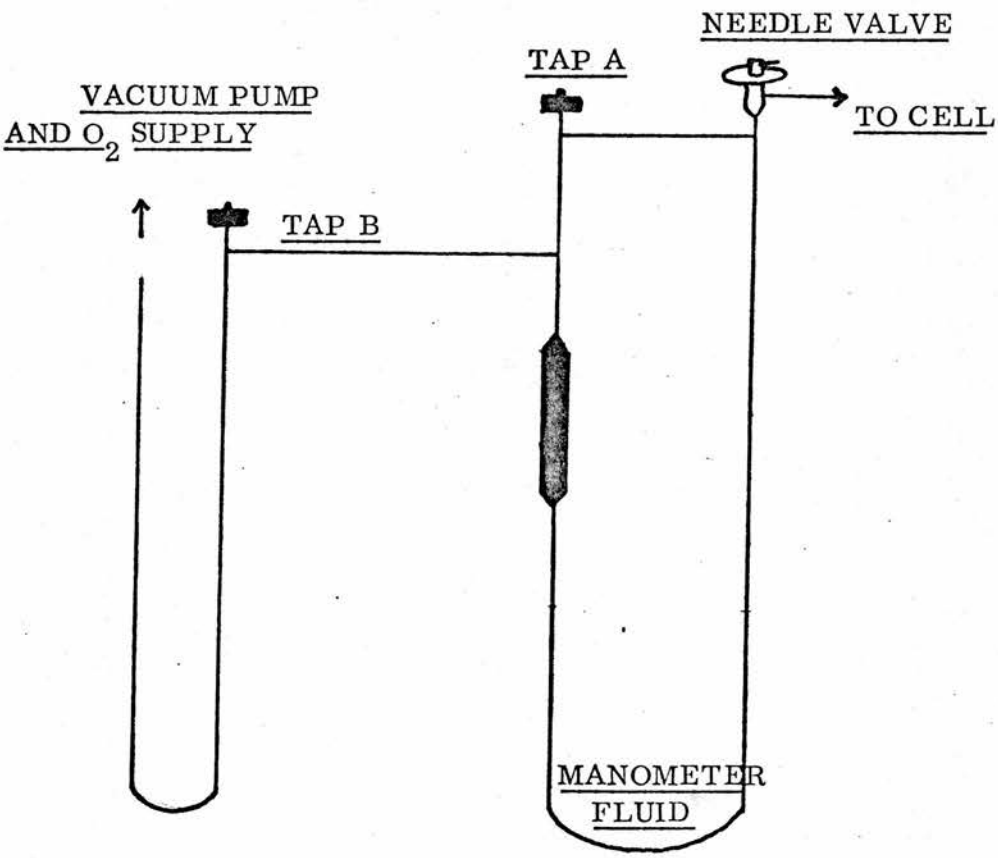

APPARATUS TWO

(MANUAL)

and B closed, the manometer fluid on the reaction side moved. The fluid was therefore zeroed, on marks on the manometer glassware and on the side of the water bath, before each reaction. With the aid of a magnifying glass (x5), positioned outside the bath, this could be done extremely accurately. During the reaction any movement of the fluid level could be monitored by rezeroing the level and reading the volume change directly from the needle valve dial and the time from a wrist watch. The pitch and area of the screw in the needle valve was measured and since each revolution was subdivided on the valve dial into one hundred units, the sensitivity of the apparatus was 5×10^{-9} moles of oxygen at atmospheric pressure. This compared extremely favourably with the sensitivity of apparatus one, 1.5×10^{-6} moles of oxygen, and that of Grassie and Weir's[21] apparatus, 2×10^{-8} moles of oxygen.

The apparatus was filled and evacuated from tap B using the same procedure as in apparatus one. The whole apparatus including the needle valve could be immersed in the water bath described previously.

e) Experimental Procedure - Apparatus Two

The experimental procedure for charging and equilibriating the cell was identical to that described for apparatus one. When the apparatus had equilibriated tap A was closed. The needle valve was then used to zero the fluid level on the reaction side of the manometer before the reaction. The lamp stabilising and positioning was also identical to apparatus one. Further readings were taken at arbitrary time intervals during the reaction by rezeroing the fluid level and reading the needle valve dial.

f) Film Casting

Because of the relatively low molecular weights of the copolymers, thin unsupported films could not be obtained. An alternative method for casting films on quartz discs was therefore devised. Figure 6 shows the casting apparatus. It consisted of a hollow brass screw and cap. A teflon ring, quartz disc and 'O'-ring were placed in the cap and screwed tightly together. 5% solutions by weight of the polymers were added dropwise from the top. Film weight and hence thickness could be controlled by the number of drops. The evenness of the films was optimised by casting on a level base and using a standard metal cutter to remove the thicker parts round the circumference. By repeating the procedure films could be cast on both sides of the quartz disc.

The solvent used for film casting for apparatus one was chloroform. This had the disadvantage of being difficult to remove and therefore required longer drying times. Any residual chloroform had a marked effect on the consistency of the results obtained. This was probably due to the photolabile nature of chloroform. Cyclohexane was used for the casting of all the films used in apparatus two. The propane/styrene copolymer did not completely dissolve at room temperature however and therefore solutions had to be heated to approximately 40 ^{o}C before being used for casting.

Polystyrene films were cast on a level tile from 5% solutions by weight with either cyclohexane at 40^{o}C or chloroform as solvent. The unsupported films were lifted from the tile after 20 to 30 minutes. A metal cutter was used to get films of uniform area.

The removal of solvent from all the films was carried out in a vacuum

FIGURE 6

FILM CASTING APPARATUS (SECTION)

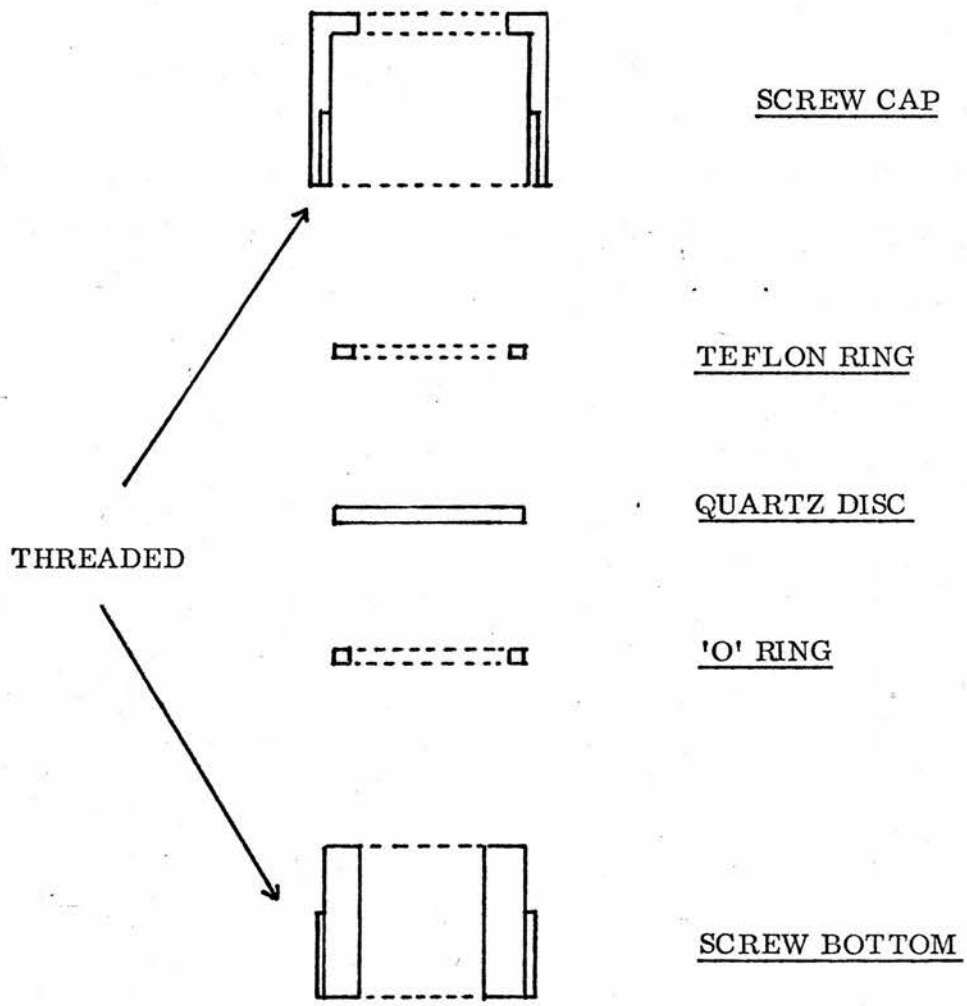

oven at room temperature. Films cast from cyclohexane were evacuated for a minimum of 14 days and those cast from chloroform for a minimum of 20 days. The surface area of all the films used was 2.835 cm^2.

Film thickness were measured by weighing a known area and checked by measuring the absorption at the λ_{max} for polystyrene and its copolymers. Good agreement between the two methods was achieved. Film thicknesses were calculated by assuming that the density of polystyrene and the copolymers was 1.0. The maximum film thicknesses of the unsupported and supported films used were 40 and 20 microns respectively. Between 3 and 4% of 253.7 nm and 90 and 95% of 313 nm incident radiation was transmitted by supported films of these thicknesses.

4. Heating Effect

When reactions were carried out in apparatus two, there was a short initial period where a 'negative' oxygen-uptake appeared to occur. This was thought to be a heating effect caused by the lamp. The effect was reduced when a quartz disc was introduced between the lamp and the cell. To find out whether the heating effect was due wholly to the lamp or if the polymer was involved in some way, cell B was constructed. Cell B is shown in figure 7. It differed from cell A in that light could pass directly through the cell via two quartz windows which could be screwed in above and below the sample. As in cell A, brass was used for the casing. 'O'-rings and grease ensured that there were no leaks at the window or sample sites and space was available for the incorporation of absorbers, Cell B was connected to a needle valve in the same way as in

FIGURE 7

CELL B (SECTION)

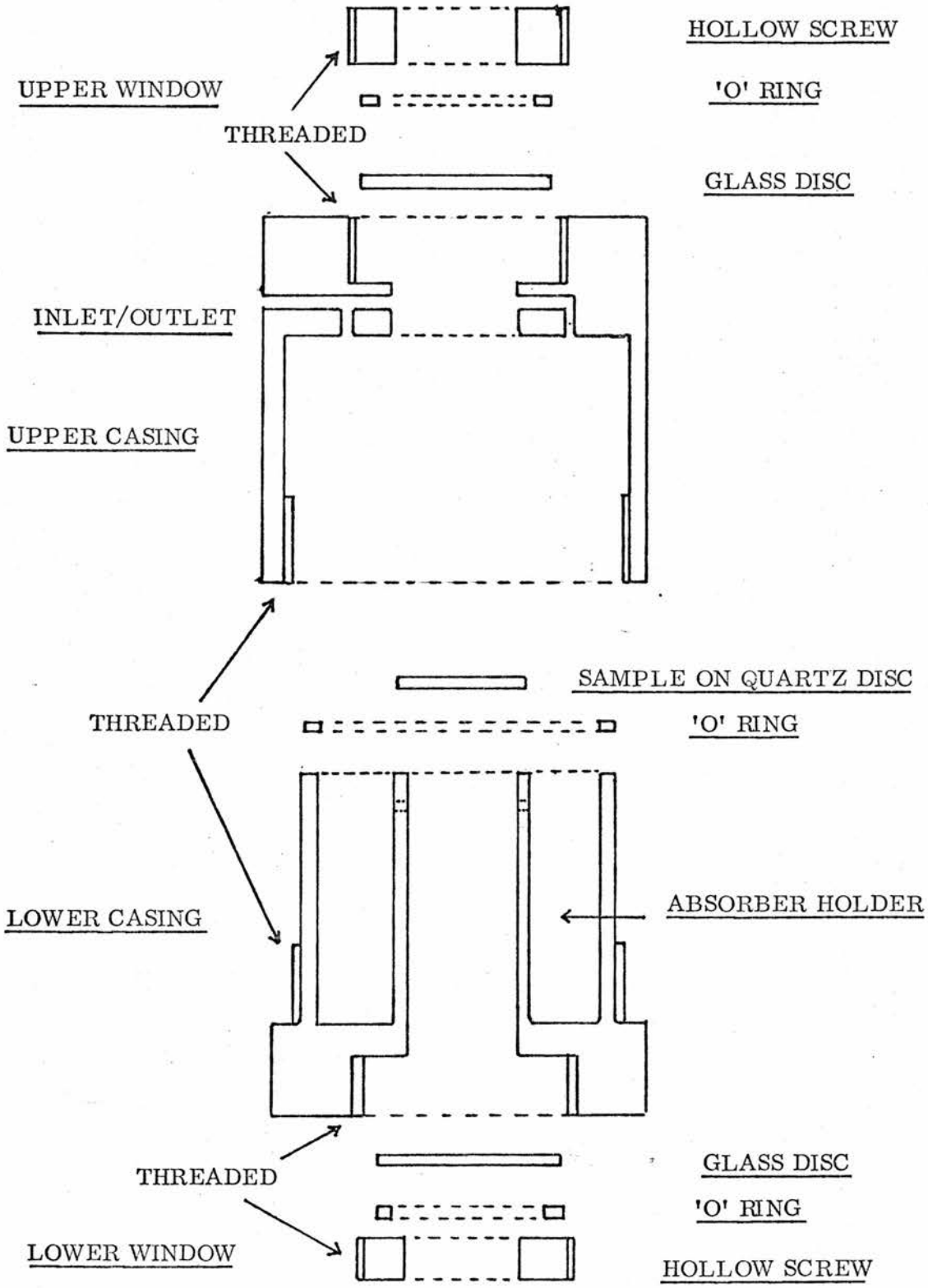

apparatus two. The needle valve the manometer system and their connection were all identical to apparatus two.

The procedure for setting up the apparatus and for monitoring the reaction was also identical to that in apparatus two. Irradiation, however, was only for periods of three minutes since the added complication of the oxidation reaction had to be avoided during the measurement of the heating effect.

5) Product Analysis

Infra-red and ultra-violet spectra of the copolymers were taken before and after each reaction. Samples were also irradiated outwith the apparatus and ultra-violet spectra taken at intervals. After irradiation in apparatus one, samples were insoluble.

The gaseous products from a few reactions were pumped out over 'cardice' (solid carbon dioxide)/acetone and liquid nitrogen traps and analysed by mass spectrometry.

CHAPTER 3

RESULTS

1. Rate Measurement and Experimental Errors for Apparatus One and Apparatus Two

The rates of oxygen-uptake of polymer samples, of known weight, at constant temperature and irradiation intensity, for both apparatus one and two were measured by plotting the number of moles of oxygen consumed versus time and taking the gradient of the resulting graph. All the reactions were carried out in the presence of carbon dioxide and water absorbers and under atmospheric pressure of oxygen unless otherwise stated. The plunger and the needle valve of apparatus one and two respectively both gave direct volume readings for the oxygen absorbed which were converted to moles of oxygen by knowing the temperature and pressure of the oxygen in the apparatus.

The estimated maximum experimental errors were as follows ; For apparatus one and two, temperature $\pm$ 0.01 ^{o}C, weight $\pm$ 0.1 mg, intensity $\pm$ 2%, pressure $\pm$ 0.5 mm of mercury ; For apparatus one, time $\pm$ 1 minute, uptake readings $\pm$ 4 x 10^{-8} moles of oxygen ; For apparatus two, time $\pm$ 10 seconds, uptake readings $\pm$ 1 x 10^{-8} moles of oxygen. Errors in temperature, intensity, pressure, time and uptake readings were common to the graphs from both apparatus one and two. The approximate error in the graphs' gradients was calculated at $\pm$ 5%. The errors in the rate of oxygen-uptake will be calculated separately for each apparatus.

2. Blank, Consistency and Film Casting Technique Checks

From time to time experiments with no polymer samples in the cell

but otherwise identical conditions were carried out as blanks. Any apparent gas-uptake in these blanks meant that the apparatus was malfunctioning. When blank experiments showed no apparent gas-uptake reaction results could be recorded.

For each apparatus a reaction was chosen as a standard. Periodically this reaction was repeated to ensure the consistency of the results. The variation in these results was in agreement with the estimated experimental errors.

The film casting technique was checked using the more sensitive apparatus two. Reactions were carried out under pyrex and quartz filters. Films were cast on both sides, only the upper side, and only the lower side of the quartz supporting disc relative to the incident radiation. It was thought that the rate of oxygen-uptake would be proportional to the weight ie. thickness of the film and the results were corrected accordingly. The results showed that, within experimental, error the rate was the same no matter which side of the quartz disc the film was cast on. This meant that the quartz disc had no effect on the reaction and the supported films could be treated in the same way as unsupported films.

To check that for apparatus two the rate of oxygen-uptake is proportional to the weight of the sample, films of different weights were irradiated under quartz and pyrex discs. Figure 8 shows that this assumption of proportionality was correct in the case of the p-xylene/styrene copolymer. Results for the other copolymers showed a similar relationship.

The rates of oxygen-uptake under quartz (Intensity = 7.6×10^{15}

FIGURE 8

RATE OF OXYGEN-UPTAKE VERSUS SAMPLE WEIGHT

FOR APPARATUS TWO

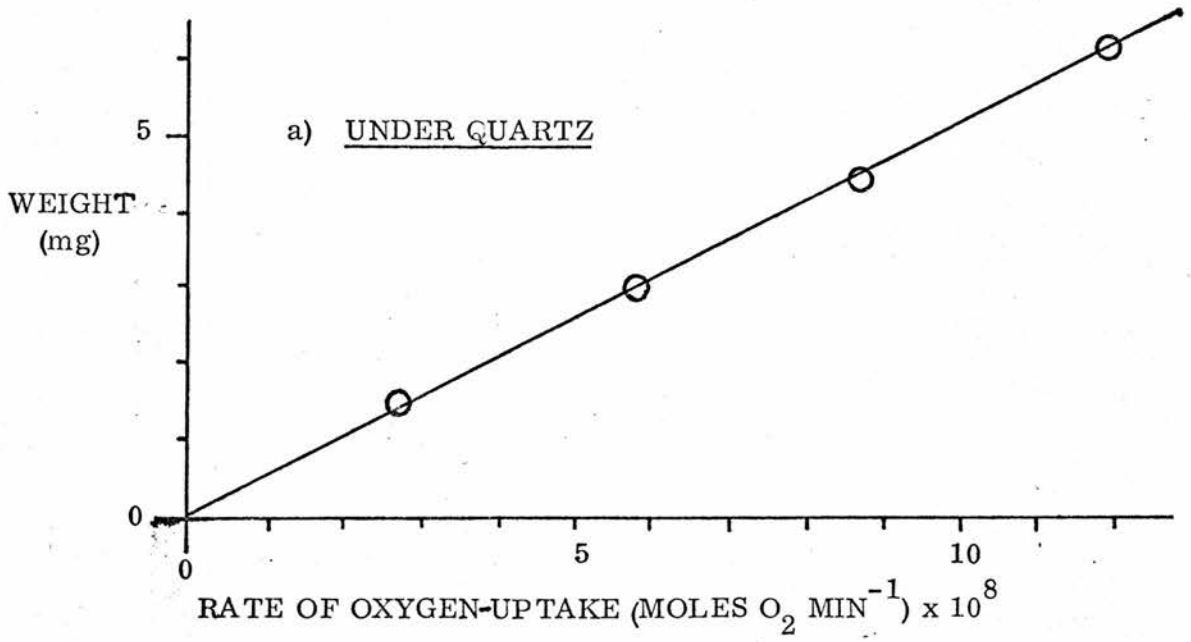

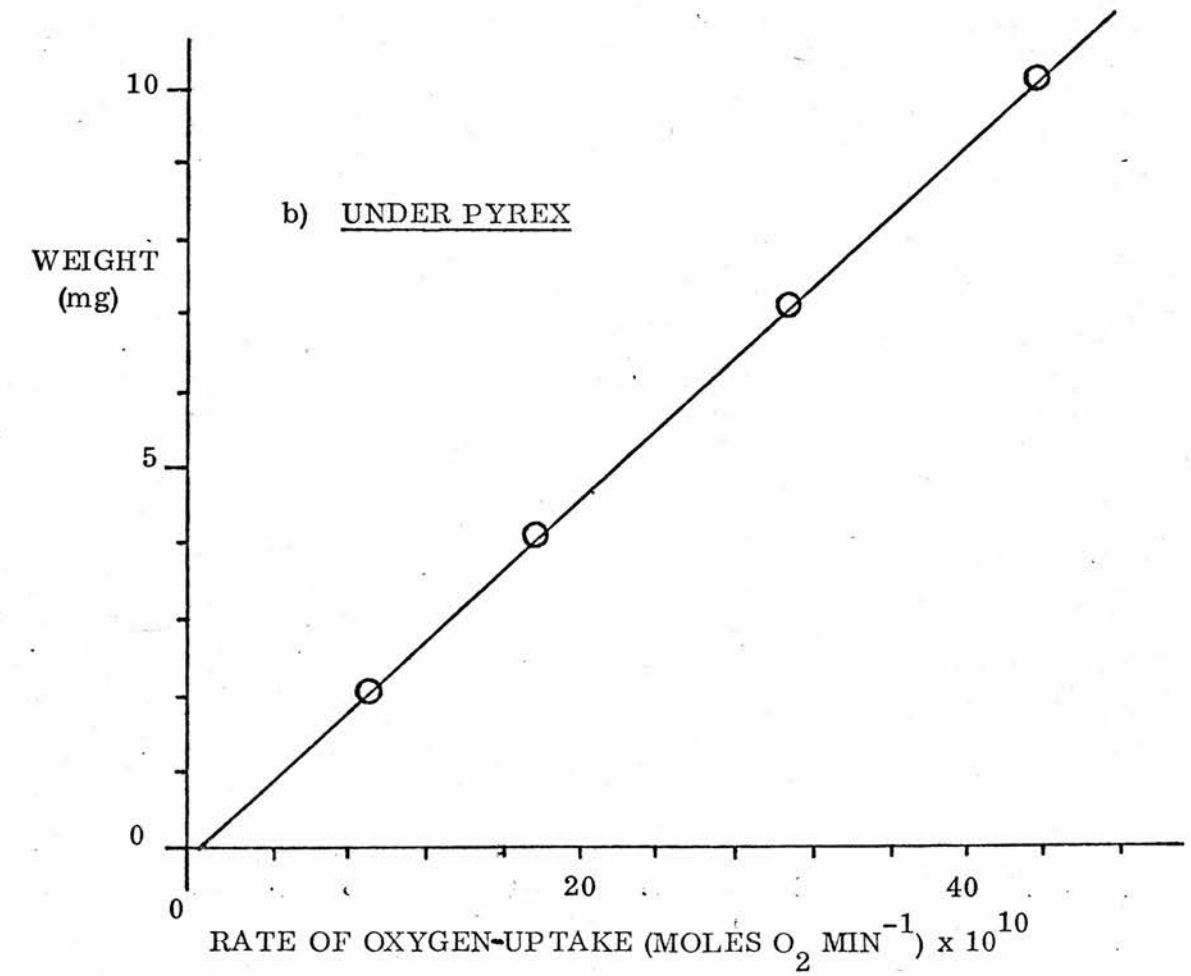

quanta cm^{-2} sec^{-1}) and pyrex (Intensity = 4×10^{15} quanta cm^{-2} sec^{-1}) for the p-xylene/styrene copolymer in apparatus two were approximately 4×10^{-8} moles O_2 cm^{-2} min^{-1} and 9×10^{-10} moles O_2 cm^{-2} min^{-1} respectively. The rate of diffusion of oxygen into polystyrene at 28°C and 600 mm oxygen pressure is 7×10^{-7} c.c. cm^{-2} mm^{-1} min^{-1} which is approximately equivalent to 2×10^{-11} moles O_2 cm^{-2} mm^{-1} min^{-1} [83]. The films used in apparatus two had maximum thicknesses of 20 microns and hence the rate of diffusion of oxygen into these films would be approximately 2×10^{-9} moles O_2 cm^{-2} min^{-1} using the data for polystyrene. These calculations suggest that the rate of oxygen-uptake under quartz should be diffusion controlled. However, because of their low molecular weight, the copolymer films are rubbers whereas the polystyrene films are glasses. The permeability (P), diffusion coefficient (D) and solubility (S) of gases in polymers are linked by the relation,

$$P = D \times S$$

The change from a glass to a rubber increases the diffusion coefficient and solubility of gases in polymers markedly and therefore the rate of diffusion of oxygen into polystyrene, used above, is far less than the rate of diffusion of oxygen into the copolymers. The fact that the photo oxidation reactions are not diffusion controlled, in the range of thicknesses used, is confirmed by the linearity of the weight versus rate graphs of all the copolymers.

3. Results From Apparatus One

Because of the relatively low sensitivity of apparatus one (1.5×10^{-6} moles of oxygen) it was useful for studying high extents of oxidation. To

maximise the rate and minimise the time, three supported films were stacked in the cell. Ultra-violet spectra of all three films together showed total absorption below 280 nm and about 90 to 95% transmittance at 313 nm.

A. Reactions Under Quartz

As an indication of the extent of reaction of the films irradiated under the full spectrum of the lamp, ultra-violet spectra were recorded before and after the reactions. The change produced in the ultra-violet spectra is shown in Figure 9. The uppermost film in the cell relative to the light source showed the greatest change in spectra, the middle one some change and the lowest no change at all. It was thought that each film was acting as an internal filter and as a result the lowest film had little or no effect on the rate of oxygen-uptake. To check this the weight of the lowest film was varied. This variation caused no change in the rate and it was concluded that,when there was total absorption by the samples at wavelengths lower than 280 nm,the rate of oxygen-uptake was independent of the total weight of the samples. The experimental error in the rate under the full spectrum of the lamp did not include the error of weighing and approximated to $\pm$ 5%.

The oxygen-uptake versus time graphs for the copolymers and for polystyrene (three unsupported films) at constant temperature, pressure and radiation intensity, are shown in Figure 10. If when one mole of oxygen is absorbed per mole of repeat unit the extent of oxidation is considered to be 100% the difference between each point on the graph corresponds to approximately 3% oxidation.

FIGURE 9

EXAMPLE OF CHANGE PRODUCED IN U.V. SPECTRA OF THE FILMS AFTER IRRADIATION

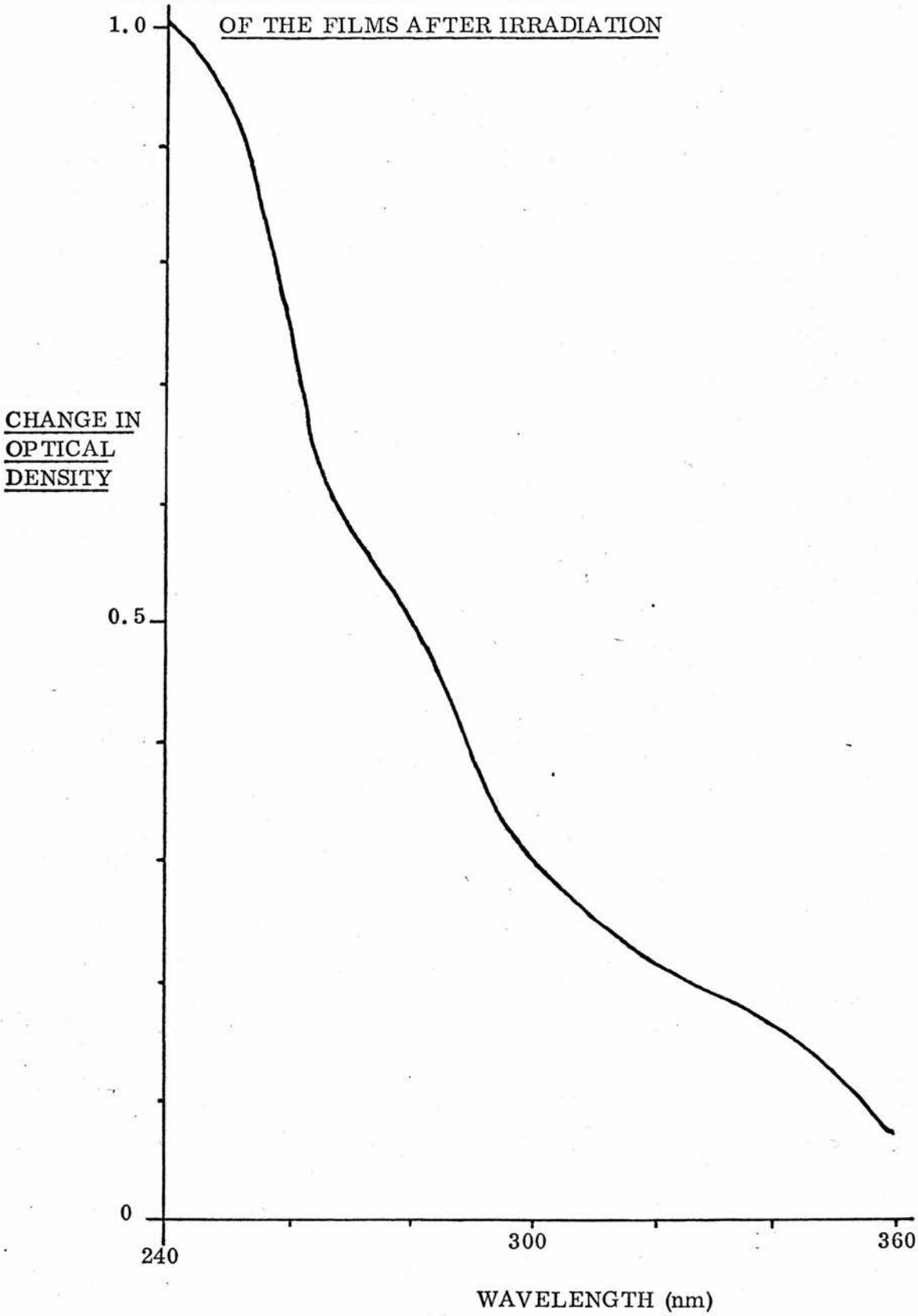

FIGURE 10

APPARATUS ONE

OXYGEN-UPTAKE VERSUS TIME UNDER QUARTZ

INTENSITY AT SAMPLE SURFACE = 7.6×10^{15} quanta cm^{-2} sec^{-1}
PRESSURE OF OXYGEN = 760 mm Hg; TEMPERATURE = 30 °C
SAMPLES OF TOTAL WEIGHT GREATER THAN 30 mg.

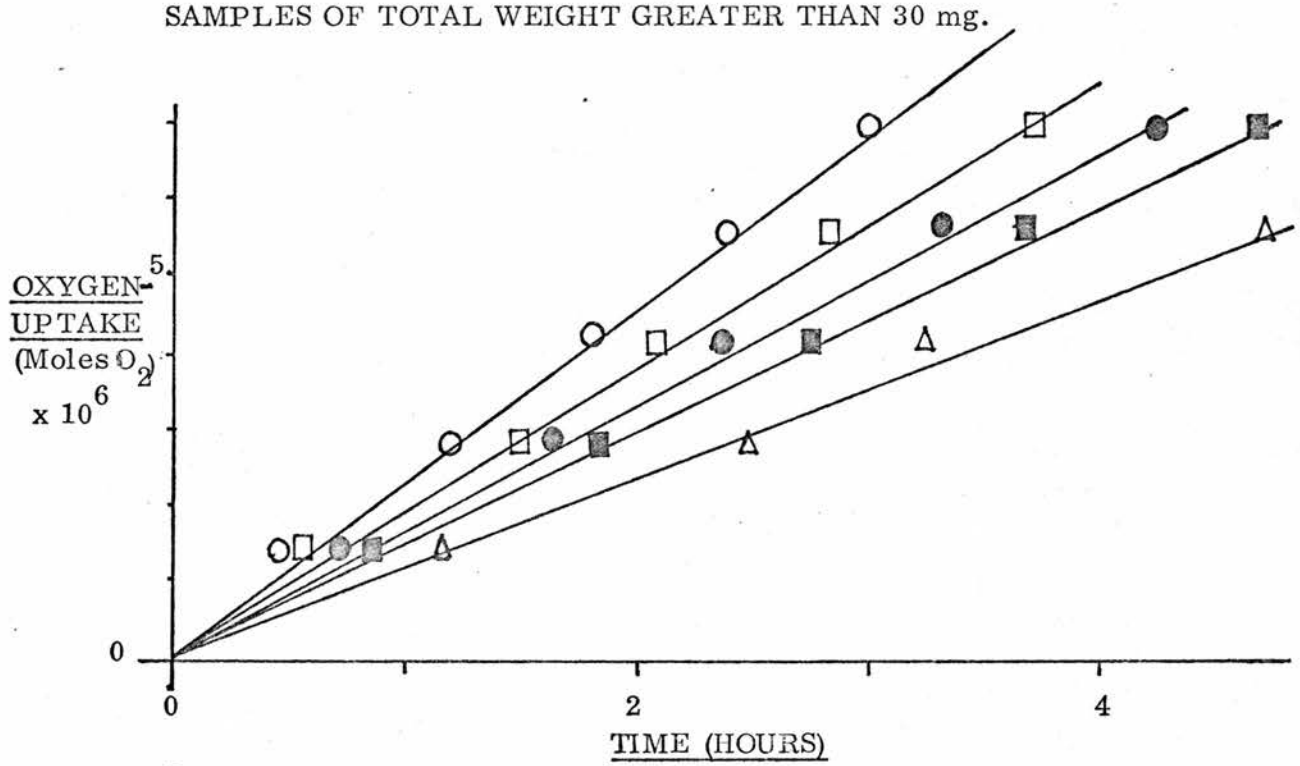

CONTINUATION OF GRAPHS ABOVE

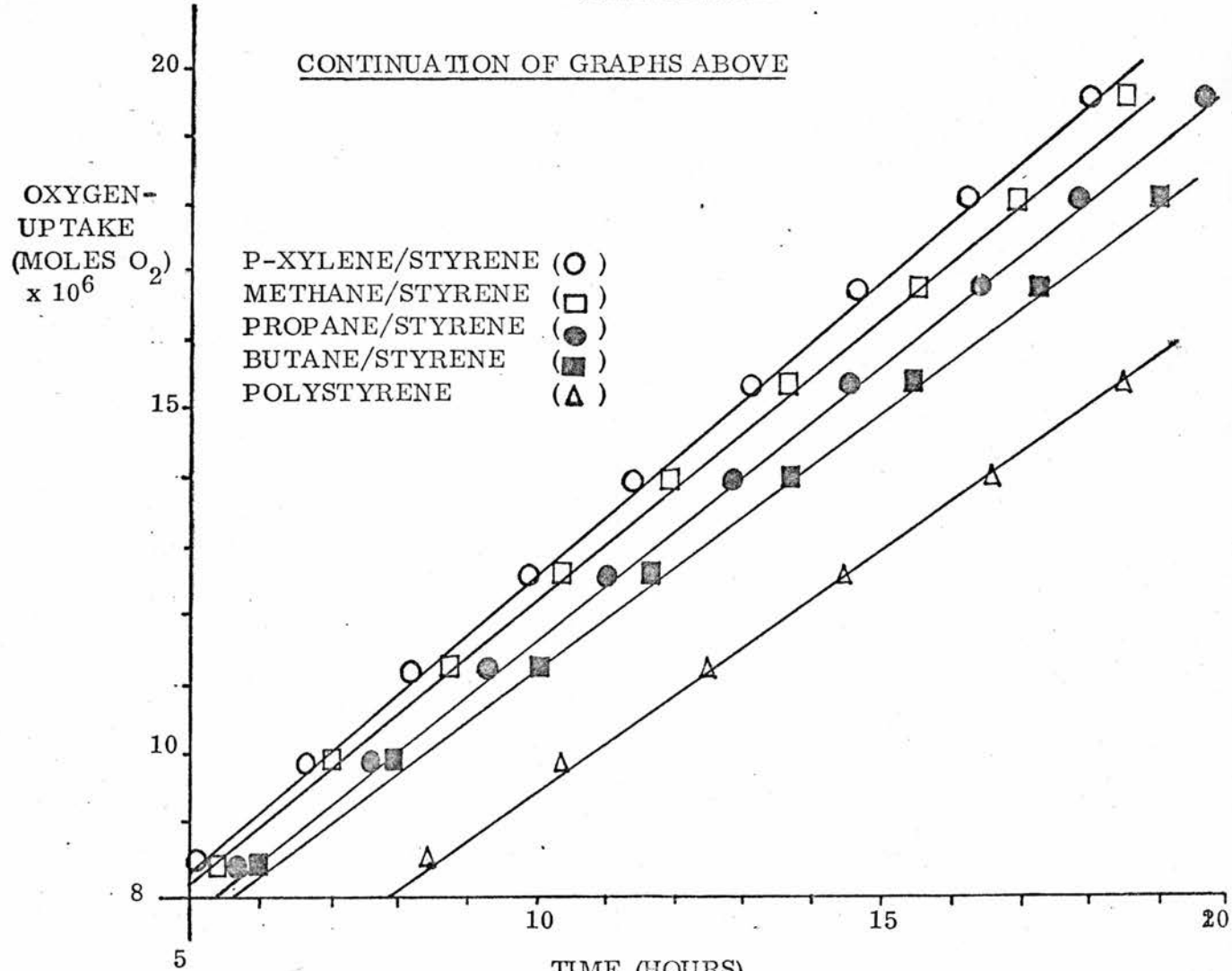

As can be seen the graphs have two distinct parts plotted separately. Initially there is a fast rate of oxygen-uptake but after approximately 5 hours (16% oxidation) a slower final rate is obtained. This could have been caused by a variety of reasons, some of which are :-

1. Filtration of the radiation by products built up on the top film.
2. Slower secondary reactions.

The initial and final rates of the photo-oxidation reactions are listed in Table 14.

Table 14

POLYMER	RATE (moles O_2. hour $^{-1}$) x 10^7	
	INITIAL	FINAL
P-XYLENE/STYRENE	33.1	14.7
METHANE/STYRENE	27.8	12.5
PROPANE/STYRENE	24.6	12.5
BUTANE/STYRENE	22.0	10.0
POLYSTYRENE	20.1	10.0

In order of photo-oxidative stability, the general trend for the initial rates was polystyrene > butane/styrene > propane/styrene > methane/styrene > p-xylene/styrene.

For reactions under the full spectrum of the lamp there was little or no dark reaction when the irradiation had ceased.

B. Reactions Under Pyrex

Reactions under pyrex were slow and meaningful results were difficult to obtain because of the low sensitivity of the apparatus. There was not total absorption by the films in the region above 280 nm so the rates may be proportional to the weight of the sample and the experimental error in the rate would then be approximately $\pm$ 7%. When reactions were carried out over several days, evaporation from the water bath became a serious problem. This evaporation and the subsequent refilling to ensure that the apparatus remained immersed caused large temperature fluctuations. In consequence, only a few reactions were carried out to see the general behaviour of the oxygen-uptake. A graph of the reaction of polystyrene under a pyrex disc is shown in figure 11. The rate of oxygen-uptake was 1.7×10^{-7} moles of oxygen.hour^{-1} for a 12.5 mg sample.

The irradiation was stopped and restarted during the reaction and a dark reaction was observed. After resuming the irradiation, there was a small induction period after which the reaction proceeded at the same rate as before.

Ultra-violet spectra of the films were taken before and after irradiation and again a change in the spectra was noted. This change was similar but smaller than that produced under full lamp spectrum irradiation on the uppermost film and no change was noticed in the middle and lowest film. This was expected since the extent of oxidation under pyrex was 4% whereas it had been 38% under quartz for the same period of irradiation.

FIGURE 11

APPARATUS ONE

OXYGEN-UPTAKE VERSUS TIME FOR POLYSTYRENE UNDER PYREX

INTENSITY AT SAMPLE SURFACE = 4×10^{15} quanta cm^{-2} sec^{-1}
PRESSURE OF OXYGEN = 760 mm Hg ; TEMPERATURE = 30 °C
TOTAL WEIGHT OF SAMPLE = 12.5 mg.

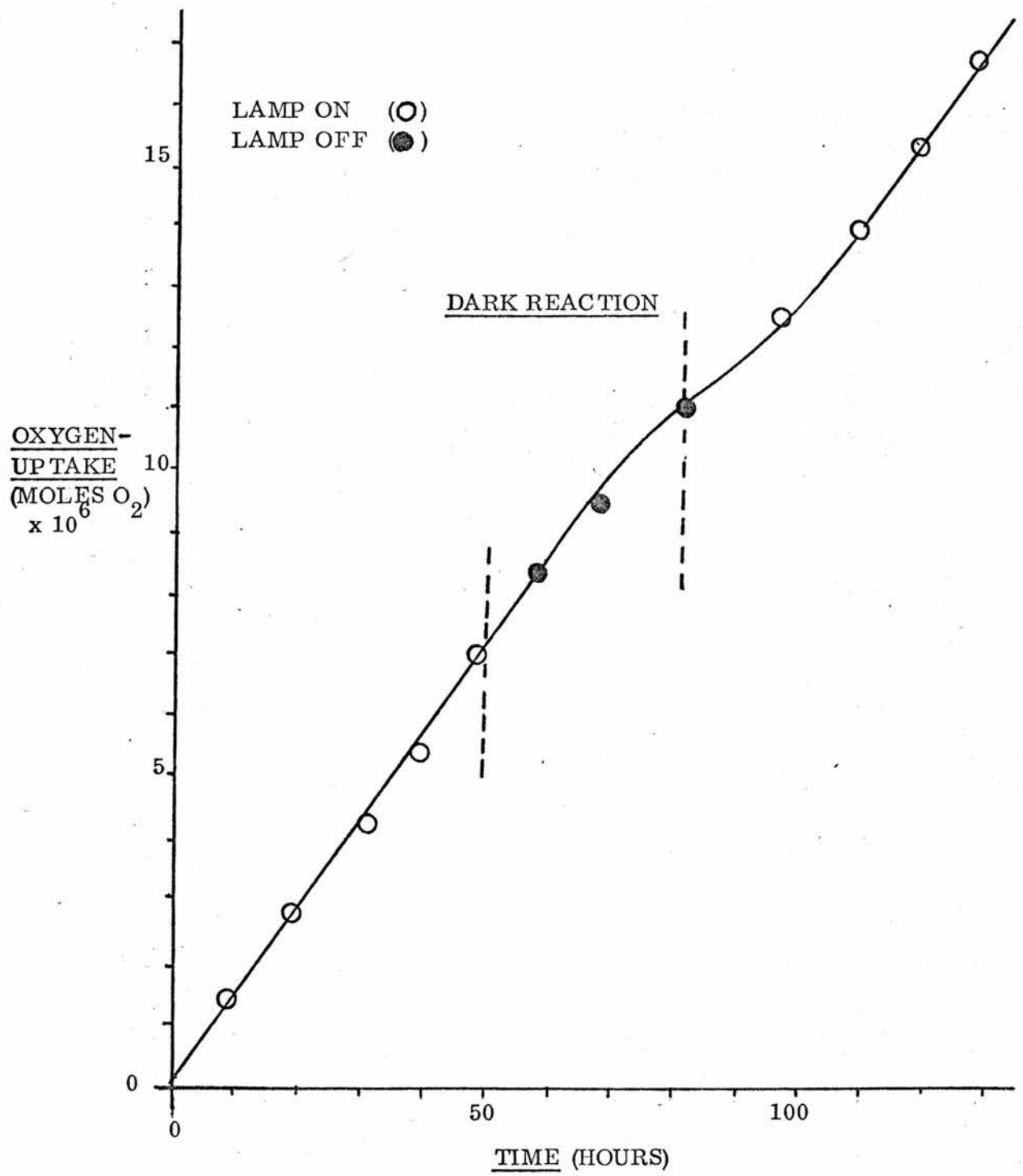

4. Results From Apparatus Two

The apparatus is extremely sensitive (5×10^{-9} moles of oxygen) and meaningful results were obtained in a matter of minutes. This apparatus was therefore useful for studying the very early stages of the reaction under either pyrex or quartz. Films were cast on only one side of the quartz disc,and since there was not total absorption by the film above 235 nm, the rate of oxygen-uptake was dependent on the weight of the sample (Chapter 3, part 2). The experimental error for the rate inclusive of the weight was $\pm$ 7%.

A. Reactions Under Pyrex

i) Relative Rates of the Copolymers

The graphs of oxygen-uptake versus time for all four copolymers corrected for weight and at constant temperature, pressure and radiation intensity are shown in figure 12. The increase in sensitivity of apparatus two compared to apparatus one was such that the first reading on apparatus one was approximately equivalent to half the entire reaction in apparatus two (6% oxidation).

The rates of oxygen-uptake are shown in table 15. These rates show the same trend in photo-oxidative stability as the rates under quartz in apparatus one.

It must be noted that,as the rates in table 15 were calculated using the molecular weight of the repeat unit, the p-xylene/styrene copolymer has three phenyl groups per repeat unit compared to the rest which have only two.

FIGURE 12

APPARATUS TWO

OXYGEN-UPTAKE VERSUS TIME UNDER PYREX

INTENSITY AT SAMPLE SURFACE 4×10^{15} quanta cm^{-2} sec^{-1}
PRESSURE OF OXYGEN = 760 mm Hg TEMPERATURE = 30 °C
WEIGHT CORRECTED TO 2×10^{-5} MOLES REPEAT UNIT

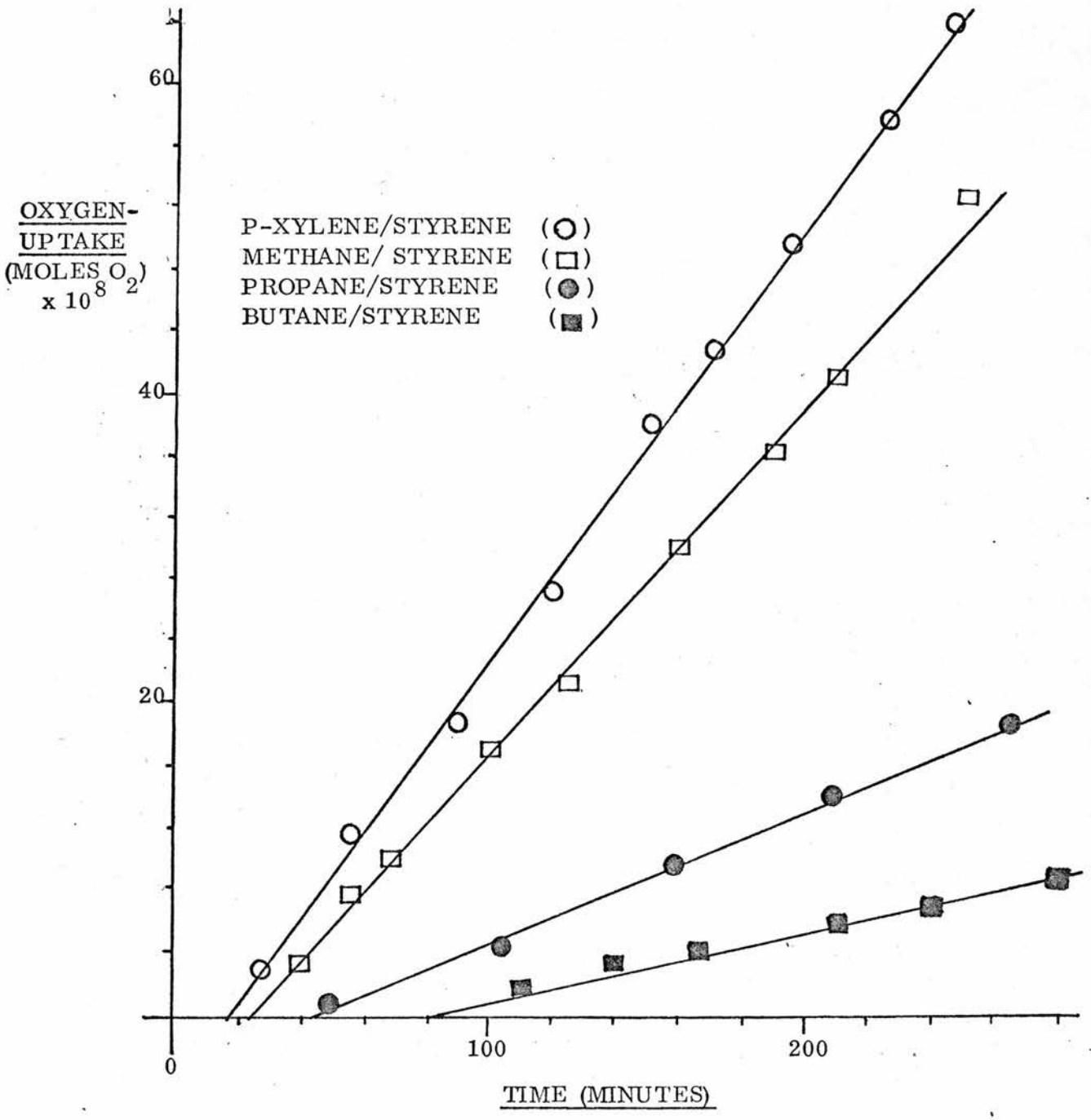

Table 15

POLYMER	RATE (moles O_2 $min.^{-1}$ (mole repeat unit)$^{-1}$ x 10^5
P-XYLENE/STYRENE	13.7
METHANE/STYRENE	11.8
PROPANE/STYRENE	4.3
BUTANE/STYRENE	2.2

The ultra-violet spectra of the films were again run before and after irradiation. No significant change was produced which showed the low extent of oxidation.

ii) Variation of Rate with Intensity

The graphs of the rate of oxygen-uptake versus the square root of intensity of all the copolymers at constant temperature and pressure and corrected for weight are shown in figure 13. The linear relationships mean that the rate of oxygen-uptake is proportional to the square root of the intensity incident on the polymer. This result is in agreement with Bolland's hydroperoxidation kinetics[53, 55].

iii) Energy of Activation

Reactions of the copolymers were carried out at different temperatures in the range 36 ^{o}C to 18 ^{o}C to find the energy of activation of the photo-oxidation reactions. Using the equation,

$$K = Ae^{-Ea/RT}$$

where K is the rate of oxygen-uptake, A is the pre-exponential constant, Ea is

FIGURE 13

APPARATUS TWO UNDER PYREX

RATE OF OXYGEN-UPTAKE VERSUS $(\text{INTENSITY})^{\frac{1}{2}}$

PRESSURE OF OXYGEN = 760 mm Hg TEMPERATURE = 30 °C

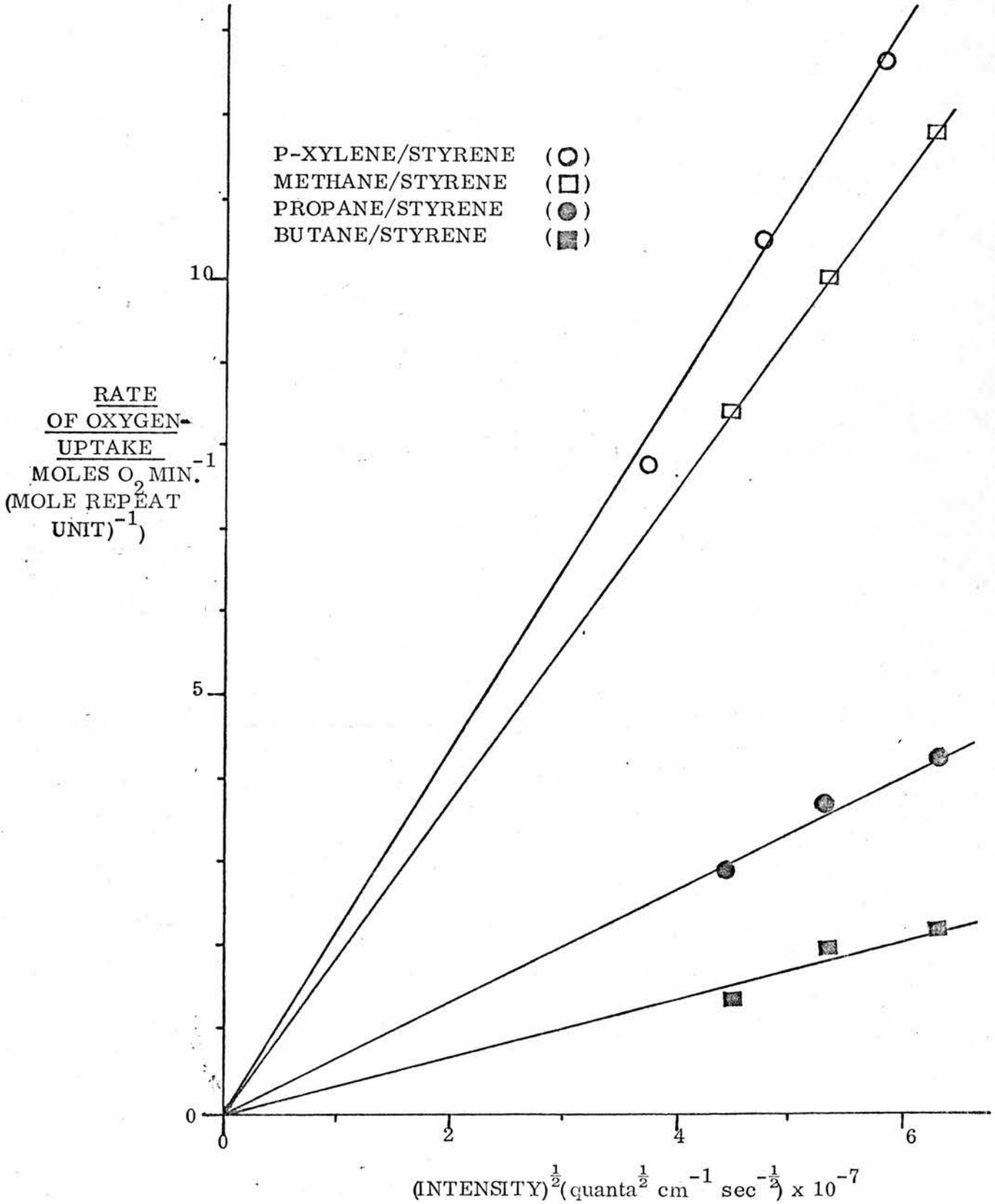

the energy of activation, R is the gas constant and T is the temperature in kelvin, plots of log (rate) versus $^1/T$ yielded the energy of activation from the gradient of the resulting graphs. The graphs for the copolymers are shown in figure 14 and the energies of activation are shown in table 16.

Table 16

POLYMER	ENERGY OF ACTIVATION (k $Jmol^{-1}$)
P-XYLENE/STYRENE	34.7
METHANE/STYRENE	21.7
PROPANE/STYRENE	34.9
BUTANE/STYRENE	61.5

The activation energies trend differs from the relative rates of oxygen-uptake by the reversal of the methane/styrene and p-xylene/styrene copolymers placings and the close similarity of the p-xylene/styrene and propane/styrene copolymers. Explanations for these results most probably lie in the variation of the copolymers' structures.

B. Reactions under Quartz

i) Relative Rates of the Copolymers

As could be expected, the rates of oxygen-uptake of the copolymers under the full lamp spectrum were faster than under pyrex. The graphs of oxygen-uptake versus time at constant temperature, pressure and radiation intensity are shown in figure 15 and the corresponding rates are listed in table 17 along with the rate of oxygen-uptake of the p-xylene/styrene copolymer

FIGURE 14

APPARATUS TWO

ENERGY OF ACTIVATION PLOTS UNDER PYREX

INTENSITY AT SAMPLE SURFACE 4 x 10^{15} quanta cm^{-2} sec^{-1}

PRESSURE OF OXYGEN = 760 mm Hg

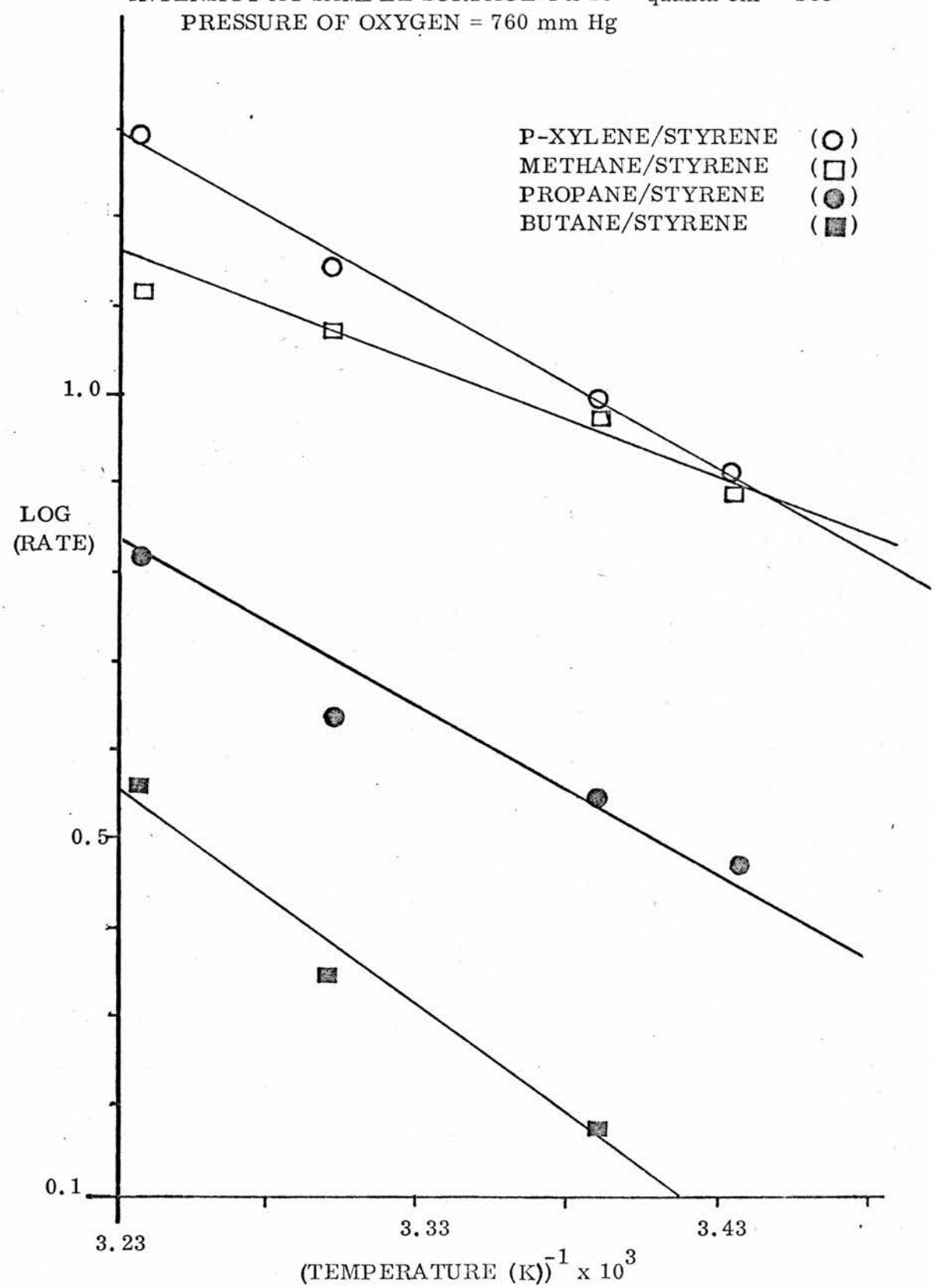

FIGURE 15

APPARATUS TWO UNDER QUARTZ

RATE OF OXYGEN-UPTAKE VERSUS TIME

INTENSITY AT SAMPLE SURFACE 7.6×10^{15} quanta cm^{-2} sec^{-1}
PRESSURE OF OXYGEN = 760 mm Hg ; TEMPERATURE = 30°C
WEIGHT CORRECTED TO 2×10^5 MOLES REPEAT UNIT

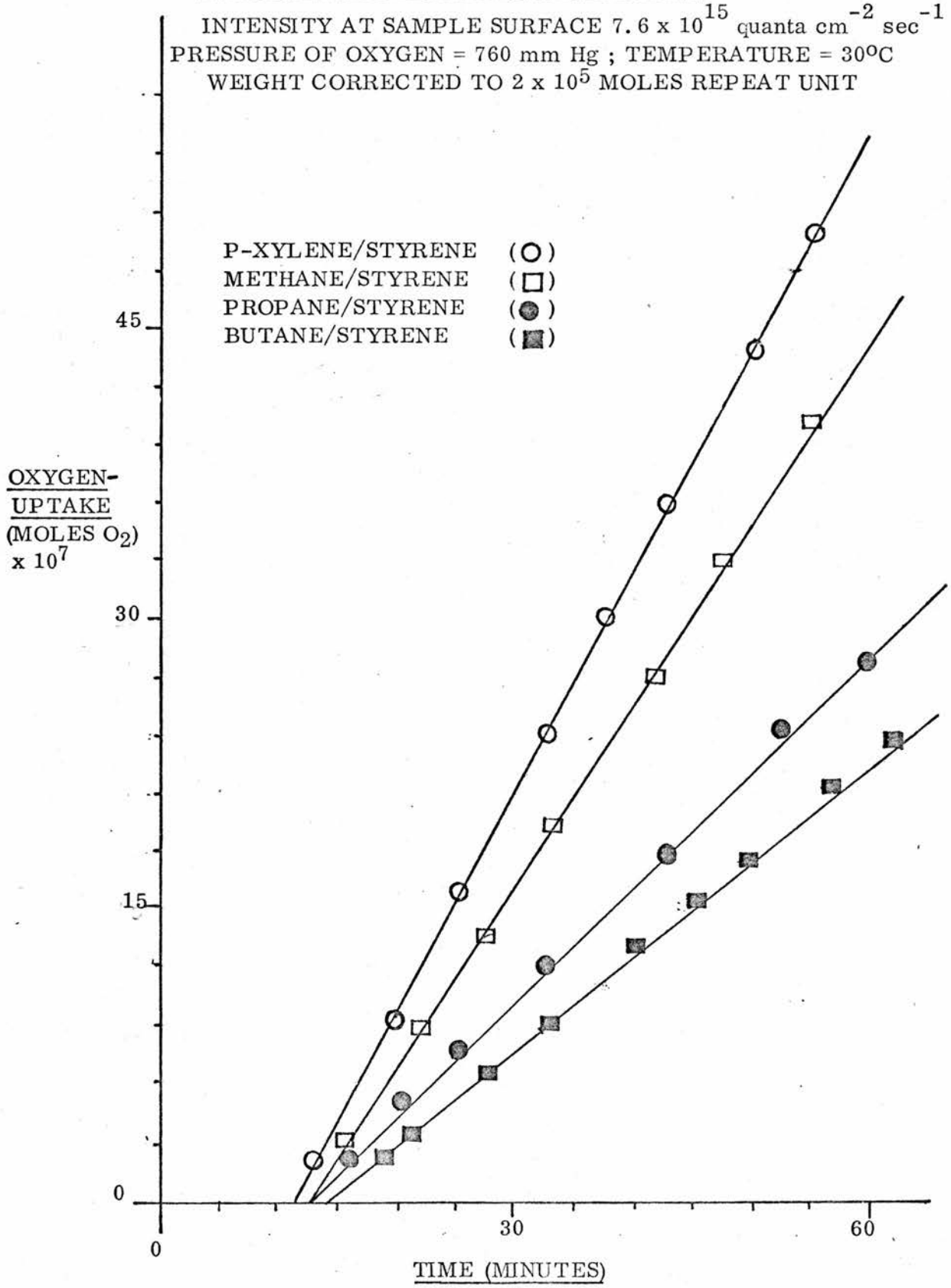

under pyrex for comparison.

Table 17

POLYMER	RATE OF OXYGEN-UPTAKE (moles oxygen $min.^{-1}$ (mole repeat unit)$^{-1}$) $x10^3$
P-XYLENE/STYRENE	6.1
METHANE/STYRENE	4.5
PROPANE/STYRENE	3.0
BUTANE/STYRENE	2.7
P-XYLENE/STYRENE UNDER PYREX	0.14

Again the general trend for photo-oxidative stability was butane/styrene > propane/styrene > methane/styrene > p-xylene/styrene.

The difference in the ultra-violet spectra after irradiation was similar in shape but less in size compared to that obtained in the reactions on apparatus one.

ii) Variation of Rate with Intensity

A plot of the rate of oxygen-uptake versus intensity for all the copolymers at constant temperature and pressure and corrected for weight is shown in figure 16. From the linearity of the graph it was evident that the rate of oxygen-uptake was proportional to the intensity of the light incident on the polymer. This is in agreement with the results obtained by Grassie and Weir who irradiated polystyrene with light of wavelength 253.7 nm[21].

FIGURE 16

APPARATUS TWO UNDER QUARTZ

RATE OF OXYGEN-UPTAKE VERSUS INTENSITY

PRESSURE OF OXYGEN = 760 mm Hg ; TEMPERATURE = 30 °C

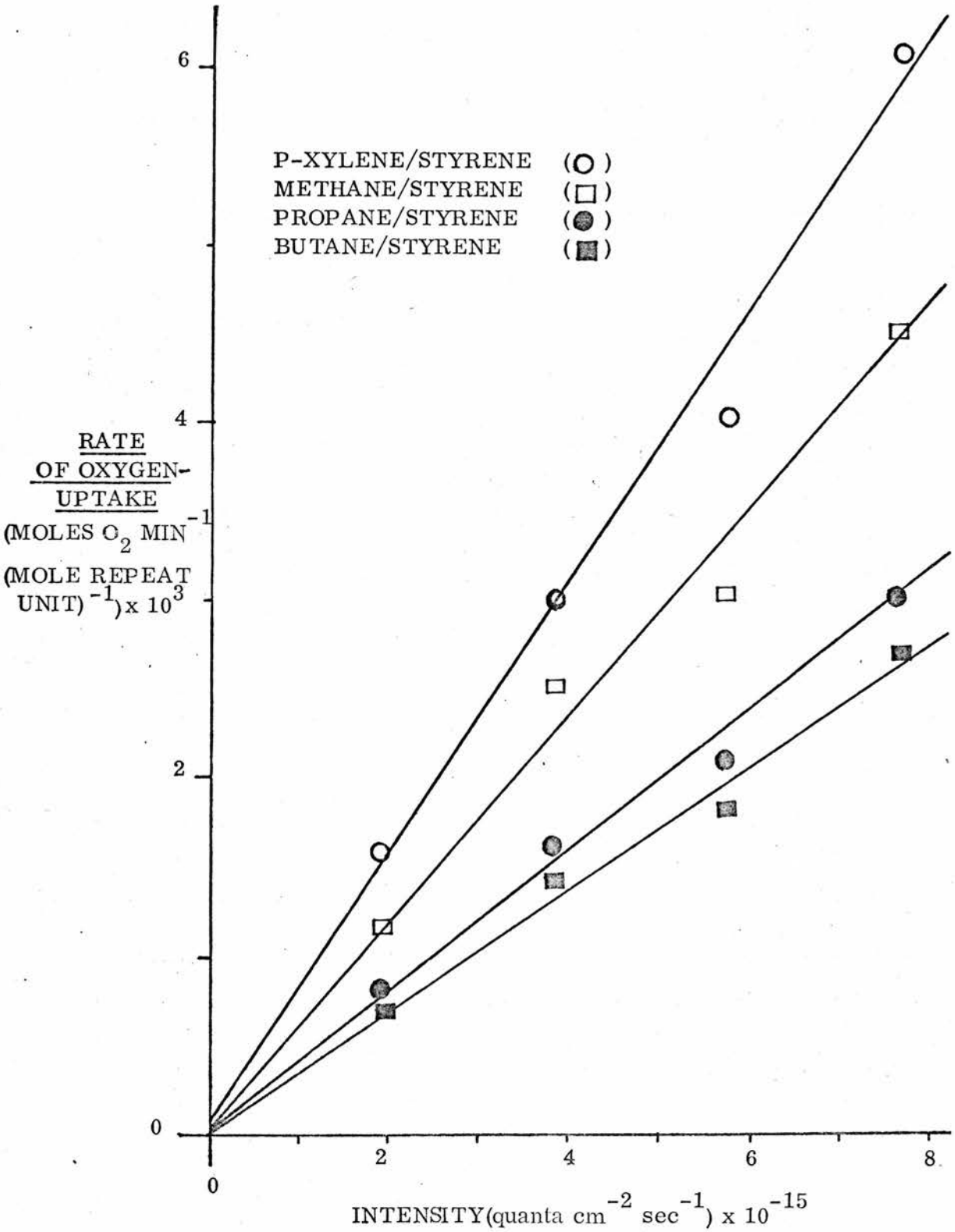

iii) Energy of Activation

Unlike the energy of activation measurements under pyrex, the temperature variation range of 36 ^{o}C to 18 ^{o}C was not wide enough to cause appreciable change in the rates of oxygen-uptake under the full spectrum of the lamp. Unfortunately, any attempt to broaden the range of temperature variation met with the loss of temperature control which was necessary for both the energy of activation measurement and more importantly the operation of the oxygen-uptake apparatus. The only conclusion therefore, which could be drawn, was that the energy of activation of all the copolymers were very much lower under the full spectrum of the lamp than they had been under pyrex.

5. Product Analysis

The uppermost films from apparatus one after irradiation under the full lamp spectrum were yellowed and insoluble. Even if nuclear magnetic resonance (n.m.r.) spectra of the sample had been possible, the complications through secondary reaction would have obscured the primary reaction products. The middle films had undergone comparitively little reaction and were still soluble but n.m.r. spectra of these showed no change from the unirradiated spectra.

Microanalysis of the uppermost film showed a reduction in the carbon and hydrogen percentages which implied that the oxygen taken up was actually being incorporated in the polymer. Accurate measurement of this content was not conducted because of the sample size, the difficulty of removing the samples from the quartz disc and the uncertainty of the extent of reaction of each film

layer.

The irradiated films from apparatus two were still soluble but n.m.r. spectra showed no change from the unirradiated samples. Microanalysis showed very little or no change in the carbon and hydrogen percentages after the film had been irradiated. These results were indicative of the low extent of oxidation of the films.

Infra-red spectra of the films irradiated under the full spectrum of the lamp in apparatus one showed various changes from the unirradiated spectra. A broad band between 3600 cm^{-1} and 3400 cm^{-1} (attributed to the formation of hydroxyl groups) and a band between 1780 cm^{-1} and 1630 cm^{-1} centred at approximately 1720 cm^{-1} (attributed to the formation of carbonyl groups) appeared. This was in agreement with a number of workers[31,66,87].

The films irradiated under pyrex in apparatus one and under pyrex and quartz in apparatus two showed no change in the infra-red spectra.

Analysis by mass spectrometry of the gaseous products after irradiation in all the reactions showed only carbon dioxide and water.

The increase in ultra-violet spectra has already been mentioned but, since this provided the most information about the reaction, additional spectra were run on films irradiated outwith the apparatus. The full lamp spectrum was used to give the maximum change and, for convenience, films were irradiated in air. Ultra-violet spectra of the films were taken at intervals during the irradiation. The general change in the ultra-violet spectra of the films under these conditions was similar to figure 9. It was decided to show

the change by plotting the optical density at four different wavelengths (240, 280, 300 and 350 nm) versus time. Figure 17 shows these changes plotted for the p-xylene/styrene copolymer. The graphs for the other copolymers were similar but the actual changes produced in the spectra for the same irradiation time decreased as the rate of oxygen-uptake of the copolymer decreased. These results suggested that the change in the ultra-violet spectra was due to the incorporation of oxygenated structures in the polymer sample. These plots showed the gradual levelling off of the spectral build up as the irradiation proceeded. Figure 18 shows plots of the total change in optical density on irradiation divided by the original optical density of all the copolymers versus wavelength. These graphs show that the products of irradiation from all the copolymers have the same general absorption patterns ; a shoulder at approximately 295 nm, a peak at approximately 280 nm and another peak below 240 nm. The spectra of the irradiated films remained unchanged long after the irradiation had ceased showing that the products were relatively stable. However, when an irradiated sample was heated in an oven at 60 ^{o}C for 1 hour, the spectral products below 300 nm were reduced (Figure 19).

6. Irradiation in Nitrogen and Vacuo

Reactions were carried out in apparatus two under quartz and pyrex in nitrogen and vacuo under similar conditions to the oxygen atmosphere experiments described previously. No gases were evolved or consumed and the polymer samples, when examined by ultra-violet spectroscopy, showed no appreciable change from the unirradiated films. This implies that the spectral

FIGURE 17

CHANGE IN ULTRA VIOLET SPECTRA IN AIR VERSUS TIME

P-XYLENE/STYRENE COPOLYMER
INTENSITY AT SAMPLE SURFACE = 7.6×10^{15} quanta cm^{-2} sec^{-1}
SAMPLE THICKNESS = APPROX 7 microns
TEMPERATURE = 22 °C ; ATMOSPHERIC PRESSURE OF AIR

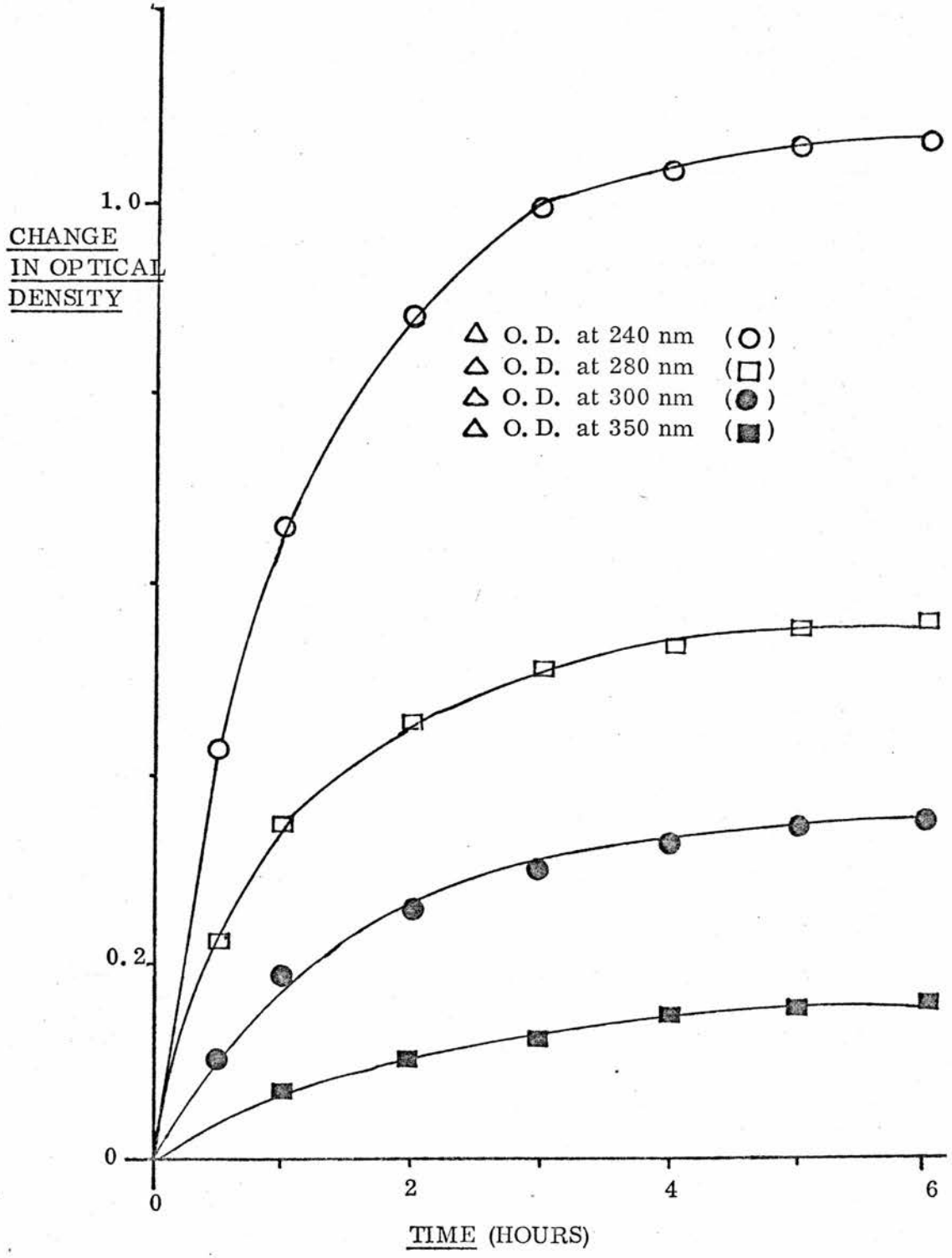

FIGURE 18

CHANGE IN OPTICAL DENSITY (Δ O. D.) AFTER 5 HOURS IRRADIATION IN AIR DIVIDED BY THE ORIGINAL OPTICAL DENSITY OF FILMS ($(O.D.)_o$) VERSUS WAVELENGTH

INTENSITY AT SAMPLE SURFACE = 7.6×10^{15} quanta cm^{-2} sec^{-1}
TEMPERATURE = 22 °C ; ATMOSPHERIC PRESSURE OF AIR

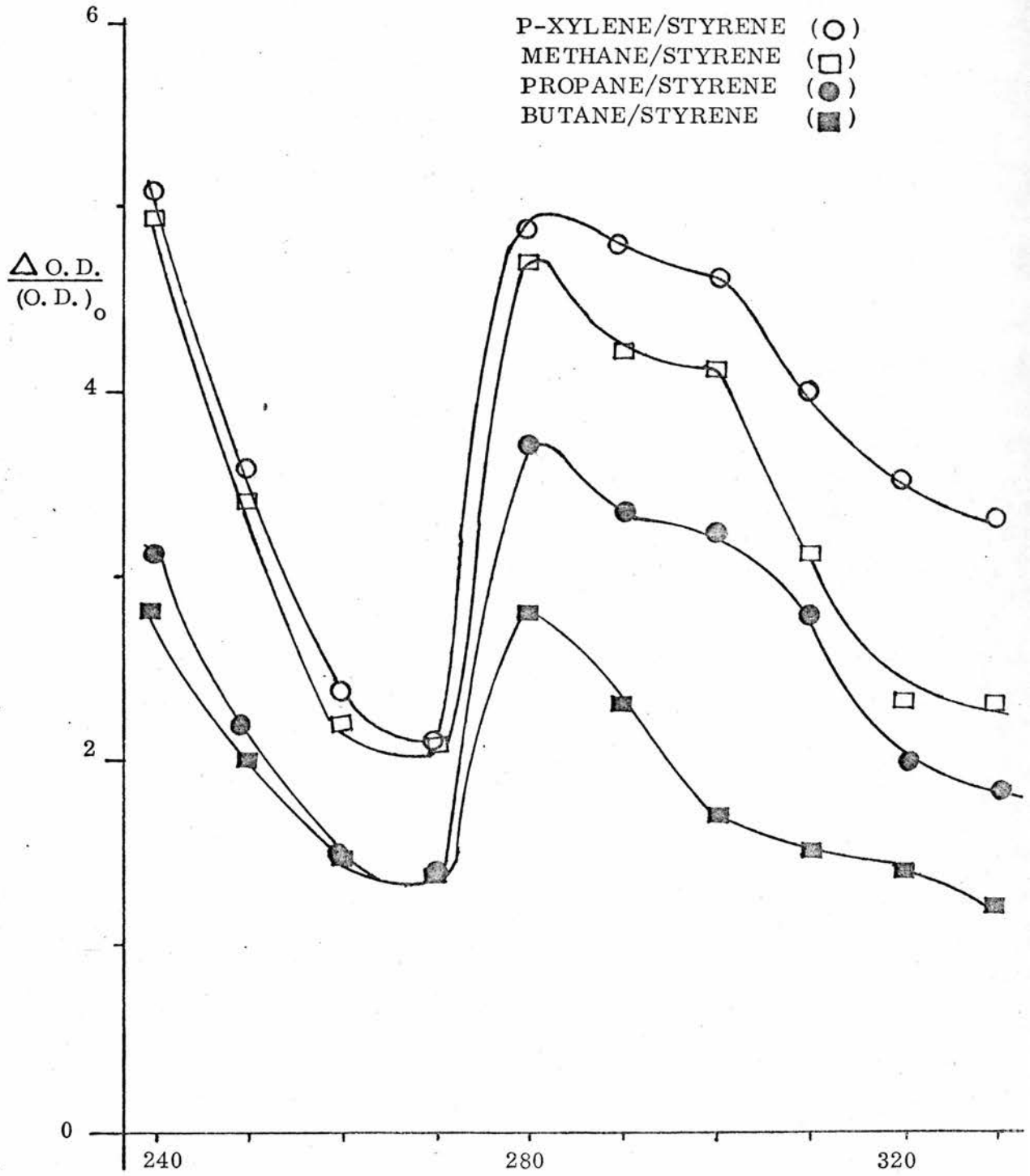

FIGURE 19

EFFECT OF HEAT ON IRRADIATION PRODUCT

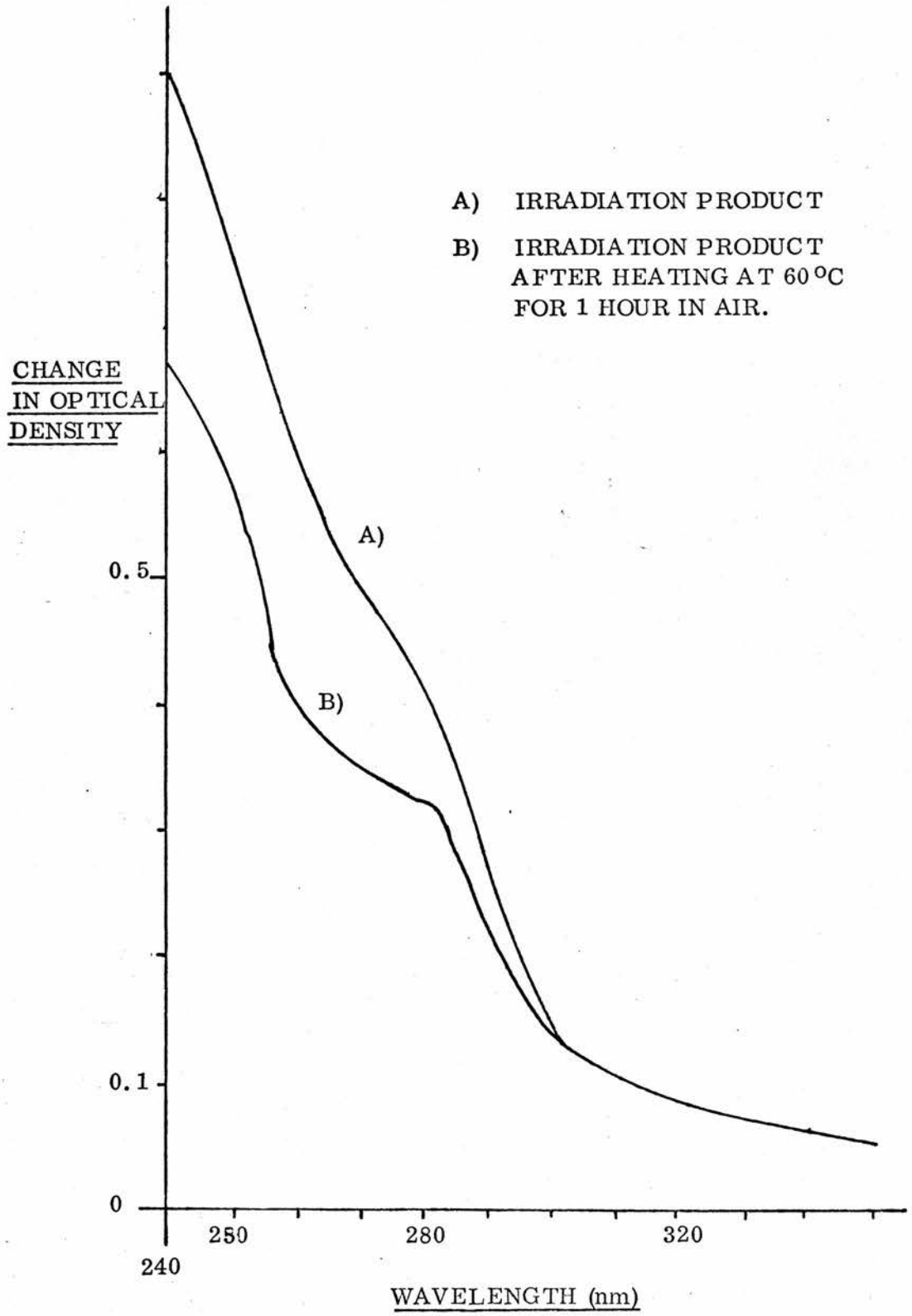

build up was due to oxygenated structures.

7. Effect of Absorber Removal on Rate

a) Under Quartz

Reactions were carried out on the copolymers under quartz to see if the removal of the carbon dioxide and water absorbers from the cell had any effect on the rate of oxygen-uptake. Figure 20 shows the effect of the removal of the absorbers on the rate of oxygen-uptake of the p-xylene/styrene copolymer corrected for weight and at constant temperature, pressure and radiation intensity.

Initially the removal of absorbers has no effect on the rate but after only a few minutes, the graphs of the samples minus one or both the absorbers began to curve away from the graph of the reaction containing both absorbers in the cell. This set of reactions was repeated for the other copolymers and, except for the relative reduction in rate for each copolymer, similar graphs were obtained. This deviation from the reaction graph with both absorbers in the cell must be due to the evolution of gas in sufficient quantities to counteract the oxygen-uptake which is initially predominant.

b) Under Pyrex

i) Absorber Removal Only

Similar reactions to those described above were carried out under pyrex. Figure 21 shows the effect of the removal of the absorbers from the p-xylene/styrene copolymers reaction corrected for weight. In this case there is little change in the rate of oxygen-uptake when both the absorbers are removed at constant temperature, pressure and radiation intensity. The removal of both

FIGURE 20

APPARATUS TWO

EFFECT OF REMOVAL OF ABSORBERS ON THE

RATE OF OXYGEN-UPTAKE UNDER QUARTZ

P-XYLENE/STYRENE COPOLYMER

INTENSITY AT SAMPLE SURFACE = 7.6×10^{15} quanta cm^{-2} sec^{-1}

PRESSURE OF OXYGEN = 760 mm Hg ; TEMPERATURE = 30 °C

WEIGHT CORRECTED TO 2×10^{-5} MOLES REPEAT UNIT

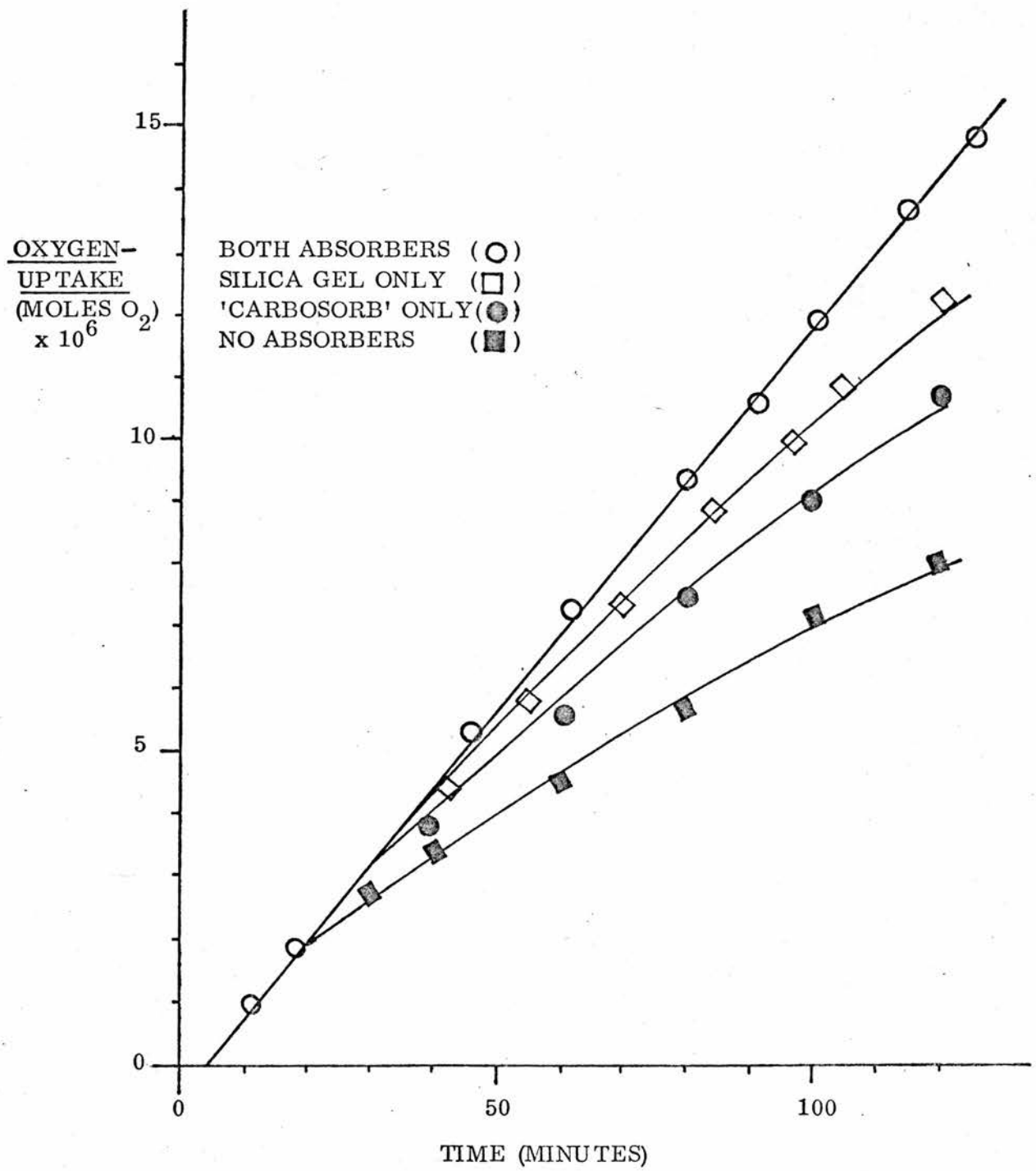

FIGURE 21

APPARATUS TWO

EFFECT OF THE REMOVAL OF BOTH ABSORBERS ON THE RATE OF OXYGEN-UPTAKE UNDER PYREX P-XYLENE/STYRENE COPOLYMER

INTENSITY AT SAMPLE SURFACE = 4×10^{15} quanta cm^{-2} sec^{-1}
PRESSURE OF OXYGEN = 760 mm Hg ; TEMPERATURE = 30 °C
WEIGHT CORRECTED TO 2×10^{-5} MOLES REPEAT UNIT

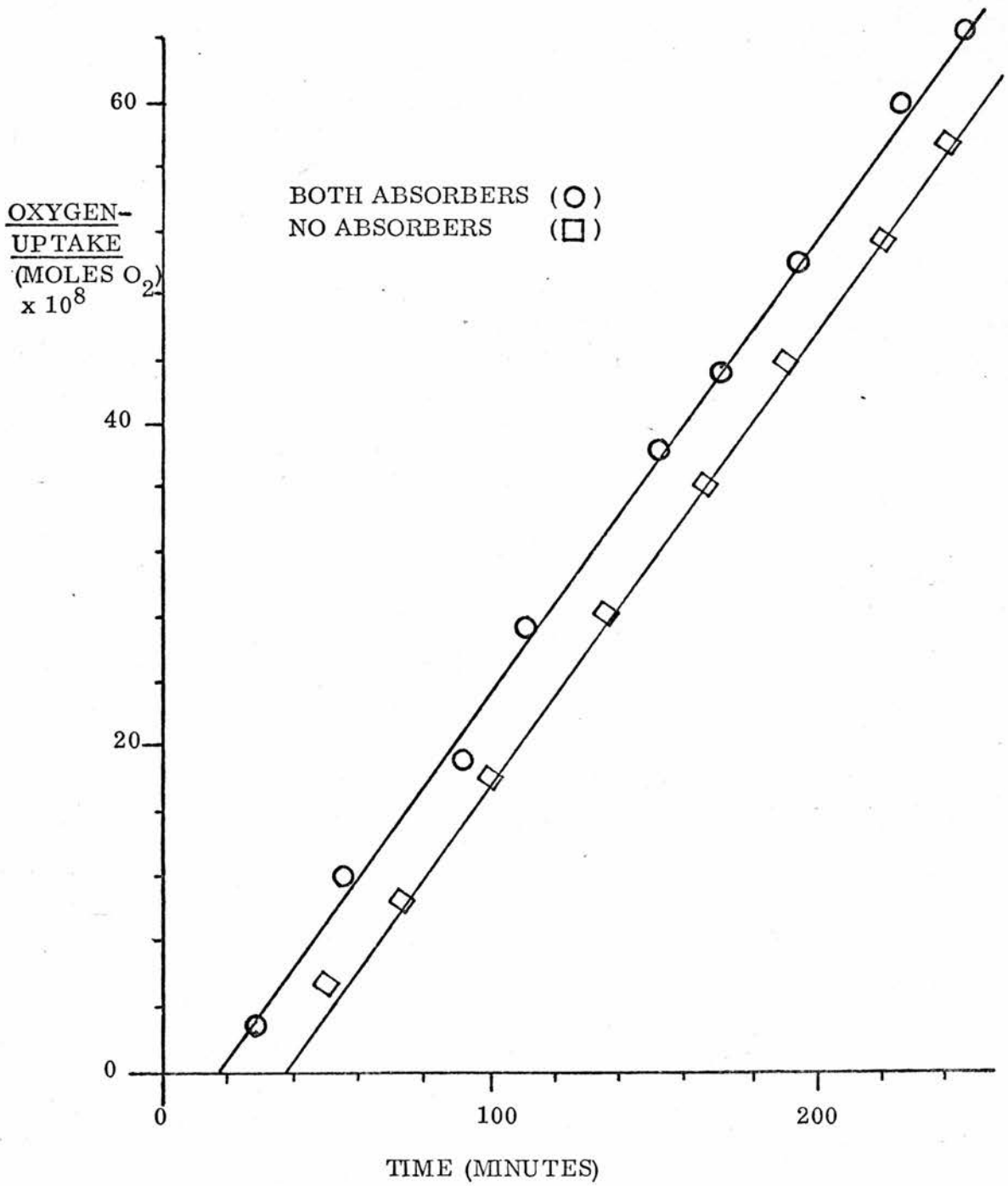

absorbers however, displaced the graph by approximately 6×10^{-8} moles of oxygen. The rate of oxygen-uptake for the p-xylene/styrene copolymer with both absorpers present was 13.7×10^{-5} moles oxygen min^{-1} (mole repeat unit)$^{-1}$. These reactions were repeated for each copolymer and, apart from the variation in rates between the copolymers, similar results were obtained. This seemed to suggest that oxygen-uptake was the predominant process throughout the reaction.

ii) Absorber Removal and Variation in 313 nm Line Intensity

When apparatus two was first set up it was found necessary to frequently clean the thermostated water bath out as a white 'greasy' film, which hampered accurate visual readings, was gradually deposited on the sides of the water bath. The bath water was tested by ultra-violet spectroscopy and the deposit was shown to have no absorption in the region of interest. For this reason and the fact that apparatus one was automatic, the water bath for apparatus one required to be cleaned out less frequently.

Possible explanations for this deposit included both the erosion of the metal clamps, bosses and rods which held the apparatus in place and an organic or inorganic growth formed by dust etc. landing on the water's surface. An attempt to remove the inconvenience of such a deposit was to tape and grease the metallic supports and add an industrial 'bath cleaner'.

Reactions on the copolymers under pyrex were now repeated to check that the removal of absorbers did not effect the rate of oxygen-uptake. Figure 22 shows the effect of removal of absorbers from the p-xylene/styrene

FIGURE 22

EFFECT OF THE REMOVAL OF ABSORBERS ON THE RATE OF OXYGEN-UPTAKE UNDER PYREX P-XYLENE/STYRENE COPOLYMER

INTENSITY AT SAMPLE SURFACE UNKNOWN BECAUSE OF THE PRESENCE OF 'BATH CLEANER' IN WATER BATH
PRESSURE OF OXYGEN = 760 mm Hg ; TEMPERATURE = 30 °C
WEIGHT CORRECTED TO 2 x 10^{-5} MOLES REPEAT UNIT
NO OXYGEN UPTAKE WHEN BOTH ABSORBERS REMOVED

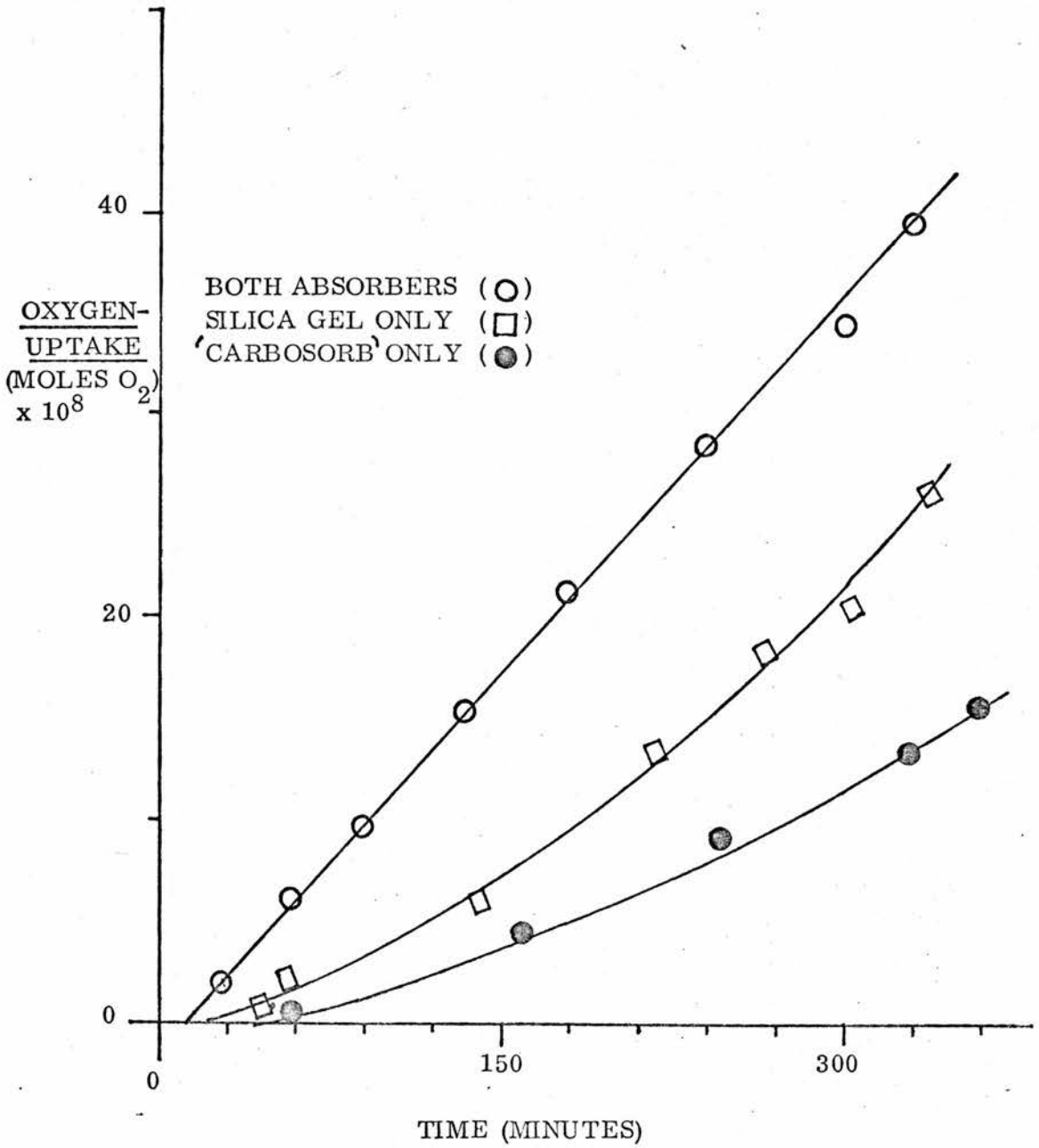

copolymer's reaction at constant temperature and radiation intensity and corrected for weight.

Along with the overall reduction in rate with both absorbers present from 13.7×10^{-5} to 5.8×10^{-5} moles O_2 min^{-1} (moles repeat unit)$^{-1}$, there were large differences, when any or all the absorbers were removed, compared to the reactions when no 'bath cleaner' was involved. This effect was checked for the other copolymers and found to be consistent.

The ultra-violet spectrum of an aqueous solution of the 'bath cleaner' showed a large absorption at 313 nm and a relatively smaller absorption at 365 nm. It was impossible, however, to find out the extent of the reduction of the intensity at the sample surface caused by this absorption as no figures were available for the concentration of the 'bath cleaner' in the water bath.

The 'bath cleaner' was removed permanently and an attempt to reproduce the effect of the 'bath cleaner' was made. When three pyrex discs were placed over the reaction cell and the lamp was moved closer to the sample to an arc to sample distance of 27.3 cm, the line intensity at 313 nm was reduced to 60% of its normal value under one pyrex disc while the 365 nm line intensity remained constant compared to that with one pyrex disc only. (Chapter 2, Part 3).

Reactions were now repeated under three pyrex discs and at an arc to sample distance of 27.3 cm. The removal of absorbers again has an effect on the rate of oxygen-uptake. Figure 23 shows this effect for the p-xylene/styrene copolymer's reaction. The experiments were repeated on the other copolymers

FIGURE 23

APPARATUS TWO

EFFECT OF THE REMOVAL OF BOTH ABSORBERS ON THE RATE OF OXYGEN-UPTAKE UNDER THREE PYREX DISCS

P-XYLENE/STYRENE COPOLYMER

INTENSITY AT SAMPLE SURFACE = 3.5×10^{15} quanta cm^{-2} sec^{-1}
PRESSURE OF OXYGEN = 760 mm Hg ; TEMPERATURE = 30 °C
WEIGHT CORRECTED TO 2×10^{-5} MOLES REPEAT UNIT

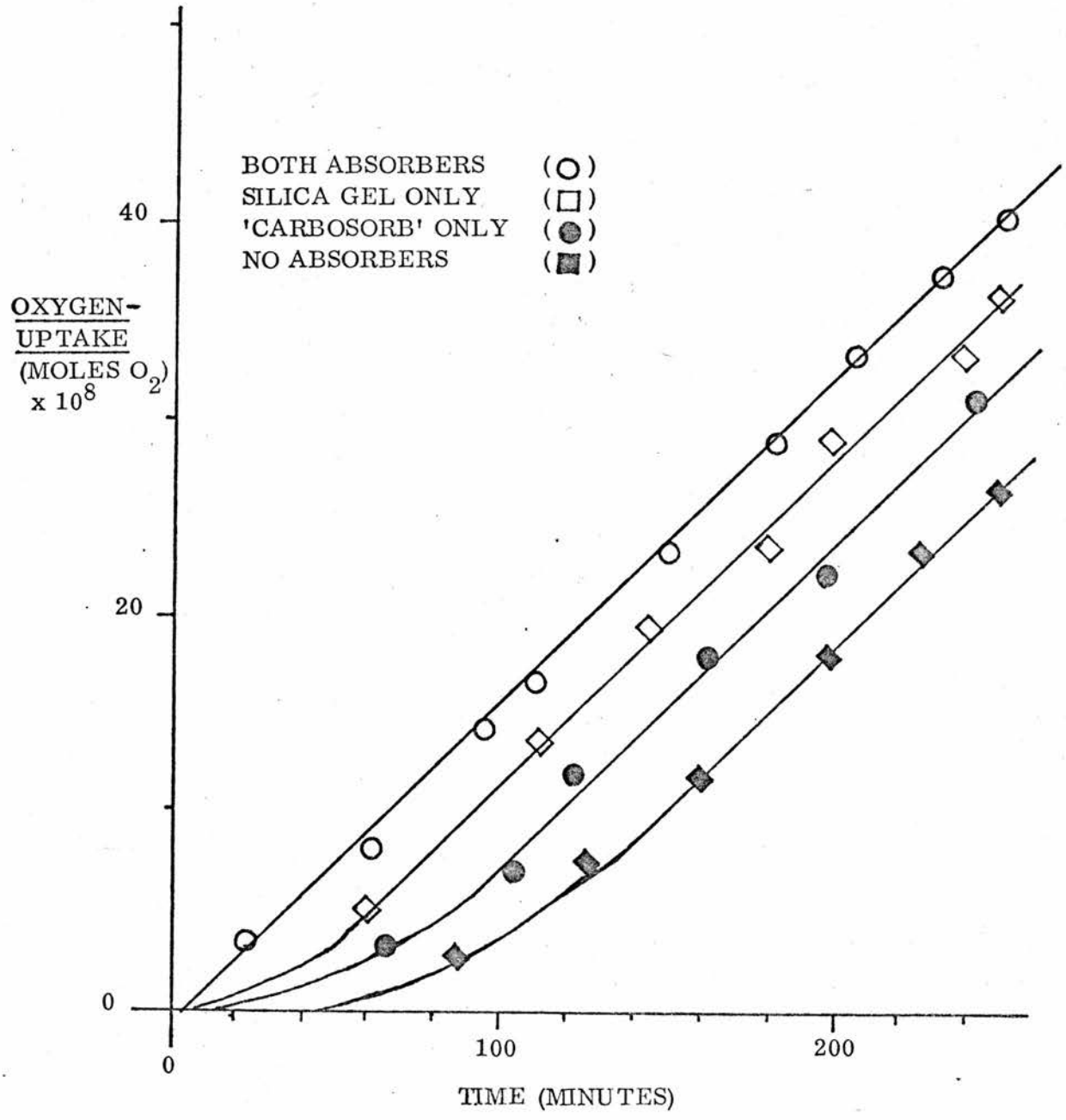

and found to be consistent.

Without the 'bath cleaner' present and with both absorbers in the cell, the rate of oxygen-uptake under one pyrex disc was approximately 40% higher than the rate with three pyrex discs over the sample and the arc to sample distance adjusted so that the 313 nm line intensity was reduced by approximately 40% while the 365 nm line intensity remained constant.

From this it could be deduced that the active wavelength for the photo-oxidation of the copolymers under pyrex was 313 nm. It could therefore be calculated that when the 'bath cleaner' was in use there was approximately a 58% reduction in the 313 nm line intensity.

In summary, figures[21, 22 and 23] show that as the 313 nm line contribution and the corresponding rate of oxygen-uptake were reduced, there was an increasing effect when absorbers were removed. The reduction in 313 nm line intensity acted as a 'magnifying' effect in that it meant that the reaction being studied became progressively closer to the point of initiation. The results therefore suggested that the photo-oxidation reaction under pyrex initially involved the evolution of gas which was superseded by oxygen-uptake later in the reaction.

8. Heating Effect

The heating effect described in chapter 2, part 4 was investigated more fully using cell B and manometer system two.

Films of the copolymers of approximately equivalent absorptions at 260 nm were each irradiated at constant intensity in oxygen for three 3 minute periods with quartz discs in both the upper and lower windows of the cell. Fifteen minutes were allowed for equilibriation between each irradiation.

The average change in volume at constant pressure was measured.

At constant pressure,

$$\frac{V_o}{T_o} = \frac{V_o + \Delta V}{T_o + \Delta T} \qquad (20)$$

Where V_o and T_o are the original volume and temperature of the gas respectively and ΔV and ΔT are the changes in volume and temperature respectively.

Rearranging equation 20

$$\Delta T = \frac{T_o}{V_o} \times \Delta V \qquad (21)$$

The total volume of cell B and the reaction side of the manometer was measured as 39 ± 1 c.c. The original temperature was 31 ± 0.01 ^{o}C. This meant that one complete revolution of the needle valve ($\Delta V = 0.01125$ c.c.) corresponded to a change of temperature in the cell of 0.0877 ± 0.0023 ^{o}C. Table 18 shows the average increase in volume and the temperature change corresponding to this increase for each of the copolymers irradiated at constant intensity and pressure for 3 minute periods.

These results are corrected for the blank experiment carried out under identical conditions except that no polymer was present in the cell. The blank gave rise to a volume increase of 1.575×10^{-3} c.c. and a corresponding temperature increase of 1.2×10^{-2} ^{o}C. The experimental error for the volume increase including both the timing and needle valve volume readings was

approximately $\pm$ 5% so the error for the change in temperature was approximately $\pm$ 8%.

Table 18

POLYMER	ΔV (c.c) x 10^3	ΔT (^oC) x 10^2
P-XYLENE/STYRENE	0.90	0.70
METHANE/STYRENE	0.68	0.53
PROPANE/STYRENE	0.90	0.70
BUTANE/STYRENE	1.69	1.32

The variation of the heating effect with intensity under quartz was checked for the p-xylene/styrene copolymer. Figure 24 shows that the temperature increase on irradiation was proportional to the incident intensity and figure 25 shows that when the lamp was switched on and off the corresponding increase and decrease in the volume caused by the heating effect was constant throughout the photo-oxidation reaction of the p-xylene/styrene copolymer under pyrex. Similar treatment of a reaction under quartz showed the same behaviour. The heating effect was also noticed when a low pressure mercury lamp was used.

From these results it was impossible to say if the effect was genuinely due to the copolymer or if some other factor was involved. Anthracene, recrystallised from ethanol, was added to 5% solutions by weight of reprecipitated commercial polystyrene in methylene chloride in concentrations of 0, 1, 2, 3, 4, 5 mg per gram of polystyrene. Films were cast on tiles, solvent removed and films of uniform area were cut out as previously described. The thickness of

FIGURE 24

HEATING EFFECT

INTENSITY VERSUS TEMPERATURE INCREASE

P-XYLENE/STYRENE COPOLYMER UNDER QUARTZ

PRESSURE OF OXYGEN = 760 mm Hg ; TEMPERATURE = 31°C
APPROXIMATE FILM THICKNESS = 10 microns

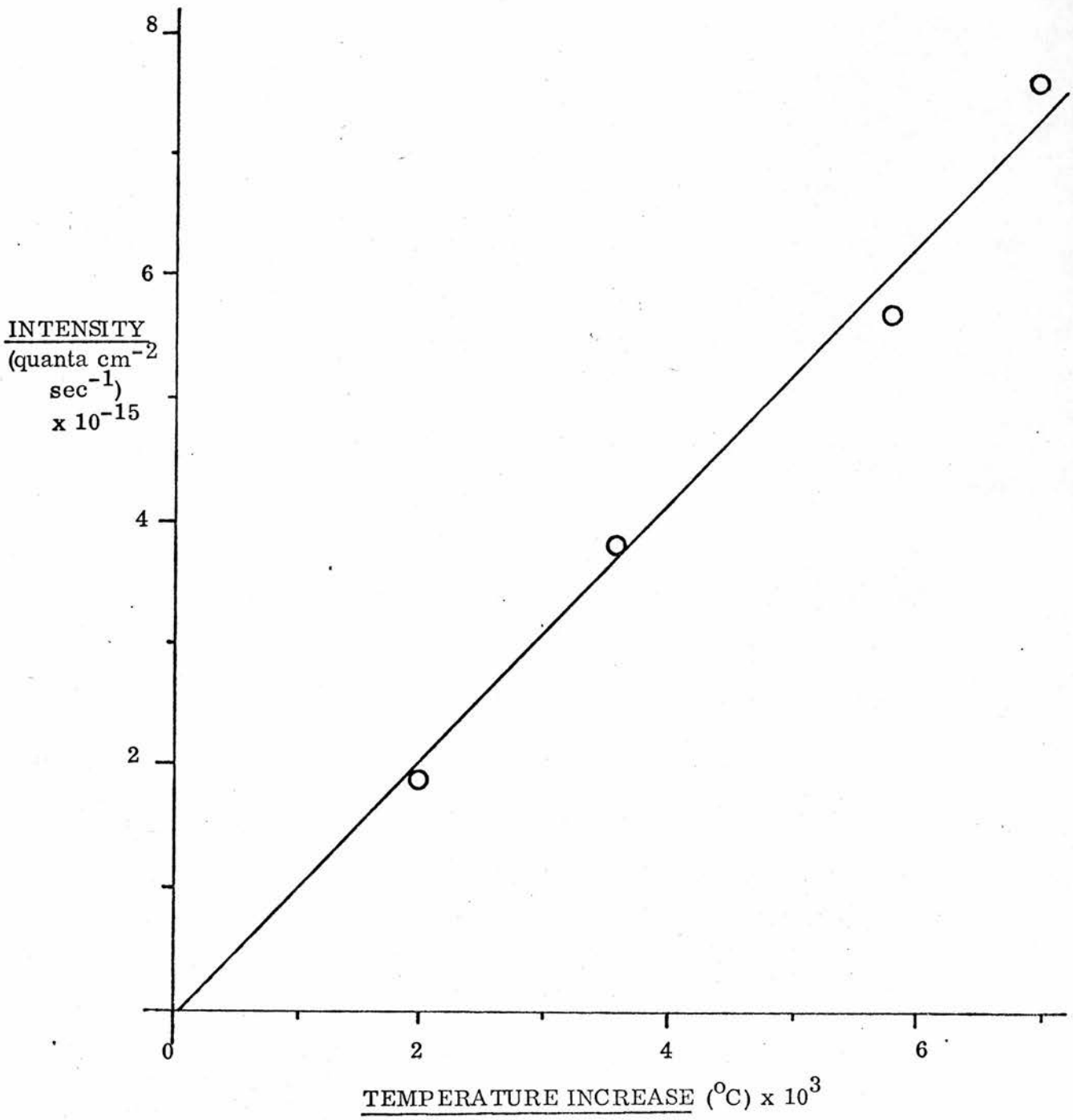

FIGURE 25

HEATING EFFECT

THE VOLUME INCREASES AND DECREASES WHEN LAMP WAS SWITCHED OFF AND ON DURING THE PHOTO-OXIDATION REACTION OF THE P-XYLENE/STYRENE COPOLYMER UNDER PYREX

PRESSURE OF OXYGEN = 760 mm Hg ; TEMPERATURE = 30 °C
INTENSITY AT SAMPLE SURFACE = 4×10^{15} quanta cm^{-2} sec^{-1}
WEIGHT CORRECTED TO 2×10^{-5} MOLES REPEAT UNIT

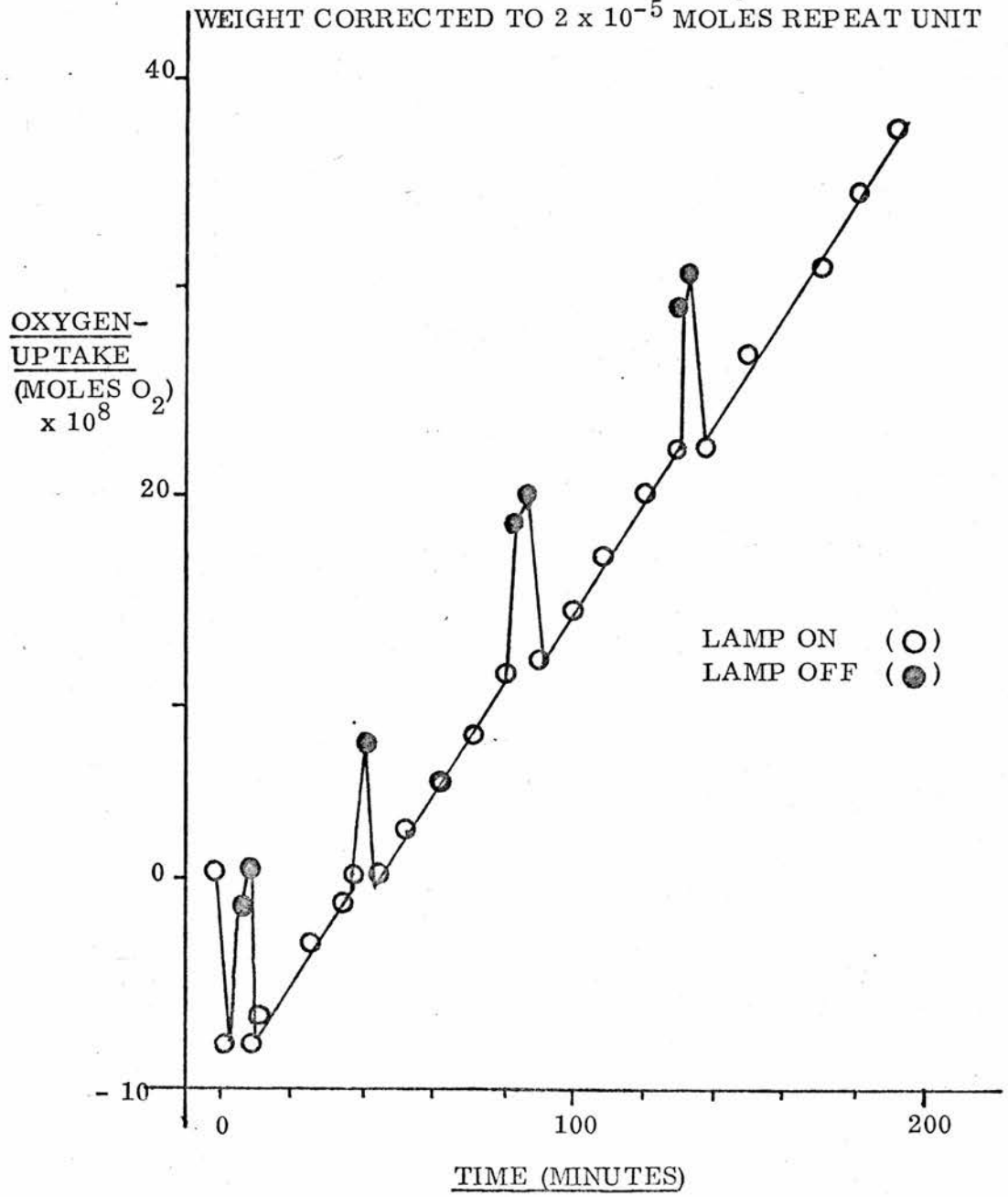

the films was 37.3 microns $\pm$ 4%. The heating effect caused by these films was measured in the same way as for the copolymers by placing the films on top of a quartz disc in the cell. The optical density maximum at 364 nm in the ultra-violet spectra of the films due to the anthracene present was plotted against the average temperature rise after 3 minutes irradiation for each film corrected for the blank experiment.

Figure 26 shows the resulting graph corrected for the heating effect caused by the polystyrene (1.8×10^{-2} °C) film itself. The experimental error for the points on the graph including the film thickness, volume and temperature errors was approximately $\pm$ 12%. The graph is linear and shows that the heating effect was indeed due to the polymer plus additive.

When a polymer is irradiated some proportion of the light absorbed is converted into heat. Using the experimental set up described the temperature rise caused by this heat can be measured. Since samples are irradiated for only a very short time before the temperature rise is calculated, any contribution to the heating effect made by the heat of chemical reaction will be negligible.

FIGURE 26

THE OPTICAL DENSITY (O. D.) MAXIMUM AT 364 nm FOR POLYSTYRENE FILMS CONTAINING ANTHRACENE VERSUS TEMPERATURE INCREASE ON IRRADIATION UNDER QUARTZ CORRECTED FOR POLYSTYRENE

INTENSITY AT SAMPLE SURFACE = 7.6×10^{15} quanta cm^{-2} sec^{-1}
PRESSURE OF OXYGEN = 760 mm Hg ; TEMPERATURE 31 °C
AVERAGE THICKNESS OF FILMS = 37.3 microns

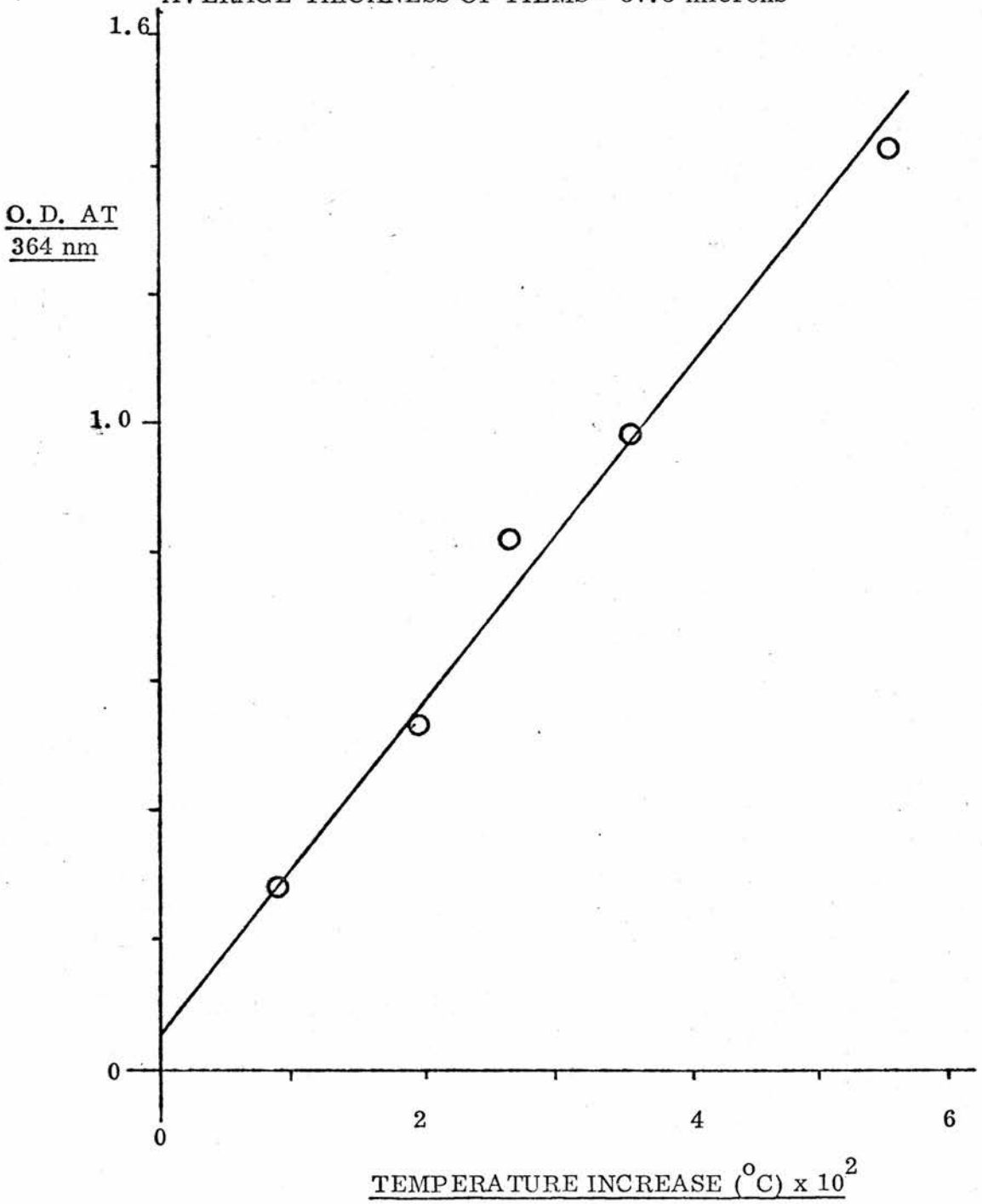

CHAPTER 4

DISCUSSION

The Photo-oxidation Reaction

It is obvious from, the dependence on intensity and the production of gaseous products, that the reactions of the polymers with oxygen and light under pyrex and under quartz are different. A mechanism must therefore be found for each which explains the results obtained.

A. The Reaction Under Quartz

i) Initiation and Oxygen-Uptake

When the polymers are irradiated under quartz the aromatic nuclei contained in the polymers absorb the light directly. By intromolecular energy transfer some of the energy absorbed is directed to a labile carbon/hydrogen or carbon/carbon bond which break to produce radicals. These radicals then react with oxygen to give the observed oxygen-uptake (scheme 7).

SCHEME 7

INITIATION Polymer $\xrightarrow{h\nu}$ Radicals

OXYGEN-UPTAKE Radicals + O_2 $\longrightarrow$ Radical Peroxides

If an active photon is described as a photon which actually causes the breaking of a bond, as the number of active photons increases so too must the number of radicals produced. Also the number of active photons increases as the intensity increases and the more radicals produced the greater the oxygen-uptake. Thus the initiation and oxygen-uptake mechanism proposed would explain the observation that the rate of oxygen-uptake is directly proportional

to the intensity of the irradiation under quartz.

ii) Relative Rates of Copolymers under Quartz

The relative extinction coefficient of the copolymers' repeat units listed in table 7 are due to the absorption of the aromatic nuclei in their respective polymeric environment. The relative rates of the photo-oxidation reactions of the copolymers obtained from apparatus two, in which there was not complete absorption by the single film, could be explained at least partially by their relative absorptions of ultra-violet light.

The ratios of the relative rates of oxygen-uptake for the copolymers in the order of p-xylene/styrene to methane/styrene to propane/styrene to butane/styrene are 2.26 : 1.67 : 1.1 : 1.0. The ratios of the relative extinction coefficients at the absorption maximum for the repeat units of the copolymers in the same order as above are 1.5 : 1.2 : 0.9 : 1.0. If the contribution to the relative rates of oxygen-uptake made by the extinction coefficients is removed by dividing the relative rates of the oxygen-uptake of the copolymers by the corresponding ratios of the extinction coefficients, the ratios of the rates of oxygen-uptake for the copolymers, in the same order as above, become 1.5 : 1.4 : 1.2 : 1.0. These ratios should now represent the contribution to the rate of oxygen-uptake made only by the polymer structures.

In apparatus one, in which there was total absorption of light below 280 nm, the relative extinction coefficients of the repeat units should have no bearing on the rates of oxygen-uptake of the copolymers as each sample should be absorbing the same amount of irradiation. The relative ratios of the rates

of oxygen-uptake in the same order as above are 1.5 : 1.3 : 1.1 : 1.0. These ratios are in close agreement with those from apparatus two with the extinction coefficient contribution removed. This confirms that there are two contributing factors to the rate of oxygen-uptake of the copolymers namely, the extinction coefficient which is initially responsible for the absorption of energy and the polymer's structure which subsequently accommodates the absorbed energy.

a) Extinction Coefficient Contribution

The variation in extinction coefficients of the copolymers with the exception of the methane/styrene copolymer can be rationalised on the basis of the numbers of aromatic nuclei per repeat unit. The methane/styrene copolymer's relatively high value, as discussed in chapter 2, seems to have no satisfactory explanation.

b) Polymer Structure Contribution

Once the copolymers have absorbed energy, the energy can be dissipated in a variety of ways.

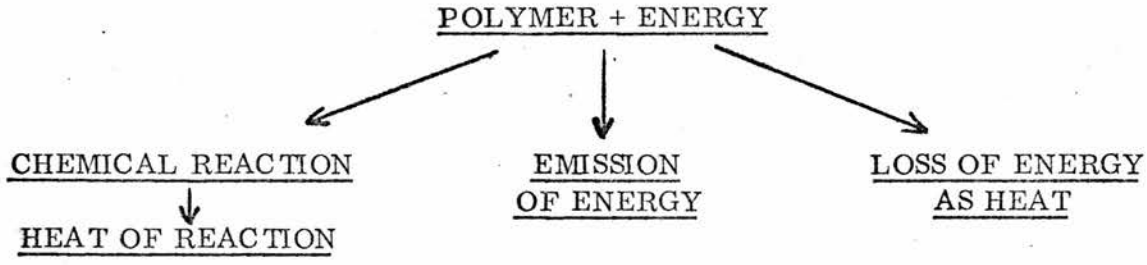

Photochemically the p-xylene/styrene copolymer has one more reaction site available in its repeat unit compared with the other copolymers, namely the main chain benzene ring. This would be expected to enhance the rate of oxygen-uptake relative to the other copolymers. Photophysically, the more

aliphatic the content of the repeat unit becomes the more vibrational and rotational modes available for energy dissipation there are. This is seen in the decrease in rate from the methane/styrene copolymer to the butane/styrene copolymer. An indication of this phenomenon is shown in the heating effects of the copolymers. From table 18, the methane/styrene copolymer appears to be the least prone to give up its absorbed energy as heat whereas the butane/styrene copolymer is about three times more likely to lose energy by this route. The methane/styrene copolymer is unique in this series of copolymers in that it has an additional dispersion route via excimer fluorescence (table 8) which will also effectively reduce the rate of oxygen-uptake by removing potentially photochemically active energy.

No direct comparisons between the rates of oxygen-uptake of the copolymers and polystyrene itself under quartz in apparatus one could be made because the polystyrene film thicknesses (approximately 40 microns) made the rate of oxygen-uptake diffusion controlled (Chapter 3). However, as can be seen in figure 10, the general behaviour of polystyrene was similar to that of the copolymers. Polystyrene shows a heating effect approximately equivalent to that for the methane/styrene copolymer but it would be expected to show more dissipation of energy via excimer compared to the methane/styrene copolymer since every benzene ring in polystyrene is in the 1,3-diphenyl propane type excimer configuration relative to either neibouring phenyl group.

iii) Propagation, Products and Termination of the Reaction

The peroxide radicals produced on oxygen-uptake can abstract a

hydrogen and form hydroperoxides (Chapter 1, IV, 4). The hydroperoxides can then react to give chain scission, crosslinking, gaseous products, carbonyl groups, hydroxyl groups etc. (Chapter 1, IV, 4).

From the change in ultra-violet spectra on irradiation, products absorbing at maxima of 295 nm, 280 nm and below 240 nm are produced (figure 18). Microanalysis, irradiation in nitrogen and vacuum and dependence on oxygen uptake all suggest that these products are oxygenated structures. The ultra-violet spectrum of acetophenone shows a peak at 279 nm and a slightly smaller peak at 287 nm (Figure 27). The acetophenone type terminal group is the only positively identified main chain secondary product[65, 66] and is reported to be the group which is responsible for the phosphorescence in photo-oxidised polystyrene[68]. It is therefore probable that the peaks obtained at 295 nm and 280 nm on irradiation are due to the formation of the acetophenone-type terminal group.

The peak with a maximum at below 240 nm is thought to be due to polymeric hydroperoxides. A study of some simple hydroperoxide ultra-violet spectra shows that the general feature is a gradual build up of absorbance from about 320 nm down to shorter wavelengths. In particular, cumene hydroperoxide has a maximum at approximately 258 nm which has an extinction coefficient of approximately 200[50]. Beachell and Smiley[66] found large quantities of hydroperoxides in polystyrene solutions after irradiation but found none in polystyrene films irradiated at 60 ^{o}C. Figure 19 offers an explanation for the absence of hydroperoxides in their work on films as it would appear that the

FIGURE 27

ULTRA-VIOLET SPECTRUM OF ACETOPHENONE

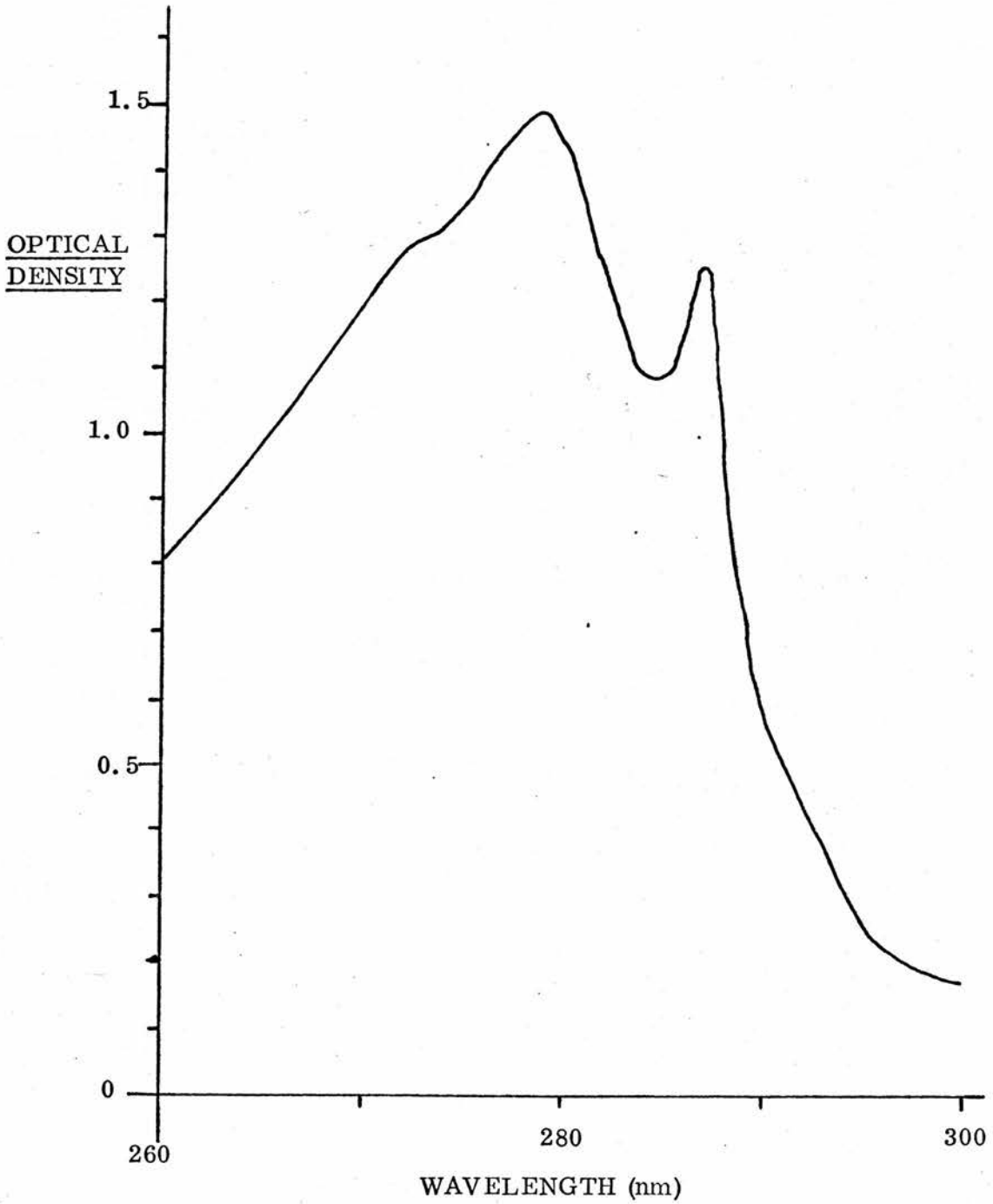

hydroperoxides formed are thermolabile.

The concentration of these products rapidly builds up on irradiation under quartz and then gradually levels off at a steady concentration at which the production must be equivalent to the breakdown (Figure 17). Carlsson and Wiles[60] reported that when polypropylene hydroperoxides built up in a polymer sample so too did the carbonyl compounds which is in agreement with Figure 17. This build up of products would eventually decrease when most of the polymer had reacted and decomposition became the predominant process.

The gaseous products evolved on irradiation were only observed after oxygen-uptake had occurred (figure 20). This endorses the initiation and oxygen-uptake reaction proposed as the production of hydroperoxides and hence gaseous products can only occur after oxygen is taken up.

From figure 20 and the results of the mass spectrometry analysis, carbon dioxide and water are the only gaseous products of the reaction and the ratio of water to carbon dioxide is approximately 2 to 1. The production of water is explained by the hydrogen abstraction reaction of hydroxylradicals (equation 22).

$$RH + HO\cdot \longrightarrow H_2O + R\cdot \qquad (22)$$

The route for the production of carbon dioxide is less obvious. Carbon monoxide is formed in the photolysis of carbonyl compounds which are produced when alkoxyl radicals from hydroperoxide breakdown undergo a β scission reaction (scheme 8).

Scheme 8

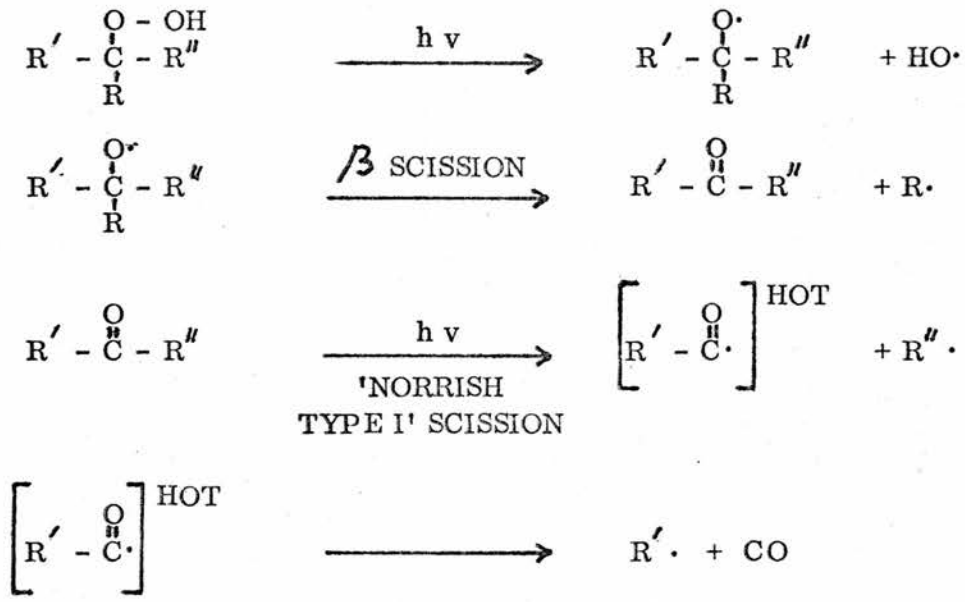

The conversion of carbon monoxide to carbon dioxide over a range of temperatures has been examined and it has been shown that carbon monoxide is converted to carbon dioxide by reaction with hydroxyl radicals or atomic oxygen in the presence of hydrogen radicals or hydrogen containing compounds[88] (equations 23 and 24).

$$CO + HO\cdot \longrightarrow CO_2 + H\cdot \qquad (23)$$

$$CO + O + M \longrightarrow CO_2 + M \qquad (24)$$

These reactions were carried out in the temperature range 310 K to 611 K and showed that reaction (23) was by far the faster of the two and had an energy of activation of only5 k J mol^{-1}. Since hydroxyl radicals are available from the breakdown of hydroperoxides, this provides a possible route for the formation of carbon dioxide.

Once carbon monoxide is formed by reaction scheme 8 it dissolves in the polymers and is converted to carbon dioxide. A competitive reaction can

be visualised as the hydroxyl radical is involved in both the production of water and carbon dioxide (reactions (22) and (23)). As two times as much water is produced as carbon dioxide, it suggests that reaction (22) is faster than reaction (23). This could have been prediced since the production of carbon dioxide is a far more complex process.

In equation (23) a hydrogen radical is produced. Because of its high reactivity, this would probably undergo a hydrogen abstraction reaction to produce hydrogen which would effect the oxygen-uptake measurement. However, if instead of reaction (23), alkoxyl radicals reacted with carbon monoxide to produce carbon dioxide the non appearance of hydrogen would be accounted for (equation 25).

$$RO\cdot + CO \longrightarrow R\cdot + CO_2 \qquad (25)$$

The predominant mode of oxygen-uptake under quartz is the reaction of radicals with oxygen. When the radicals combine to give products which are no longer reactive with oxygen the reaction is terminated. However, if these products are photo-active, further radicals can be produced which will react with oxygen. Because of the insolubility of the polymers after high extents of oxidation, the ultimate products are most probably crosslinked which would explain the embrittlement observed.

The lack of dark reaction under quartz confirms the suggestion that the oxygen-uptake is dependent on the presence of radicals not involved in a chain reaction.

B The Reaction under Pyrex

i) Initiation

The fact that a photo-oxidation reaction occurs in polystyrene and its copolymers under pyrex proves that some species are absorbing light above 295 nm. Because of the purity and preparation of the sample used, it is extremely unlikely that any chromophoric impurities had been incorporated in the polymers. It is suggested that the source of absorption which is present is a charge transfer complex of oxygen with benzene rings of the copolymers since no precaution was taken to exclude oxygen from the polymer solutions before casting the films.

Weak oxygen complexes of benzene derivatives have been observed which cause an absorption at the long-wavelength side of the benzene derivatives' absorption edge[38-43]. This type of complex has also been proposed as a possibility for the absorption at long wavelengths in polystyrene[31]. The ultraviolet spectra of the copolymers showed that there was approximately 85-95% transmittance of the incident light at 313 nm. Klöpffer[68] calculated that the concentration of oxygen in polystyrene was approximately 2×10^{-3} molar and concluded that the contribution of the oxygen complex in polystyrene was of the order of several precent of the total absorption.

When light is absorbed by these complexes, it is thought that the excited complex gives up its oxygen which then undergoes an insertion reaction with, most probably, the relatively weak tertiary benzylic carbon/hydrogen bond. This produces the hydroperoxide directly. Because the oxygen molecule

is a diradical, it is thought that this insertion is a one-step concerted reaction similar to that of a carbene (equation 26).

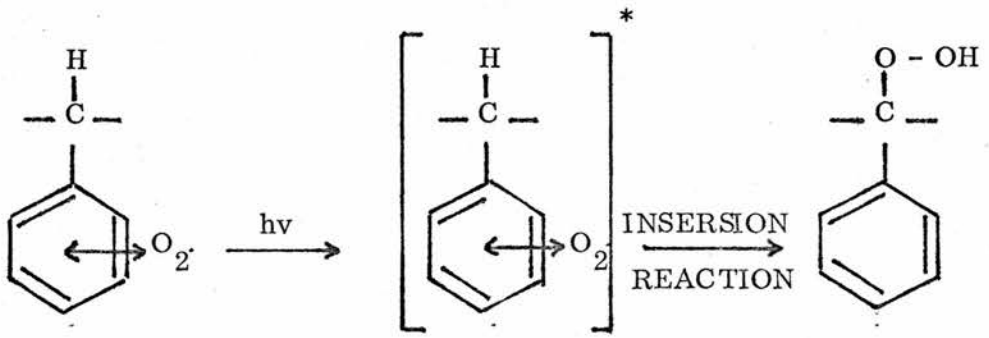

(26)

ii) Relative Rates of the Copolymers Under Pyrex in Apparatus Two

The relative rates of the oxygen-uptake reaction under pyrex are between forty and one hundred and twenty times slower than under quartz. The main reason for this is that that absorption of the copolymers under pyrex is far smaller. The ratios of the relative rates of oxygen-uptake for the copolymers are 6.23 : 5.36 : 1.95 : 1.0 (in the order, p-xylene/styrene : methane/styrene : propane/styrene : butane/styrene). These ratios, although in the same order, show a marked change in magnitude for the same ratios of rates under quartz which is an indication of the different mechanisms involved. The extinction coefficients at 313 nm for all the copolymers give the approximate ratios, in the same order as above, of 7 : 5 : 1.5 : 1.0. The extinction coefficient for the p-xylene/styrene copolymer at 313 nm is 21. This implies that the greater the absorbance per mole of repeat unit at 313 nm the greater the rate of oxygen-uptake. The absorbance at 313 nm is most probably due to

the charge transfer complexes in the copolymers and therefore, assuming that the phenyl/oxygen complex absorbs the same amount of light regardless of its polymeric environment, the rate of oxygen-uptake is proportional to the concentration of phenyl/oxygen complexes capable of promoting the reaction.

The p-xylene/styrene copolymer has one benzene ring per repeat unit more than the other copolymers and therefore has a statistically higher probability of forming a charge transfer complex with oxygen. This is reflected in the ratios of the extinction coefficients at 313 nm but not to the same extent in the relative rates of oxygen-uptake of the p-xylene/styrene and methane/styrene copolymers. It is therefore implied that the main chain phenyl/oxygen complex, when it has absorbed light, reacts relatively slowly. By inference,this would show that the rate of the insertion reaction is determined by the strength of the carbon/hydrogen bond available because the nearest carbon/hydrogen bond, not incorporated in the benzene ring, is secondary in the case of the p-xylene/styrene copolymer's main chain phenyl group whereas it is tertiary in the case of the methane/styrene copolymer's pendant phenyl group.

The difference between the ratios of the extinction coefficients and the rates of oxygen-uptake of the copolymers apart from the p-xylene/styrene copolymer is also probably due to the copolymer's structure. From the results,it is found that the more aliphatic content in the repeat unit the lower the extinction coefficient. This may be due to a decrease in the accessability of the phenyl groups caused by steric hindrance of the oxygen by the aliphatic groups.

The relative rates of the oxygen-uptake of the copolymers are influenced, not only by the extinction coefficients of the phenyl/oxygen complexes, steric hindrance and ease of the insertion reaction, but also by similar heating effects to those described previously for reactions under quartz. It is, however, unlikely that any excimer is formed when the methane/styrene copolymer is irradiated at wavelengths over 300 nm as the excimer emission maximum is at approximately 320 nm.

The energies of activation for the photo-oxidation reactions of the polymers are in the order, butane/styrene $>$ propane/styrene $\doteqdot$ p-xylene/styrene $>$ methane/styrene. The results would be consistent with photo-oxidative stability if the p-xylene/styrene copolymer's energy of activation was lower than that of the methane/styrene copolymer. A possible explanation for the inconsistently high value of the p-xylene/styrene copolymer could be that it has two possible insertion reactions. From chapter one, the difference in bond energies between the secondary and tertiary carbon/hydrogen bonds is approximately 21 k J mol $^{-1}$ and therefore the insertion reaction in the p-xylene/styrene copolymer should be predominantly into the tertiary carbon/hydrogen bond. However, the oxygen released by the main chain phenyl in the p-xylene/styrene copolymer has four times the chance of inserting into a secondary carbon/hydrogen bond as does the oxygen released by the pendant phenyl group into a tertiary carbon/hydrogen bond.

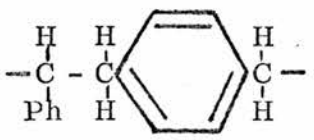

This increase in the possible reaction paths could increase the reaction coefficient of the insertion into a secondary bond and bring both insertion reactions into direct competition or make the insertion into the secondary bond the major reaction. Either of these situations would lead to an increased contribution to the apparent energy of activation by the secondary insertion reaction. This would explain the higher than expected activation energy in the p-xylene/styrene copolymer. Once the secondary and tertiary insertion reactions have taken place they necessarily produce more sites for subsequent breakdown and oxygen- uptake which maintains the p-xylene/styrene copolymer's oxygen-uptake reaction as the fastest in the series.

The polymer structures of all the copolymers must in some way be affecting the rate of the insertion reaction. As one descends the reactivity series for the copolymers there is an increase in the unreactive aliphatic content in the repeat units. This probably involves an increase in the steric hindrance to the insertion reactions, as it did in the formation of the charge transfer complexes, and therefore causes the increase in activation energy.

iii) Oxygen-uptake, Propagation, Products and Termination of the Reaction

Once the hydroperoxides are formed their breakdown is similar to that described previously. It is at this stage that radicals are formed which react with oxygen from the gas environment and produce the observed oxygen uptake. The rate of oxygen-uptake for the copolymers was found to be proportional to the square root of the incident light intensity which is in agreement with the Bolland hydroperoxidation mechanism[53-55]. The reaction after the hydroperoxide

(ROOH) has been formed by the insertion reaction is as shown in scheme 9.

SCHEME 9

HYDROPEROXIDE BREAKDOWN

$$ROOH \xrightarrow{h\nu} RO\cdot + HO\cdot$$

FORMATION OF PRODUCTS

$$RO\cdot + RH \longrightarrow ROH + R\cdot$$

$$HO\cdot + RH \longrightarrow H_2O + R\cdot$$

$$RO\cdot + HO\cdot \longrightarrow \text{PRODUCTS + RADICALS}$$

etc.

HYDROPEROXIDATION AND OXYGEN-UPTAKE

$$R\cdot + O_2 \longrightarrow RO_2\cdot$$

$$RO_2\cdot + RH \longrightarrow RO_2H + R\cdot$$

The reactions carried out with and without absorbers, while reducing the 313 nm line intensity and keepting the 365 nm line intensity constant, showed that the active wavelength for the photo-oxidation of the copolymers under pyrex was 313 nm and that initially gaseous products were evolved which were superseded by oxygen-uptake later in the reaction. The suggested mechanism agrees with these experimental results in that hydroperoxide decomposition must necessarily start before any radicals capable of taking up oxygen are produced. 313 nm is known to be the active wavelength in the breakdown of hydroperoxides and it is thought that the absorption of the copolymers at 313 nm determines the rate of hydroperoxide formation by promoting the oxygen insertion reaction.

Also, initially gaseous products are evolved from the hydroperoxide decomposition.

The gases evolved initially in the reactions under pyrex were water and carbon dioxide in the approximate ratio of 2 to 1 (figure 23). These results are similar to those obtained in the later stages of the reaction under quartz and it is likely that the same mechanisms for gaseous product formation as described previously are involved.

Because of the low extent of oxidation ($< 2\%$) under pyrex, there is no direct information available for the polymeric products of irradiation. However, since all the copolymers are thought to produce similar hydroperoxides to those involved in the reactions under quartz, the ultimate products under quartz and pyrex will be the same.

In the reactions under quartz, when irradiation had ceased, very little dark reaction was observed because the main route for oxygen-uptake was thought to be via the radicals produced outwith the hydroperoxide breakdown. Under pyrex, however, a dark reaction was observed. This reaction is probably caused by the continuation of the short chain reaction of the hydroperoxide breakdown. Termination of the reaction is likely to be radical combination as described previously.

BIBLIOGRAPHY

1. Hawkins, W.L. , 'Polymer Stabilisation', Wiley-Interscience, (New York), 1972.

2. Bowen, E.J. and B. Brocklehurst, Trans. Faraday Soc., 51, 774 (1955).

3. Bowen, E.J. and B. Brocklehurst, Trans. Faraday Soc., 49, 1131 (1953).

4. Noyes , W.A., Jr., and H.Ishikawa, J. Amer. Chem. Soc., 84, 1502, (1962) and J. Chem. Phys., 37, 583 (1962).

5. Noyes, W.A., Jr., G. Porter, and J.E. Jolley, Chem. Rev., 56, 49 (1956).

6. Rånby, B., and J.F. Rabek, 'Photodegradation, Photo-oxidation and Photostabilisation of Polymers', Wiley-Interscience, (New York), 1975.

7. Chien, J.C.W. and W.P. Conner, J. Amer. Chem. Soc., 90, 1001 (1968).

8. Klöpffer, W., 'Organic Molecular Photophysics', Vol. 1, Ed. J.B. Birks, Wiley-Interscience (New York), 1973.

9. Klöpffer, W., J. Chem. Phys, 50, 4, 1689 (1969).

10. Yanari, S.S., F.A. Bovey and R. Lumry, Nature, 200, 242 (1963).

11. Hirayama, F., J. Chem. Phys., 42, 3163 (1965).

12. Vala, M.T., Jr., J. Haebig and S.A. Rice, J. Chem. Phys., 43, 886 (1965).

13. Klöpffer, W., Chem. Phys. Letters, 4, 193 (1969)

14. Chandross, E.A. and C.J. Dempster, J. Amer. Chem. Soc., 92, 3586 (1970).

15. Wall, L.A., M.R. Harvey and M. Tyron, J. Phys. Chem, 60, 1306 (1956).

16. Hansen, R.H., W.H. Martin and T. De Benedictis Trans. Inst. Rubber Ind., (London), 39, (6), T301, (1963).

17. Keith, H. D. and F. J. Padden, Jr., J. Appl. Phys., 34, 2409 (1963).

18. Keith, H. D. and F. J. Padden, Jr., J. Appl. Phys., 35, 1270, 1286 (1964).

19. Hawkins, W. L., W. Matreyek and F. H. Winslow, J. Polymer Sci., 41, 1, (1959).

20. Winslow, F. H. and W. Matreyek, ACS Polym. Preprints, 3 (1) 229 (1962).

21. Grassie N. and N. A. Weir, J. Appl. Polym. Sci., 9, 975, 987 (1965).

22. Cozzens, R. F., J. Chem. Phys., 48, 581 (1968).

23. Rankin, C. T., Ph. D. Thesis, St. Andrews University (1972).

24. Foote, C. S. and S. Wexler, J. Amer. Chem. Soc., 86, 3879 (1964).

25. Foote, C. S. and S. Wexler, J. Amer. Chem. Soc., 90, 975 (1968).

26. Trozzolo, A. M. and F. H. Winslow, Macromolecules, 1, 98 (1968).

27. Kaplan, M. L. and P. G. Kelleher, J. Polymer Sci., B, 565 (1971).

28. Kaplan, M. L. and P. G. Kelleher, Science, 169, 1206, (1970).

29. Kaplan, M. L. and P. G. Kelleher, J. Polymer Sci., A1, 8, 3163 (1970).

30. Zweig, A. and W. A. Henderson, Jr., J. Polymer Sci., (Chem. Ed.), 13, 3, 717 (1975).

31. Rånby, B. and J. F. Rabek, J. Polymer Sci., A1, 12, 273 (1974).

32. Kwei, K. S., J. Polymer. Sci., A1, 7, 1075 (1969).

33. Cooper, G. D. and M. Prober, J. Polymer Sci., 44, 397 (1970).

34. Razumovskii, S. D., A. A. Kefeli and G. E. Zaikov, Eur. Polym. J., 7, 275 (1971).

35. Razumovskii, S. D., O. N. Karpukhin, A. A. Kefeli, T. V. Pokholok and G. E. Zaikov, Vysokomol. Soedin., A, 13, 782 (1971). Chem. Abs. 21351 d (1971).

36. Abasov, S., M. Bagirov, T. Gueseinov and U. Kabulov, Izv. Akad. Nauk S. S. S. R., Ser. Fiz-Tekh. Mat. Nauk, 75, 57 (1970). Chem. Abs. 110769 p (1971).

37. Welge, K. H., Canad. J. Chem., 52, 8ii), 1424 (1974).

38. Chien, J. C. W., J. Phys. Chem., 69, 4317 (1965).

39. Carlsson, D. J. and J. C. Robb., Trans. Faraday Soc., 62, 3403 (1966).

40. Betts, J. C. and J. C. Robb, Trans. Faraday Soc., 64, 2402 (1968).

41. Evans, D. F., J. Chem. Soc., 345 (1953) and 1351 (1957).

42. Tsubomura, H. and R. S. Mulliken, J. Amer. Chem. Soc., 82, 5966 (1960).

43. Munck, A. V. and J. R. Scott, Nature 177, 587 (1956).

44. Achhammer, B. G., M. J. Reiney and F. W. Reinhart, J. Res. Nat. Bur. Standards (U. S.), 47, 116 (1951).

45. Lawrence, J. B. and N. A. Weir, J. Polymer Sci., A1, 11, 105 (1973).

46. Cameron, G. G. and G. P. Kerr, Eur. Polym. J., 6, 423 (1970).

47. Ingold, K. U., Chem. Rev., 61, 563 (1961).

48. Mesrobian, R. B., J. Polymer Sci., 2, 463 (1947)

49. George, G. A. and P. J. Burchill, J. Appl. Polym. Sci., 18, 2, 419 (1974).

50. Calvert, J. G. and N. J. Pitts, Jr., 'Photochemistry', Wiley-Interscience, (New York) 1966 .

51. Plooard, P. I. and J. E. Guillet, Macromolecules, 5, 405 (1972).

52. Hartley, G. H. and J. E. Guillet, Macromolecules, 1, 165, (1968).

53. Bolland, J. L., Quart. Rev., 3, 1 (1949).

54. Bolland, J. L. and H. R. Cooper, Proc. Roy. Soc., A, 225, 405 (1954).

55. Bolland, J. L. and G. Gee, Trans. Faraday Soc., 42, 236, 244 (1946).

56. Jellinek, H. H., J. Polymer Sci., 4, 1 (1949).

57. Russel, G. A. and R. F. Bridger, J. Amer. Chem. Soc., 85, 3765 (1963).

58. Ingold, K. U., Pure Appl. Chem., 15, 19, (1967).

59. Hendry, D. G. and G. A. Russel, J. Amer. Chem. Soc., 86, 2371 (1964).

60. Carlsson, D. J. and D. M. Wiles, Macromolecules, 2, 587, 597 (1969).

61. Chien, J. C. W., J. Polymer Sci. A1, 6, 375, 381, 393 (1968).

62. Benson, S. W., J. Chem. Ed., 42, 502 (1965).

63. Walling, C., Pure and Appl. Chem., 15, 69 (1967).

64. Wall, L. A. and M. Tyron, J. Phys. Chem., 62, 697 (1958).

65. Charlesby, A. and R. H. Partridge, Proc. Roy. Soc., A, 283, 312, 329 (1965).

66. Beachell, H. C. and L. H. Smiley, J. Polymer Sci., A1, 5, 1635 (1967).

67. Grassie, N. and N. A. Weir, J. Appl. Poly. Sci., 9, 999 (1965).

68. Klöpffer, W., Eur. Poly. J., 11, 203, (1975).

69. Richards, D. H., N. F. Scilly and F. J. Williams, Polymer, 10, 603 (1969).

70. Szwarc, M., Makromol. Chem., 35, 132 (1960).

71. Szwarc, M., Nature, 178, 1168 (1956).

72. Richards, D. H., N. F. Scilly and S. M. Hutchison, Polymer, 10, 611 (1969).

73. Szymanski, H. A., 'I. R. Theory and Practice of Infra-red Spectroscopy', Plenum Press (New York), 1964.

74. Paterson, K., Ph.D. Thesis, St. Andrews University (1971).

75. Bovey, F.A., F.P. Hood, E.W. Anderson and L.C. Snyder, J. Chem. Phys., 42, 3900 (1965).

76. Tunnicliff, D.D., R. Robert Brattain and L.R. Zumwalt, Analyt. Chem., 21, 890 (1949).

77. Berlman, I.B., 'Handbook of Fluorescence Spectra of Aromatic Molecules', Second Ed., Academic Press, 1971.

78. Atkinson, J., Ph.D. Thesis, St. Andrews University (1971).

79. Richards, D.H., N.F. Scilly and F.J. Williams, Chem. Comm., 1285 (1968).

80. Parker, C.A., Proc. Roy. Soc. (London), A 220, 104 (1953).

81. Parker, C.A. and C.G. Hatchard, Proc. Roy. Soc. (London), A 235, 518 (1956).

82. Longhurst, R.S., 'Geometrical and Physical Optics', Longmans (London), 1963.

83. Grassie, N. and N.A. Weir, J. Appl. Polym. Sci., 9, 963 (1965).

84. Brandrup, J. and L.H. Peebles, Jr., Macromolecules, 1, 64 (1968).

85. Russel, G.A. and J.V. Pascale, J. Appl. Polym. Sci., 7, 959 (1963).

86. Volman, D.H. and K.J. Laidler, J. Chem. Phys., 30, 589 (1959).

87. Ghaffer, A., A. Scott and G. Scott, Eur. Poly. J., 11, 271 (1975).

88. Wong, E.L., A.E. Potter, Jr., and F.E. Belles, N.A.S.A. Report, No. 129-01-03-01-22, 1967 (JUNE).